PHOENIX: A REACTOR BURNUP CODE WITH UNCERTAINTY QUANTIFICATION

A Dissertation

by

GRANT REID SPENCE

Submitted to the Office of Graduate and Professional Studies of
Texas A&M University
in partial fulfillment of the requirements for the degree of

DOCTOR OF PHILOSOPHY

Chair of Committee,	William S. Charlton
Committee Members,	Sunil S. Chirayath
	David R. Boyle
	James Olson
Head of Department,	Yassin A. Hassan

December 2014

Major Subject: Nuclear Engineering

ABSTRACT

Codes for accurately simulating the core composition changes for nuclear reactors have developed as computing technology developed. The desire to understand neutronics, material compositions, and reactor parameters as a function of time has been, and will continue to be, an area of great interest in nuclear research. Several methods have been developed to simulate reactor burnup; however, quantifying the uncertainty in reactor burnup simulations is in its relative infancy. This research developed a fundamentally different approach to calculate burnup simulation uncertainty using perturbations and regression methods. In this work, a computer software package called PHOENIX was developed that simulates reactor burnup and provides a quantitative prediction of the systematic uncertainty associated with simulation modeling parameters. PHOENIX is a "linkage" code that connects the Monte Carlo N-Particle transport code MCNP6 to the buildup and depletion code ORIGEN-S.

A verification and validation analysis was performed on four different reactor configurations using PHOENIX. The validation analysis consisted of two separate components: a code-to-code validation with MONTEBURNS 2.0 and a perturbation validation analysis using two different perturbation methods. Each analysis observed differences in reactor parameters and gram compositions for a selected isotopic suite, and compared them to a pre-determined validation criteria. For the code-to-code validation component, every reactor configuration simulated in PHOENIX produced reactor parameter values within five percent of the values provided by MONTEBURNS

2.0. A majority of the isotopes simulated in each code also produced gram quantities with differences of less than five percent. Similarly, the perturbation validation analysis confirmed that the simulation parameters produced by PHOENIX using each perturbation method contained differences of less than five percent for a majority of the cases. The outlying instances where a reactor parameter or isotopic composition did not pass validation criteria are explained in detail. The results from the validation analysis showed that PHOENIX produces valid estimates of reactor core compositions throughout burnup.

ACKNOWLEDGEMENTS

I would first like to thank my committee chair, Dr. Charlton for putting up with all of my foolishness. Without his help and guidance I would never be leaving with my Ph.D. I would also like to thank Dr. Chirayath for all of the help he has given me over the course of my research. He was instrumental in helping me through difficult segments of my research. I would also like to thank Dr. Vanderlinde at Zel Technologies and Dr. Smith at AFTAC for their guidance in completing this research.

A large degree of thanks goes to my family as well. Without their support I would not be finishing my third college degree. Lastly I want to thank my beautiful wife Katie Spence. If not for her help, love, support, and humor, I would not be the man I am today.

NOMENCLATURE

MCNP	Monte Carlo N-Particle transport code
EOB	End of burn
LWR	Light water reactor
HWR	Heavy water reactor
BWR	Boiling water reactor
PWR	Pressurized water reactor
ODE	Ordinary differential equation
ORNL	Oak Ridge National Laboratory
ENDF	Evaluated nuclear data files
LANL	Los Alamos National Laboratory
CANDU	Canada Deuterium Uranium
wt%	Weight Percent
MWth	Megawatt thermal
PFBR	Prototype fast breeder reactor
FBR	Fast breeder reactor
MOX	Mixed oxide
HEU	Highly enriched uranium
EFPD	Effective full power days
DSR	Diluent safety rod
CSR	Control safety rod

JAERI	Japanese Atomic Energy Research Institute
nps	A mode of running MCNP6 using a standard source definition

TABLE OF CONTENTS

Page

LIST OF FIGURES

Page

LIST OF TABLES

Page

1. INTRODUCTION

Most industrialized nations have accorded high priority to the development of nuclear reactors and research facilities. [1] As a result of their operations, these facilities can produce large quantities of actinides and fission products in the form of spent fuel and radioisotopes. [2] The United States' (US) fleet of light-water reactors (LWR) alone outputs over 2000 tonnes of spent fuel heavy metal each year. [3] Nuclear facilities are indispensable for various basic research techniques, industrial processes, and many medical procedures. [4, 5] Additionally, the material from these facilities can also be used to make nuclear and radiological weapons. [4, 6, 7, 8, 9, 10] In order to promote the former uses while inhibiting the latter, there is a desire for greater comprehension of reactor isotopic content during and after reactor operation. [11, 12] This increased understanding of isotopic content can be accomplished through modeling and simulations of reactor burnup.

Reactor burnup is defined as a measure of the energy expended over a length of time the reactor was operated per weight of the initial fuel loaded in the reactor. [13] Burnup simulations aim at following the time development of material compositions and neutronics during reactor operations. [14, 15] These simulations are a relatively cheap and time efficient alternative when compared to experimental burnup measurements. [16] Current versions of burnup software are used to aid experts in the fields of nuclear nonproliferation, spent fuel reprocessing, reactor operation, and many nuclear intelligence applications. Developing burnup software, like any computational software,

can be a difficult process. It requires defining the parameters necessary to solve isotopic depletion equations, developing the mathematical models to solve these equations, writing the burnup software, and accomplishing a large amount of software verification and validation to ensure accuracy and precision.

Since reactor burnup software has been developed for more than a decade, the mathematical models to solve burnup calculations, as well as the parameters used in the isotopic depletion equations, have been well researched. In computational burnup calculations, isotopic cross-sections and neutron fluxes are needed to solve the isotopic depletion equations. Both of these burnup parameters can be solved via stochastic (Monte Carlo) or deterministic methods. [17] Each method, whether it be stochastic or deterministic, has its own set of advantages and disadvantages related to geometric modeling capabilities, computational time, and simulation accuracy. There are also various ways to develop burnup software. Deterministic burnup software often includes neutron transport calculations, which solve for the neutron flux and isotopic depletion calculations in the same package. Various Monte Carlo codes run two separate pieces of software, one to solve for the neutron flux, and the other to solve the isotopic depletion equations, and then link them together as necessary. These are known as "linkage" codes. Similar to calculating burnup parameters, each software development method offers varying degrees of advantages and disadvantages that can affect the burnup simulation's accuracy and computational time.

Regardless of the method selected for parameter calculation or software development, an extensive process of verification and validation is needed. Verification

and validation is an engineering practice that produces confidence that the system software was built adequately and will meet the needs that required its creation. [18] In software development, verification is the process of evaluating software to determine whether the products of a given development phase satisfy the conditions imposed at the start of that phase. [19] In the case of burnup software development, verification is achieved by comparing the methods used to calculate important parameters, such as neutron flux and isotopic cross-sections, and comparing the produced results to well understood phenomena. An example of this would be observing the behavior of reactor criticality and flux, or ensuring a near-linear production rate for isotopes like Cs-137. Verifying that these phenomena are behaving correctly provides burnup software verification. Software validation is defined as the process of evaluating software to determine whether it satisfies the specified reasons for its creation. [19] During validation, the software is executed and simulated results are compared to stated functional and performance requirements. In effect, the correctness of the test results validates the system against the specifications required of the software. [20] Burnup software validation is achieved by comparing simulated results to experimental results, or by comparing results to other burnup codes that have been verified and validated with experimental data.

Inherent in the use of burnup codes is a desire to gain precise and accurate predictions for reactor constituents over a period of time. [21, 22, 23] Without the ability to quantitatively determine isotopic precision and accuracy, the researcher has no way of presenting the simulation's fidelity except through comparison to experimental data.

Since the exact operating parameters of a nuclear reactor are unknown in most cases, verifying the accuracy of burnup simulations can be difficult. Until the past decade, the ability to calculate and quantify uncertainties in the predicted values from these simulations has gone relatively unexplored. Recent efforts have been made to quantify stochastic uncertainty in burnup simulations theoretically and numerically through large numbers of simulations. Conversely, the systematic error component of burnup simulations is under-researched. This systematic error can be introduced through inaccurate measurements of input model characteristics, such as fuel enrichment or geometry, or by the method used to calculate reactor parameters. The ultimate goal is to quantify both of these types of errors and provide them to the user to reduce the dependence on experimental validation. If a method to quantify systematic uncertainty in burnup software were developed, this goal would be achieved.

The objective of this research was to develop a package of computer software, called PHOENIX, which simulated reactor burnup, as well as provided a quantitative prediction of the systematic uncertainties associated with simulation modeling parameters. PHOENIX is a "linkage" code that links MCNP6 to the buildup and depletion code ORIGEN-S. The use of MCNP6 allows for the calculation of complex geometries and material compositions in radiation transport calculations. [24] Similarly, the use of ORIGEN-S allows for a deterministic calculation of isotope concentrations, radioactivity, fission rates, and neutron absorption rates as a function of time. [25] In addition to performing standard burnup calculations, PHOENIX also provides a prediction of the systematic uncertainties caused by uncertainties in initial modeling

parameters. This means that PHOENIX can essentially predict the change to End of Burn (EOB) values caused by measurement uncertainties in the simulation input material density, isotopic composition, and cross-section, while only running the simulation a single time. This ability provides an enormous benefit to researchers using the code for spent fuel reprocessing, safeguards, nuclear nonproliferation, and intelligence applications.

2. BURNUP SOFTWARE BACKGROUND

The development of reactor burnup software has increased with developments in computing technology. The desire to understand neutronics, material compositions, and reactor parameters as a function of time has been, and will continue to be, an area of great interest in nuclear research. For this reason, successive generations of reactor burnup software have significantly improved relative to previous generations. With each new generation, burnup software becomes more efficient, the mathematical solution methods become more refined, and processes like uncertainty quantification become more important.

2.1. Burnup Software Operation

Although different reactor burnup software have different solution and operation methods, burnup software, in general, tend to follow the same basic processes for calculating important parameters as a function of time. The first step to simulating reactor burnup is to model the physical system as accurately as possible. The simulation model includes important problem dependent parameters such as reactor geometry, material compositions, material temperatures, material cross-sections, reactor power level, reactor operating history, and problem boundary conditions. In certain situations, assumptions are made to model input parameters to improve simulation accuracy and computational time. In cases where model input parameters do not have a high degree of accuracy (e.g., specific reactor operating history or initial material compositions), assumptions are made to improve the accuracy of the simulation. In cases where

simulation input parameters are well known (e.g., problem boundary conditions), assumptions are made to reduce the computational time of the simulation.

Burnup calculations are divided into two main distinct solvers: neutron transport and isotope depletion. The neutron transport component calculates the neutron flux and energy dependent interaction cross-sections in the system. The isotope depletion component calculates isotopic gram quantities and other reactor parameters such as burnup, radioactivity, and power. The goal of reactor burnup software is to track each of these reactor parameters through time. The method for calculating these parameters over time is to divide the reactor operating history into a certain number of user defined time-steps. Reactor parameters are calculated at every time-step to provide an approximation of the physical system over the course of its operation. Initial time-step parameters are calculated using the information input into the simulation model. Using the system geometry and material specifications, the neutron flux and material interaction cross-sections are calculated at an initial time-step (i = 0). These flux (ϕ) and cross-section (σ) values are input into depletion ODEs that give updated nuclide number densities (N) for the next time-step (i + 1). Once calculated, the updated nuclide number densities for the next time-step (i + 1) replace the input material compositions of the previous time-step (i). If the time-step is not equal to EOB, the time-step is iterated and a new set of flux and interaction cross-sections are calculated for the next time-step (i + 2). This process of calculating fluxes and cross-sections and using them to solve ODEs for updated nuclide number densities is repeated for every remaining time-step in the simulation. A graphic example of this can be seen in Figure 1.

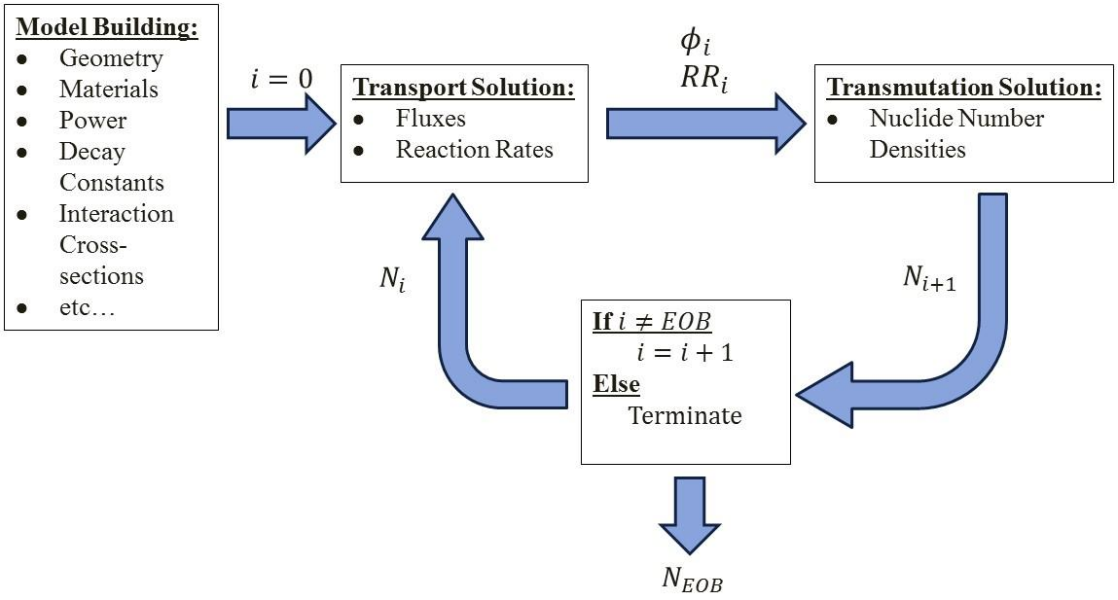

Figure 1. Diagram of burnup software operation.

The procedure described above outlines the general behavior of reactor burnup software. Each particular set of software has its own methods for improving the accuracy of neutron flux, material cross-section, and nuclide number density calculations. Furthermore, different methods exist to calculate each of these parameters, and each of these methods has their own set of advantages and disadvantages.

2.2. Deterministic vs. Monte Carlo Methods

Regarding neutron transport solutions, the two prominent methods used to calculate neutron flux and material interaction cross-sections are Monte Carlo methods and deterministic methods. Monte Carlo stochastic methods of radiation system analysis are among the most popular of computation techniques. [26] This method tracks each particle (i.e., neutrons, photons, and charged particles) for a given number of source particles from birth to absorption. Neutrons and photons are tracked on an interaction-

by-interaction basis using random numbers to fit both theoretical and experimental probability distribution functions. These probability distribution functions describe the differential behavior of a particular interaction type. By using these distribution functions combined with point wise cross-section data, Monte Carlo codes have the ability to calculate surface currents, flux tallies, energy deposition in a cell, pulse height tallies, and other tallies resulting from particle transport. Electrons and other charged particles are tracked using a condensed history approximation, which is effective in predicting the average behavior of an energetically charged particle after undergoing many interactions.

Simulating neutron transport using Monte Carlo methods has both advantages and disadvantages. The main advantage to the Monte Carlo method is the capability to model geometry and interaction physics without making major approximations. [27] In fact, it is often the only type of model possible for simulating complex systems. Simulating a reactor system model by means of deterministic methods frequently becomes infeasible when large heterogeneities are involved. [28] Monte Carlo methods also allow for sensitivity analysis and optimization of a real system without the need to physically operate that system. The main disadvantage to using Monte Carlo methods is that solutions generally require much more computer time when compared to deterministic methods. Furthermore, using random numbers in probability distribution functions creates statistical variance inherent in Monte Carlo simulation results. In some cases multiple simulations of the same model are required to ensure precision. Deterministic solutions, on the other hand, require only a single iteration because they

are exact values provided by the analytical solution of mathematical models. Although Monte Carlo methods require extensive computational time and have inherent statistical uncertainty, the advantage afforded by modeling complex geometries and interaction physics make it an ideal choice for neutron transport solutions.

Deterministic methods for neutron transport solutions involve directly solving the space and energy dependent transport equation. [29] Thus, a reliable computation of the neutron flux distribution within a reactor core would require the solution of the space-, energy-, and angle-dependent neutron transport equation for the full heterogeneous nuclear reactor core. Due to the large amount of heterogeneities present in reactor materials, temperatures, and power, it is not feasible to solve the neutron transport equation for reactor core geometries in detail. Therefore, the simulations are split into two steps: cell and lattice calculations, and core simulations. Cell and lattice calculations are based on static multi-group transport methods applying detailed geometry. Core simulations are based on static and transient nodal codes employing only a few energy groups and coarse mesh homogenized geometry. These two processes are linked via the few group cross-section libraries, which are produced by the cell and lattice calculations. These libraries are used as input for multi-dimensional core simulations. [30]

Deterministic analysis calculation methods are less widely employed because their large memory requirements inhibit their ability to accomplish three-dimensional modeling. As a result, deterministic codes are often limited to diffusion type solvers with transport solution corrections, or limited geometry capabilities such as one- or two-dimensional geometry approximations. [26, 31] In general, deterministic codes have

applicability during the reactor design process to perform scoping studies, evaluate reactivity coefficients and delta-reactivity effects, and other types of simulations involving iterative design parameter changes. Deterministic codes have much shorter computation times and are not subject to the same statistical effects as Monte Carlo reference codes. This is particularly useful when evaluating small perturbations where statistical effects may mask the desired results. [32, 33]

2.3. Existing Burnup Software

Most reactor burnup codes use Monte Carlo methods to calculate fluxes and cross-sections because of the geometric freedom allowed when creating a model. The MONTEBURNS 2.0 package, developed by Holly R. Trellue of Los Alamos National Laboratory, links MCNP5 to the isotope build up and depletion code ORIGEN2.2. [34] Since MCNP5 and ORIGEN2.2 are two separate codes linked together, MONTEBURNS 2.0 is considered a "linkage" code. ORIGEN2.2 is a deterministic code developed at ORNL that predicts solutions to the Bateman depletion equations using a matrix exponential method to solve a large system of coupled, linear, first-order ODEs with constant coefficients. [35, 36] ORIGEN2.2 includes standard libraries for many reactor systems including pressurized water reactors (PWR), boiling water reactors (BWR), Canadian-deuterium uranium (CANDU) reactors, and liquid-metal fast breeder reactors (LMFBR).

Another widely used Monte Carlo burnup code is MCNPX2.7. [37] Similar to MONTEBURNS 2.0, MCNPX2.7 also uses stochastic methods to calculate fluxes and cross-sections. Unlike MONTEBURNS 2.0, MCNPX2.7 uses the Markov chain based

Monte Carlo buildup and depletion code CINDER90 instead of ORIGEN2.2. [38] CINDER90 uses intrinsic cross-section and decay data for 63 neutron energy groups to track the time-dependent reactions of 3400 isotopes. CINDER90 tracks immediate daughter products used by the burn material interactions and any user-specified isotopes. Ternary fission cross-sections are absent from the data. [39] Conversely, ORIGEN2.2 tracks only 1700 nuclides but it contains cross-sections for all reaction types including ternary fission. For these reasons MCNPX2.7 has the capability to be slightly more accurate than MONTEBURNS 2.0; however, the computational time is much greater since CINDER90 tracks significantly more isotopes and the Markov chain Monte Carlo solution is slow for long decay chains. [40]

There has also been a significant amount of research dedicated to creating burnup software using deterministic methods. The inherent downfall in using any deterministic burnup solver is its limited dimensional modeling ability. One of the most popular deterministic burnup codes used today is HELIOS-2. [31] HELIOS-2 is a neutron and gamma transport code for lattice burnup in two-dimensional geometry. The transport calculations are performed with either a collision probabilities or a method of characteristics solver. HELIOS-2 uses ENDF/B-VII evaluated data files, which are the most comprehensive evaluations available. Deterministic codes are useful for simplified systems that are infinite in one dimension, because the computing time necessary is approximately170 times less than Monte Carlo methods. [33]

The deterministic software DRAGON is also widely used to simulate reactor burnup. Similar to HELIOS-2, DRAGON performs lattice calculations in a two

dimensional plane and has a parameterized treatment of the neutron flux. [41] The two main components of the code DRAGON are its multigroup flux solver and its one-group collision probability tracking modules. [42] The multigroup flux solver can use various algorithms to solve the integral neutron transport equation for the spatial and angular distribution of the flux. Each of these algorithms is presented in the form of a one-group solution procedure where the contributions from other groups are considered as sources. The multigroup solution algorithms solve the integral neutron transport equation in one and two dimensions, and are capable of solving three dimensional fuel assembly calculations after assumptions are made. [43] Isotopic depletion calculations in DRAGON are performed using the matrix exponential solution method to the Bateman depletion equations similar to ORIGEN-2.2. Both HELIOS-2 and DRAGON have been benchmarked against experimental measurements and performed well. [44, 45]

Before deciding which type of burnup software to use, a general understanding of the system to be modeled is needed. Does the system have complicated geometry with a large amount of material heterogeneities? Can the system be modeled effectively in two dimensions? Are there significant temperature differences in the system, and will these impact the calculated cross-sections? These are just a few examples of the questions that need to be asked before the type and solution method for burnup calculations can be selected. Monte Carlo based software provides robust geometric modeling capabilities allowing the user to model a highly heterogeneous system. Using a Monte Carlo neutron transport solution method means the user needs less a priori knowledge of how the system operates relative to deterministic transport solution methods. However,

MONTEBURNS 2.0 uses outdated ORIGEN-2.2 reactor cross-section libraries, and MCNPX-2.7 can have a drastically increased computational time due to the Markov chain method. HELIOS-2 and DRAGON, contrarily, use the most up to date ENDF/B-VII.1 cross-section libraries and have computational times that are orders of magnitude faster than Monte Carlo methods. However, the assumptions needed to deterministically solve the integral neutron transport equations in three dimensions inhibit modeling of highly heterogeneous systems. It is also extremely important to note that none of the software mentioned above have any kind of uncertainty quantification capability. If burnup software were developed that included updated reaction cross-sections and reactor cross-section libraries, the capability to model highly heterogeneous systems, and uncertainty quantification, it would greatly benefit the field of reactor burnup simulation.

2.4. PHOENIX Software

As mentioned in Section 1, PHOENIX is a "linkage" code. It links the latest version of the Monte Carlo radiation-transport code MCNP, which is MCNP6, to the newest version of the isotopic depletion code ORIGEN, which is ORIGEN-S.

2.4.1. MCNP6

All versions of the Monte Carlo code MCNP are written and maintained by Los Alamos National Laboratory. [24] It is the most widely used Monte Carlo transport code and is capable of modeling almost any geometry in three-dimensions. [26] The popularity of this code is largely due to its versatility, comprehensive geometry features, and its overall physics capabilities, including continuous energy treatment. Today, MCNP calculations are sufficiently accurate and considered of benchmark quality (i.e.,

in lieu of experimental data). [46, 47] A downside to using Monte Carlo based codes, particularly MCNP, is that the neutron flux is obtained via simulation requiring a very large number of particles; the number of particles is especially large if spatially detailed information is required. This neutronics solution procedure is time-consuming and, therefore, less suitable for the very large number of repetitive simulations needed in optimization applications. [29]

The latest version of MCNP, MCNP6, represents the culmination of a multi-year effort to merge the MCNP5 and MCNPX codes into a single product comprising all features of both. Although MCNP6 is simply and accurately described as the merger of MCNP5 and MCNPX capabilities, the result is much more than the sum of these two computer codes. As a consequence of the merger, and five years of development by the MCNP code development teams, new capabilities, features, and options are now available to the entire MCNP/X user base. The new capabilities of MCNP6 provide improvements to particle physics, source declarations, tallies, material declarations, variance reduction techniques, and geometry creation. [48]

2.4.2. ORIGEN-S, COUPLE, AND SCALE

The isotopic depletion and decay portion of PHOENIX is performed using ORIGEN-S. ORIGEN-S is no longer offered independently and is only provided as part of the nuclear software package SCALE. The SCALE code package is a comprehensive modeling and simulation suite for nuclear security safety analysis and design that is developed and maintained by ORNL. SCALE provides a comprehensive, verified and

validated, user-friendly tool set for criticality safety, reactor physics, radiation shielding, radioactive source term characterization, and sensitivity and uncertainty analysis. [49]

Both ORIGEN-2.2 and ORIGEN-S apply a matrix exponential expansion model to calculate time-dependent concentrations, activities, and radiation source terms for a large number of isotopes simultaneously generated or depleted by neutron transmutation, fission, and radioactive decay. Provisions are made to include continuous nuclide feed rates and continuous chemical removal rates that can be described with rate constants for application to reprocessing or other systems that involve nuclide removal or feed. [25, 50] ORIGEN-S maintains the capabilities of ORIGEN-2.2 to be used as a standalone code, but also has the added ability to utilize multi-energy-group cross-sections processed from standard ENDF/B evaluations. [50]

The cross-section libraries used in PHOENIX by ORIGEN-S are generated using COUPLE, which is also included in the SCALE package. The COUPLE code generates binary format nuclear data libraries that are used by ORIGEN-S to calculate isotopic concentrations and the associated radiation sources and decay heat during irradiation and decay. COUPLE combines problem-dependent cross-sections generated using MCNP6, with state-of-the-art ENDF/B-VII nuclear decay data and energy-dependent fission product yields, and continuous-energy cross-section evaluations of the JEFF-3.0/A neutron activation file, to produce binary libraries that can be used by ORIGEN-S for analyzing a broad range of nuclear applications. [51]

2.5. Uncertainty in Burnup Calculations

As described in section 2.3, years of research and computational developments have provided different methods for reactor burnup simulation; however, quantifying the uncertainty in reactor burnup simulations is in its relative infancy. This research proposes a fundamentally different approach to calculate burnup simulation uncertainty using perturbations and regression methods. In this section, the present status of uncertainty quantification and propagation in burnup software will be discussed.

2.5.1. Uncertainty Quantification

Uncertainty in burnup calculations can be classified into two groups: stochastic and systematic. Stochastic uncertainty results from a lack of precision in burnup calculations. It is a direct result of the system's ability to behave in many different ways. Thus, it is a property of the calculation method. Due to the random nature of these errors, there is an equal chance that they will be above or below the 'true' value. Systematic uncertainty results from a lack of knowledge about elements that make up the burnup model, and is, therefore, a property of the burnup model itself. These errors are typically skewed in a single direction and can be difficult to quantify. [52]

For the purposes of this work, it is important to discuss the stochastic uncertainties associated with using Monte Carlo based burnup software. Inherent in all Monte Carlo calculations is a stochastic uncertainty created from applying random numbers to particle histories. This stochastic uncertainty is present in any quantity derived from particle history sampling in Monte Carlo transport calculations. This means that quantities such as particle flux, surface tallies, energy spectra tallies, reaction rates,

and eigenvalue calculations all contain some degree of stochastic error. The quantities containing these stochastic errors are used in depletion equations to provide estimated isotopic concentrations at the end of a burnup time-step. Since the stochastic error in a Monte Carlo burnup calculation varies directly with the quantity of particles in each simulation, it can be regulated by increasing the number of particle histories per simulation. [53, 54, 32] Work was performed by Matthew R. Sternat to quantify the stochastic uncertainties in burnup calculations using MONTEBURNS 2.0. [55] In this work, Sternat quantifies the stochastic uncertainty in a particular burnup model by running many identical input decks with different random starting seeds. Statistical methods were used to gain a quantification of the model's stochastic uncertainty.

There are also systematic uncertainties in every Monte Carlo burnup model. These exist because there will always be some degree of uncertainty in the specification of the parameters used in transport and depletion calculations. These parameters, such as decay constants, fuel isotopic composition, fuel density, and interaction cross-sections, are all measured experimentally and contain uncertainties in their measurements. The experimental cross-section measurement uncertainties in particular are difficult to quantify because many transport codes use the same cross-section libraries; however, recently developed techniques can evaluate the upper and lower bounds for the measurement of cross-section uncertainties. [56] Using these parameters without accounting for their uncertainties introduces a systematic error into the burnup model.

2.5.2. Uncertainty Propagation

Although a large number of Monte Carlo based burnup codes exist, few studies have been devoted to theoretical formulation to quantify the effect of uncertainty propagation. [57] Takeda, Hirokawa, and Noda completed one of the first studies which presented a burnup matrix method aimed at estimating uncertainty propagations on the nuclide number densities in Monte Carlo burnup calculations. Its shortfall is the failure to address how to calculate the propagated uncertainties in Monte Carlo tallies. [57, 58]

More recently, Tojoh et al. examined the effects of both statistical errors from reaction rate estimates, and propagated uncertainties from nuclide number densities. They provide a supposedly useful calculation for approximating nuclide number density uncertainties after burnup calculations have completed. [57, 59] Garcia-Herranz et al. has also offered a formulation that can be used to quantify the uncertainty propagation of nuclide number densities with burnup. Because their formulation focuses on nuclide number density uncertainties alone, it is not enough to quantify the systematic effects of the uncertainties in Monte Carlo tallies described above. [57, 60]

3. UNCERTAINTY QUANTIFICATION DEVELOPMENT

Outlined in Section 2 are the prominent burnup codes being used today, as well as some current research methodologies used to quantify and propagate the uncertainties associated with these codes. Many of the uncertainty quantification methods involve running multiple Monte Carlo simulations to provide uncertainty estimates. These are estimates of the stochastic uncertainty in nature. They are also specific to the simulation performed; they do not have the ability to extrapolate these uncertainties to similar simulations. [61, 62] It is the goal of this research to create burnup software capable of quantifying stochastic and systematic uncertainty estimates through the use of model perturbations.

3.1. Uncertainty Quantification & Propagation Methodology

In order to quantify and predict uncertainty in burnup calculations, it is important to understand how that uncertainty is propagated. As seen from the previously referenced literature, stochastic uncertainty quantification and propagation has been well explored. To quantify each parameter's systematic uncertainty, we must first verify that we can rigorously propagate the uncertainty through the transmutation equations. Once the uncertainty is propagated, we can attempt to quantify it by fitting a functional form to its variance. To begin to understand uncertainty propagation we can observe a simple system in which isotope X can be produced via decay from isotope A or absorption in isotope B. The general buildup and decay equation for isotope X is given by:

$$\frac{dN_X}{dt} = P_X - L_X \tag{1.1}$$

$$\frac{dN_X}{dt} = \lambda_P N_A(t) + \sigma_P \phi N_B(t) - \lambda_L N_X(t) - \sigma_A \phi N_X(t) \tag{1.2}$$

$$\frac{dN_X}{dt} + (\lambda_L + \sigma_A \phi) N_X(t) = \lambda_P N_A(t) + \sigma_P \phi N_B(t) \tag{1.3}$$

where N_X is the isotopic concentration of isotope X, λ_P is the decay constant for isotope A which results in the production of isotope X, P_X is the grouped isotopic production terms for isotope X, L_X is the grouped isotopic loss terms for isotope X, $N_A(t)$ is the isotopic concentration of isotope A at time t, σ_P is the absorption cross-section of isotope B which results in the production of isotope X, ϕ is the neutron flux, λ_L is the decay constant for isotope X, and σ_A is the absorption cross-section for isotope X . Let us assume that over the time of interest $N_A(t) = N_A$ and $N_B(t) = N_B$. Also we shall assume that $N_X(t = 0) = N_{X0}$. Solving this first order differential equation via exponential integrating factor yields:

$$N_X(t) = \frac{\lambda_P N_A + \sigma_P \phi N_B}{\lambda_L + \sigma_A \phi}\left\{1 - e^{-(\lambda_L + \sigma_A \phi)t}\right\} + N_{X0} e^{-(\lambda_L + \sigma_A \phi)t} \tag{2}$$

Every isotope has its own set of production and destruction mechanisms that make propagating parameter uncertainties difficult. In this solution, the following parameters could all have systematic errors in their recorded measurement: λ_P, N_A, σ_P, ϕ, N_B, λ_L, σ_A, and N_{X0}. In order to determine the burnup model's sensitivity to these

errors we can assess the change in N_X due to perturbations in each of these parameters ($\delta\lambda_P$, δN_A, $\delta\sigma_P$, $\delta\phi$, δN_B, $\delta\lambda_L$, $\delta\sigma_A$, δN_{X0}). If we can derive a common functional form that characterizes the propagated variance of the perturbed isotopic quantity N_X , the systematic uncertainty can be quantified by implementing small perturbations in the burnup model. We can attempt to propagate parameter uncertainty, as well as characterize a common variance functional form, by looking at a number of simplified cases that represent general isotope behavior in a reactor.

3.1.1. Case 1: Cs-137 Type Isotopes

In cases using isotopes like Cs-137, the isotopes are produced in large quantities in the reactor and undergo relatively little destruction or decay. Therefore, we can assume that that $\lambda_P N_A = 0$ and $(\lambda_L + \sigma_A\phi) \to 0$. To approximate the total propagated variance in the system we can use the partial derivatives method to propagate uncertainty:

$$x = f(u, v, \dots) \tag{3.1}$$

$$s_x^2 \cong s_u^2 \left(\frac{\partial x}{\partial u}\right)^2 + s_v^2 \left(\frac{\partial x}{\partial v}\right)^2 + \cdots \tag{3.2}$$

where s_x^2, s_u^2, and s_v^2 are the variances for component x, u, and v respectively. [63] It is important to note that we are assuming covariance terms are negligible in this propagation analysis. This assumption is valid because the covariance terms between parameters are either zero or are so small they become negligible. Using the

methodology from Equation Set 3 and the simplifications for Cs-137 type isotopes outlined above, Equation 2, with propagated variances, can be written as:

$$s_{N_X}{}^2 = s_{N_{XO}}{}^2 + \left(\frac{s_{\sigma_p}{}^2}{\sigma_p{}^2} + \frac{s_{\phi}{}^2}{\phi^2} + \frac{s_{N_B}{}^2}{N_B{}^2}\right) s_P{}^2 \phi^2 N_B{}^2 \tag{4.1}$$

$$s_{N_X}{}^2 = \underline{s_{N_{XO}}{}^2} + \underline{s_{\sigma_p}{}^2} \phi^2 N_B{}^2 + \sigma_P{}^2 \underline{s_{\phi}{}^2} N_B{}^2 + \sigma_P{}^2 \phi^2 \underline{s_{N_B}{}^2} \tag{4.2}$$

where $s_{N_X}{}^2$, $s_{N_{XO}}{}^2$, $s_{\sigma_p}{}^2$, $s_{\phi}{}^2$, $s_{N_B}{}^2$ are the variances for the isotopic composition of isotope X at time t, at time $t = 0$, the production cross-section, the particle flux, and isotope B respectively. In Equation 4.2 the underlined components are the elements being perturbed in the simulation. As variances, we can call these components linear functionals because the variances do not operate on one another. Furthermore, since they are linear functionals we only need to know the slopes of these functionals to characterize them. These slopes can be discovered using only a single perturbation in the original model's parameters.

3.1.2. Case 2: Pu-239 & Ru-105 Type Isotopes

In the Cs-137, case we assumed both of the potential loss terms$(\lambda_L + \sigma_A \phi) \to 0$. In this scenario, the production of Cs-137 occurs linearly with respect to time due to its lack of destruction mechanisms. For Pu-239 and Ru-105, one of the destruction mechanisms can be assumed to be zero while the other is comparatively large. Pu-239 has a large absorption cross-section but a very long half-life; conversely, Ru-105 has a relatively low absorption cross-section but a very short half-life (on the order of hours).

These conditions lead to near-linear isotopic production in a reactor with respect to time. Looking specifically at the Pu-239 case where $\lambda_L \to 0$, Equation 2 can be rewritten as:

$$N_X(t) = \frac{\lambda_P N_A + \sigma_P \phi N_B}{\sigma_A \phi}\left\{1 - e^{-(\sigma_A \phi)t}\right\} + N_{X0} e^{-(\sigma_A \phi)t} \tag{5}$$

Furthermore, using the methods outlined in Equation 3 we can derive each parameter's propagated uncertainty component:

$$s_{N_{XO}}^2 \left(\frac{\partial N_x}{\partial N_{XO}}\right)^2 = s_{N_{XO}}^2 \left(e^{-(\sigma_A \phi)t}\right)^2 \tag{6.1}$$

$$s_{N_A}^2 \left(\frac{\partial N_x}{\partial N_A}\right)^2 = s_{N_A}^2 \left[\frac{\lambda_P}{\sigma_A \phi}\left(1 - e^{-(\sigma_A \phi)t}\right)\right]^2 \tag{6.2}$$

$$s_{N_B}^2 \left(\frac{\partial N_x}{\partial N_B}\right)^2 = s_{N_B}^2 \left[\frac{\sigma_P}{\sigma_A}\left(1 - e^{-(\sigma_A \phi)t}\right)\right]^2 \tag{6.3}$$

$$s_{\lambda_P}^2 \left(\frac{\partial N_x}{\partial \lambda_P}\right)^2 = s_{\lambda_P}^2 \left[\frac{N_A}{\sigma_A \phi}\left(1 - e^{-(\sigma_A \phi)t}\right)\right]^2 \tag{6.4}$$

$$s_{\sigma_P}^2 \left(\frac{\partial N_x}{\partial \sigma_P}\right)^2 = s_{\sigma_P}^2 \left[\frac{N_B}{\sigma_A}\left(1 - e^{-(\sigma_A \phi)t}\right)\right]^2 \tag{6.5}$$

$$s_{\phi}^2 \left(\frac{\partial N_x}{\partial \phi}\right)^2 = s_{\phi}^2 \left[\frac{e^{-(\sigma_A \phi)t}\left(\lambda_P N_A\left(\sigma_A \phi t - e^{(\sigma_A \phi)t} + 1\right) + \sigma_A \phi^2 t(\sigma_P N_B - \sigma_A N_{XO})\right)}{\sigma_A \phi^2}\right]^2 \tag{6.6}$$

$$s_{\sigma_A}^2 \left(\frac{\partial N_x}{\partial \sigma_A}\right)^2 = s_{\sigma_A}^2 \left[\begin{array}{c} \dfrac{e^{-(\sigma_A \phi)t}\left(\lambda_P N_A\left(\sigma_A \phi t - e^{(\sigma_A \phi)t} + 1\right)\right)}{{\sigma_A}^2 \phi} - \\ \dfrac{\phi\left(\sigma_A \phi t(\sigma_A N_{XO} - \sigma_P N_B) + \sigma_P N_B\left(e^{(\sigma_A \phi)t} - 1\right)\right)}{{\sigma_A}^2 \phi} \end{array}\right]^2 \tag{6.7}$$

with the total variance, ${s_{N_X}}^2$, being a summation of each component. Although the contributions in Equation Set 6 are considerably more complex than those seen in Equation Set 4, the propagated variance functionals are again considered linear because they do not operate on one another. This linear nature allows each parameter's propagated variance to be calculated using perturbations.

3.1.3. Case 3: Xe-135 Type Isotopes

The previous two isotopic cases had either one or both of the destruction mechanisms assumed to be approaching zero. In Xe-135 type isotopes, both the absorption and decay loss mechanisms are considered relatively large. This makes the isotopic production of Xe-135 with respect to time obey a quadratic shape. Due to both destruction mechanisms being present, the production at later time-steps becomes less linear and plateaus. These factors prevent us from making any simplifying assumptions to Equation 2. Without any assumptions, the contribution to the total isotopic variance from each parameter's propagated uncertainty is:

$$s_{N_{XO}}^2 \left(\frac{\partial N_x}{\partial N_{XO}}\right)^2 = s_{N_{XO}}^2 \left(e^{-(\lambda_L+\sigma_A\phi)t}\right)^2 \tag{7.1}$$

$$s_{N_A}^2 \left(\frac{\partial N_x}{\partial N_A}\right)^2 = s_{N_A}^2 \left[\frac{\lambda_P}{\lambda_L+\sigma_A\phi}\left(1-e^{-(\lambda_L+\sigma_A\phi)t}\right)\right]^2 \tag{7.2}$$

$$s_{N_B}^2 \left(\frac{\partial N_x}{\partial N_B}\right)^2 = s_{N_B}^2 \left[\frac{\phi\sigma_P}{\lambda_L+\sigma_A\phi}\left(1-e^{-(\lambda_L+\sigma_A\phi)t}\right)\right]^2 \tag{7.3}$$

$$s_{\lambda_P}^2\left(\frac{\partial N_x}{\partial \lambda_P}\right)^2 = s_{\lambda_P}^2\left[\frac{N_A}{\lambda_L+\sigma_A\phi}\left(1-e^{-(\lambda_L+\sigma_A\phi)t}\right)\right]^2 \tag{7.4}$$

$$s_{\sigma_P}^2\left(\frac{\partial N_x}{\partial \sigma_P}\right)^2 = s_{\sigma_P}^2\left[\frac{\phi N_B}{\lambda_L+\sigma_A\phi}\left(1-e^{-(\lambda_L+\sigma_A\phi)t}\right)\right]^2 \tag{7.5}$$

$$s_{\phi}^2\left(\frac{\partial N_x}{\partial \phi}\right)^2 = s_{\phi}^2\left[\begin{array}{c}\dfrac{\sigma_A t\left(e^{-(\lambda_L+\sigma_A\phi)t}\right)(\lambda_P N_A+\sigma_P\phi N_B)}{\lambda_L+\sigma_A\phi}- \\ \dfrac{\sigma_A\left(1-e^{-(\lambda_L+\sigma_A\phi)t}\right)(\lambda_P N_A+\sigma_P\phi N_B)}{(\lambda_L+\sigma_A\phi)^2}+ \\ \dfrac{\sigma_P N_B\left(1-e^{-(\lambda_L+\sigma_A\phi)t}\right)}{\lambda_L+\sigma_A\phi}-\sigma_A N_{XO}t\left(e^{-(\lambda_L+\sigma_A\phi)t}\right)\end{array}\right]^2 \tag{7.6}$$

$$s_{\sigma_A}^2\left(\frac{\partial N_x}{\partial \sigma_A}\right)^2 = s_{\sigma_A}^2\left[\begin{array}{c}\dfrac{\phi t\left(e^{-(\lambda_L+\sigma_A\phi)t}\right)(\lambda_P N_A+\sigma_P\phi N_B)}{\lambda_L+\sigma_A\phi}- \\ \dfrac{\phi\left(1-e^{-(\lambda_L+\sigma_A\phi)t}\right)(\lambda_P N_A+\sigma_P\phi N_B)}{(\lambda_L+\sigma_A\phi)^2}+ \\ \phi N_{XO}t\left(e^{-(\lambda_L+\sigma_A\phi)t}\right)\end{array}\right]^2 \tag{7.7}$$

$$s_{\lambda_L}^2\left(\frac{\partial N_x}{\partial \lambda_L}\right)^2 = s_{\lambda_L}^2\left[\begin{array}{c}\dfrac{t\left(e^{-(\lambda_L+\sigma_A\phi)t}\right)(\lambda_P N_A+\sigma_P\phi N_B)}{\lambda_L+\sigma_A\phi}- \\ \dfrac{\left(1-e^{-(\lambda_L+\sigma_A\phi)t}\right)(\lambda_P N_A+\sigma_P\phi N_B)}{(\lambda_L+\sigma_A\phi)^2}+ \\ N_{XO}t\left(e^{-(\lambda_L+\sigma_A\phi)t}\right)\end{array}\right]^2 \tag{7.8}$$

with the total variance, ${s_{N_X}}^2$, being a summation of each component. Similar to the previous two cases, the propagated variance functionals are linear and can be calculated using parameter perturbations. Through the three most common transmutation cases, we have proven that systematic uncertainties in burnup calculations can be rigorously propagated and quantified using perturbations.

3.2. Fuel Enrichment Perturbations & Linear Regression

In the previous section, we outlined how perturbations can be used to propagate and quantify systematic uncertainties in burnup calculations. In PHOENIX, the goal of our uncertainty quantification methodology is not just to quantify the uncertainties associated with burnup simulations alone, but to also create a function that can characterize the relative change in EOB quantities (such as gram compositions, reactor flux, burnup, and criticality) due to small perturbations in the initial input model. The use of perturbations allows us to effectively quantify the systematic uncertainty in the model parameters using the sensitivity analysis methods outlined in the previous subsection. This uncertainty quantification methodology is useful when considering the systematic uncertainty in the initial enrichment of fresh reactor fuel. In real systems, the measured enrichment of fuel is not exact and contains some degree of systematic uncertainty. Having a tool that can predict EOB reactor parameter quantities as a function of different fuel starting enrichments will greatly benefit the field of reactor burnup simulation.

Combining fuel enrichment perturbations with regression analysis techniques provides the ability to observe the propagated variance functional of the systematic uncertainty in the system. To test this theory, a sensitivity analysis was performed using fuel enrichment perturbations in MONTEBURNS 2.0 on three separate reactor configurations: the GODIVA model provided as benchmark for MCNP verification from LANL, the Flat Top Pu model provided as benchmark for MCNP verification from LANL, and the CANDU-type NRX research reactor. Burnup simulations for each of

these reactor types were performed with zero perturbations to create a control for our analysis. Perturbations were made to increase the initial enrichment of the fuel for each model in increments of 1 wt%, 2 wt%, 3 wt%, 4 wt%, and 5 wt% of the original fissile isotopics. For example, perturbing the initial enrichment of the NRX reactor's natural uranium fuel by five percent of its original enrichment would change the isotopics to those seen in Table 1

Table 1. Perturbation of Initial Fuel Enrichment

NatU Fuel	Unperturbed	Perturbed*
U-234 wt%	5.400E-03	5.398E-03
U-235 wt%	7.114E-01	7.470E-01
U-238 wt%	9.928E+01	9.925E+01

*Perturbed at +5 wt% of initial enrichment of U-235

Results from the iterations on each model were compared to their respective unperturbed control cases. Parameters of interest included criticality, flux, burnup, activation product gram quantities, and actinide gram quantities. A regression analysis was performed on each of the above parameters using the six simulations for each model (control plus five iterations) to understand their relationship to fuel enrichment perturbations. With the control case as a starting point, the slope of the regression curve was used to interpolate parameter values at every time-step for any enrichment up to the maximum perturbed enrichment. Using the example from Table 1 above, this method would interpolate the criticality, flux, burnup, and gram quantities for varying initial fuel enrichments up to five weight percent of the measured enrichment at every time-step simulated. The results of the GODIVA reactor configuration and their associated

regression functionals can be seen in Figures 2-8. Many of the gram quantities for "Case 1" and "Case 3" isotopes remained constant between enrichment perturbations. Looking at gram compositions for Xe-135 in Figure 8 for example, the difference in gram quantity calculated was sufficiently small enough that statistical effects from the Monte Carlo simulations became important.

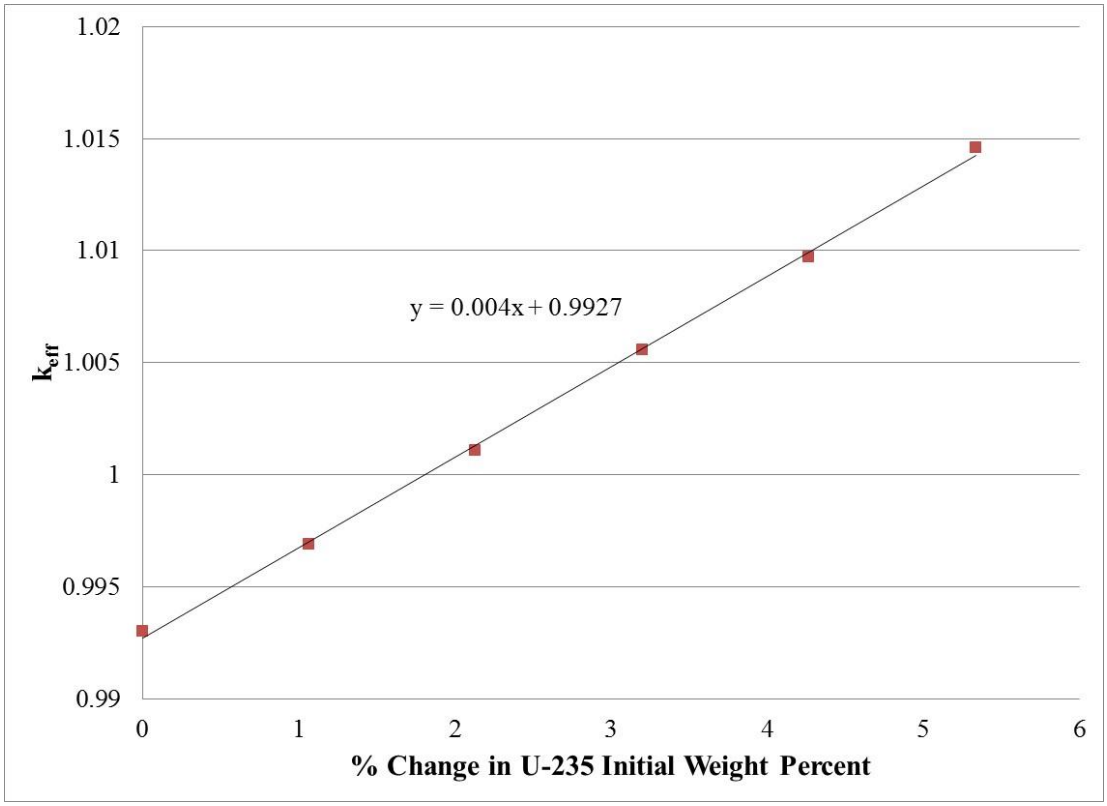

Figure 2. GODIVA criticality versus perturbation of +1-5 wt% of U-235.

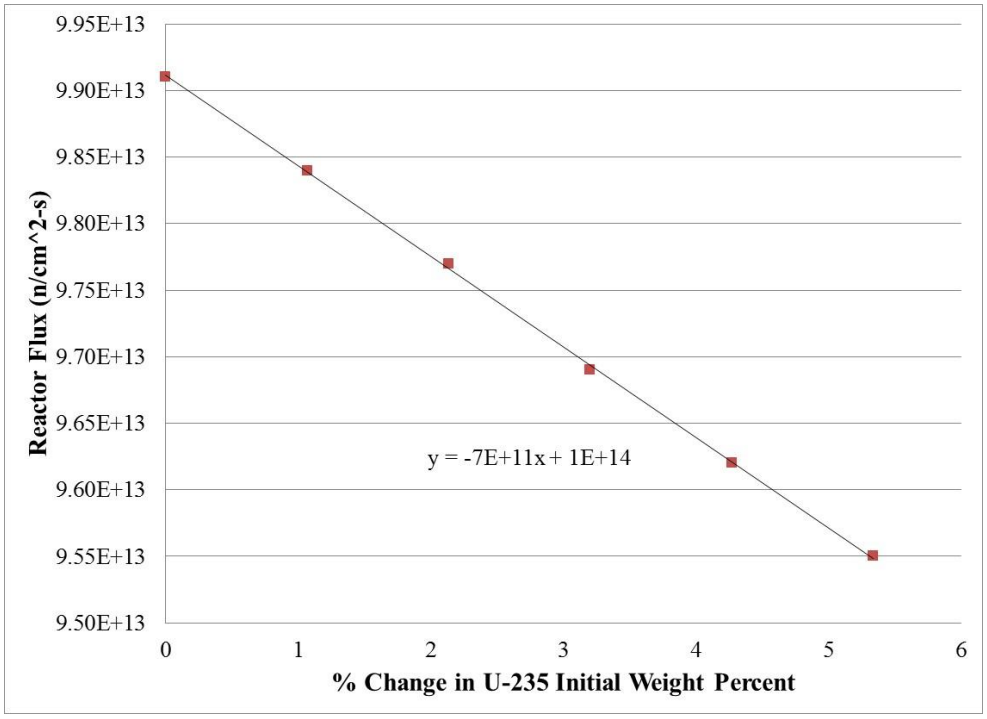

Figure 3. GODIVA reactor flux versus perturbation of +1-5 wt% of U-235.

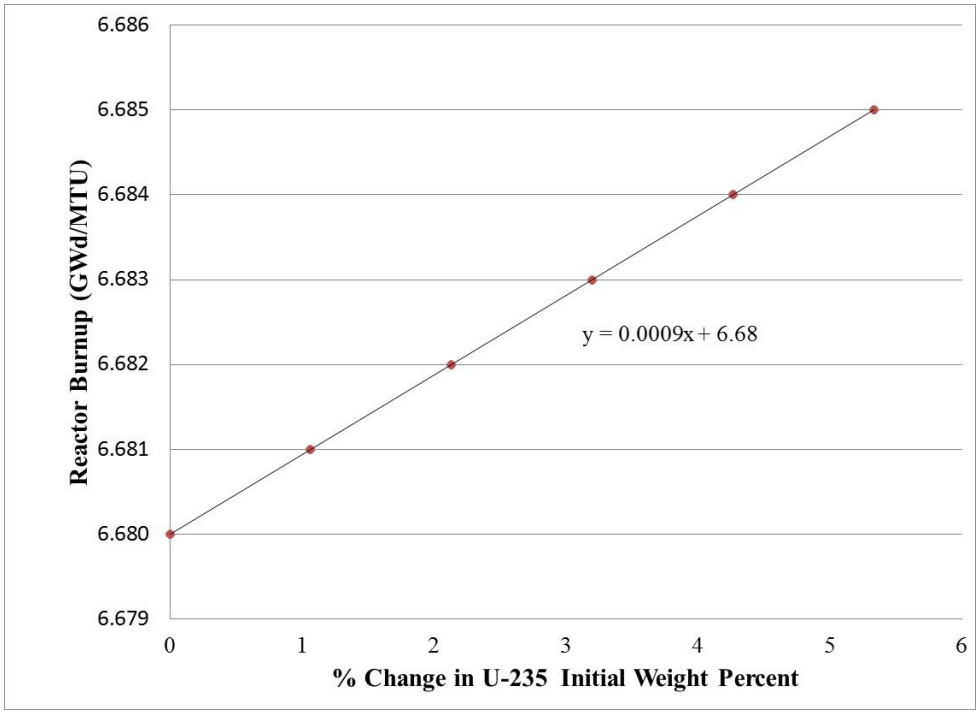

Figure 4. GODIVA reactor burnup versus perturbation of +1-5 wt% of U-235.

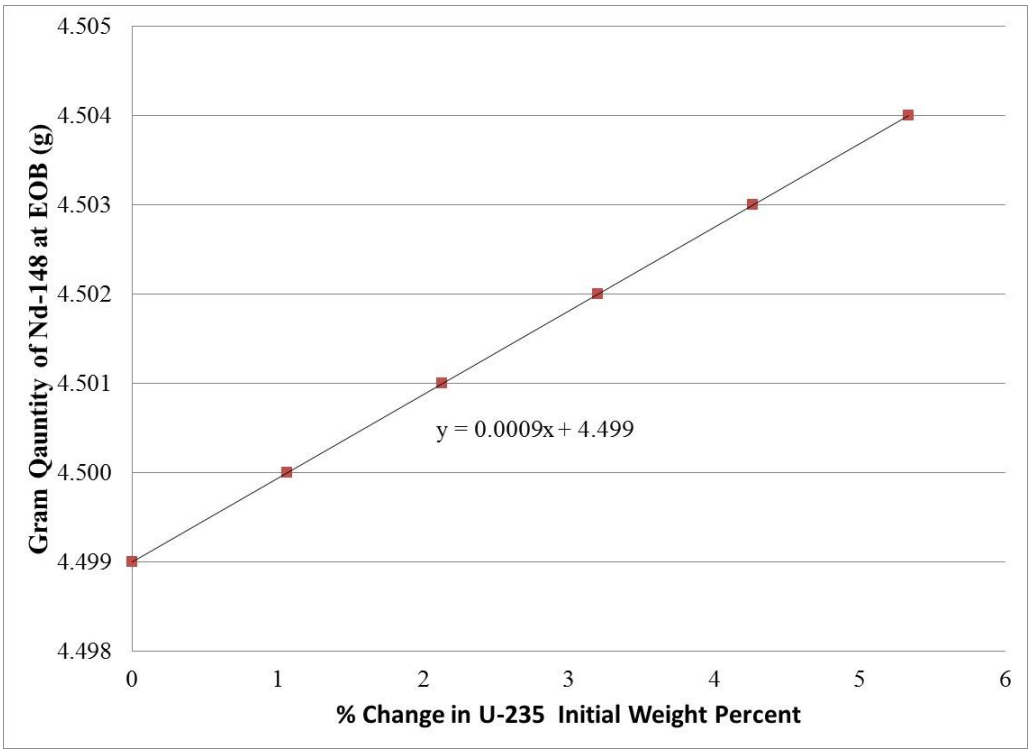

Figure 5. GODIVA Nd-148 production at EOB versus perturbation of +1-5 wt% of U-235. Nd-148 is a "Case 1" isotope.

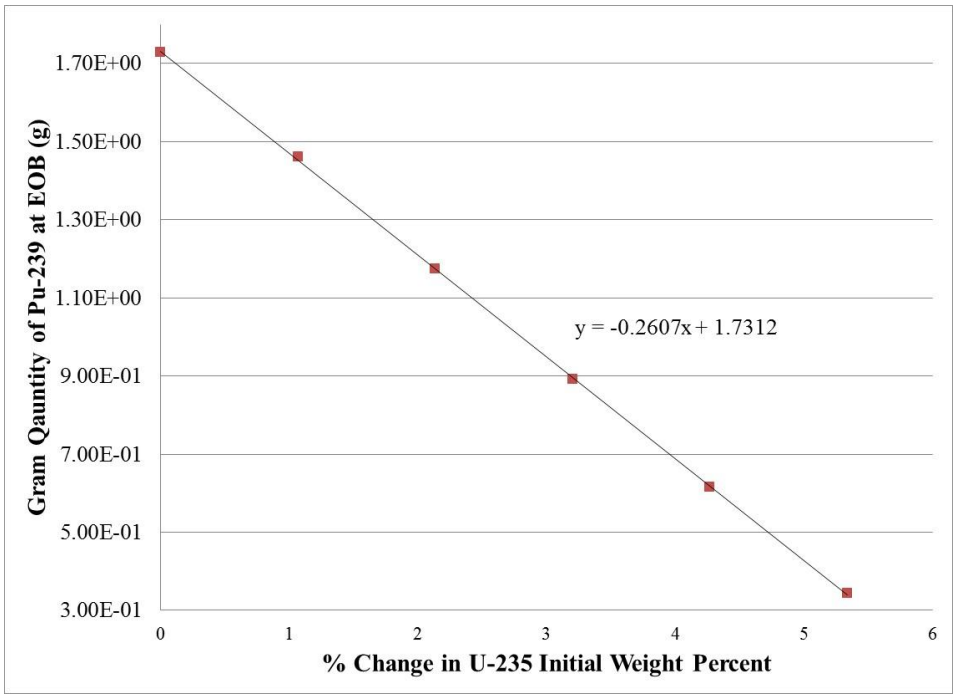

Figure 6. GODIVA Pu-239 production at EOB versus perturbation of +1-5 wt% of U-235. Pu-239 is a "Case 2" isotope.

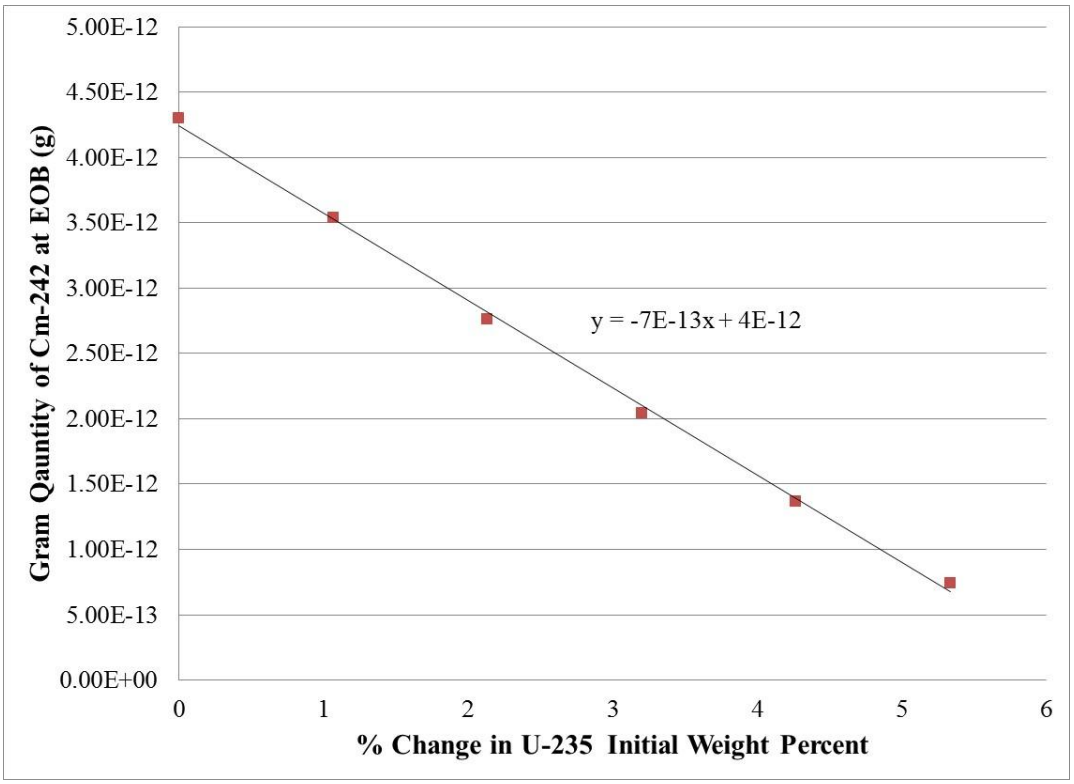

Figure 7. GODIVA Cm-242 production at EOB versus perturbation of +1-5 wt% of U-235. Cm-242 is a "Case 3" isotope.

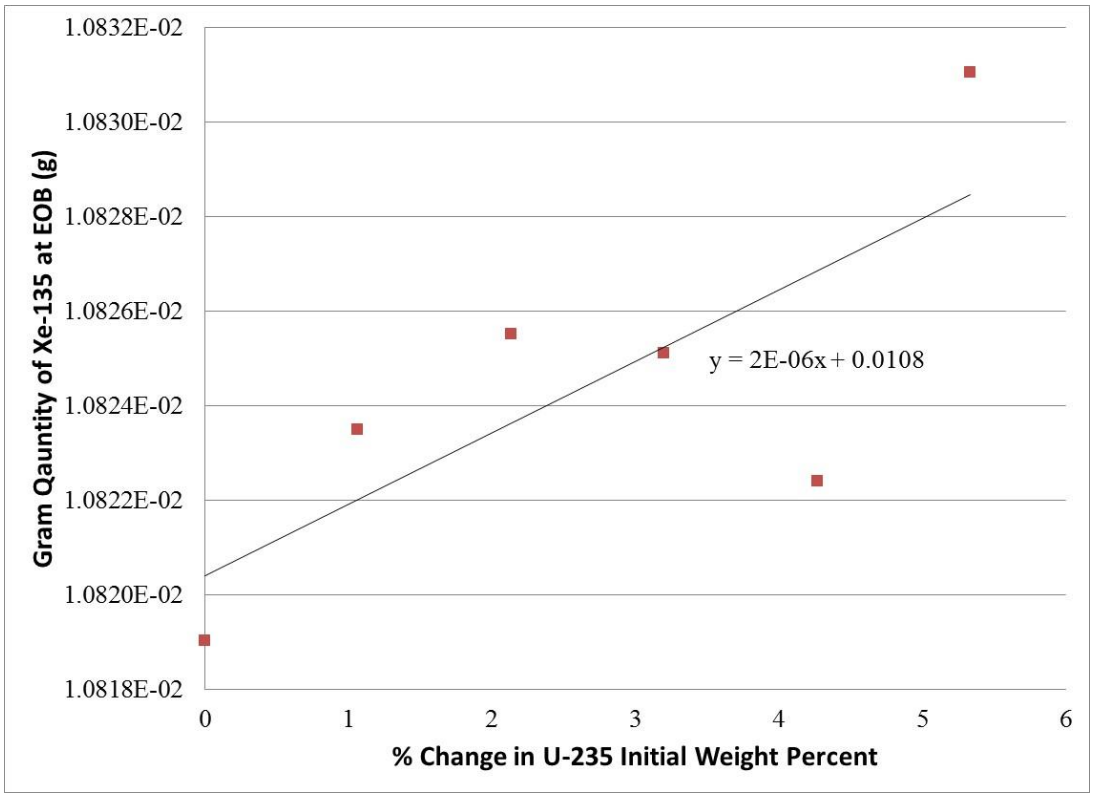

Figure 8. GODIVA Xe-135 production at EOB versus perturbation of +1-5 wt% of U-235. Xe-135 is a "Case 3" isotope.

For all reactor configurations, it was determined that with small enough perturbations (less than 20 wt%) the systematic uncertainty in each parameter could be quantified and interpolated using linear regression. The interpolated parameters for the linear regression are:

$$y_{interpolated} = y_{control} + \frac{\sum_i(\overline{x}-x_i)(\overline{y}-y_i)}{\sum_i(\overline{x}-x_i)^2} x_{desired} \quad (8)$$

where $y_{interpolated}$ is the interpolated simulation parameter of interest, $y_{control}$ is the control parameter value with no perturbed enrichment, $x_{desired}$ is the desired

enrichment, $\overline{x}$ is the calculated average enrichment between all perturbation iterations, x_i is the enrichment at each iteration i, $\overline{y}$ is the average parameter value from all perturbation iterations, and y_i is the parameter value at each enrichment iteration.

To verify the rigorousness of the calculated regression function, 20 separate simulations containing random starting fuel enrichment perturbations between ±3 wt% were performed on the GODIVA model in MONTEBURNS 2.0. The starting fuel enrichment and the other major parameters of interest were averaged over the 20 simulations. The averages of the initial fuel enrichment and major reactor parameters over the 20 simulations was compared to interpolated parameters calculated using linear regression methods on the GODIVA model. Some of these results can be seen in Table 2.

Table 2. GODIVA Regression Analysis Comparing Simulated Values to Interpolated Values at the End of Time-step One

	Simulation Average	**Regression Prediction**	**% Difference**
k_{eff}	1.000E+00	9.997E-01	0.03%
Flux (n/cm^2-s)	9.827E+13	9.827E+13	0.00%
Burnup (GWd/MTU)	1.908E+00	1.909E+00	-0.03%
Nd-148 (g)	5.621E-01	5.622E-01	-0.01%
Pu-239 (g)	2.081E-01	2.083E-01	-0.11%
Cm-242 (g)	1.193E-15	1.176E-15	1.45%
Xe-135 (g)	1.082E-02	1.082E-02	-0.01%

The percent difference between the average simulated parameters and the interpolated parameters was found to lie between 0.001% and 2.4%. A majority of the parameters were found to have differences of <1%, with the outliers being “Case 2” (see

Section 3.1.2) activation products with extremely low gram quantities such as Cm-242 and Cm-244. The small difference between these predicted and simulated values gives fidelity to our uncertainty quantification and interpolation methodology.

4. PHOENIX THEORY AND OPERATION

An ideal reactor burnup software package should include the capability to model complex geometric heterogeneities, have a low computational time, use updated cross-section and decay information, and include a mechanism for uncertainty quantification. Many of the reactor burnup codes discussed in Section 2.0 include some, but not all, of this criteria. MONTEBURNS 2.0, for example, contains all of the above components except for uncertainty quantification. PHOENIX was developed similar to the MONTEBURNS 2.0 package, but includes uncertainty quantification. Like MONTEBURNS 2.0, PHOENIX is also a "linkage" code. The major advantage to developing a "linkage" code is that it connects software that has been thoroughly benchmarked for both errors and accuracy. Another advantage to creating a "linkage" code is that PHOENIX can be operated without requiring detailed training in either the transport or depletion software being linked. [64]

PHOENIX uses MCNP6 for neutron transport calculations even though its computational cost, relative to deterministic transport solutions, is high. MCNP6's capability to model complex systems offers a large advantage when compared to deterministic transport solvers. In PHOENIX, MCNP6 was "linked" to ORIGEN-S and COUPLE from the SCALE6.1 package. ORIGEN-S was chosen because it provides accurate depletion calculations using time efficient deterministic methods. Similarly, the use of COUPLE allowed for the creation of problem dependent cross-section libraries for use in ORIGEN-S which increased burnup calculation accuracy. In this section the

theory behind the development and operation of PHOENIX will be discussed. The burnup parameters PHOENIX calculates, as well as the uncertainty quantification methodology used in PHONEIX, will be outlined in detail.

4.1. Description of PHOENIX

PHOENIX is a computer program written exclusively in C++ for UNIX operating systems. PHOENIX contains 18 separate modules linked together by the file main.cpp. PHOENIX is capable of calling a multiprocessing MCNP6 executable, but it must run SCALE processes chronologically. There are no disadvantages to running both COUPLE and ORIGEN-S serially since both codes are deterministic and have low computational time; however, running MCNP6 in parallel greatly reduces computational time. In order to use PHOENIX, the user must provide two separate input files: an MCNP6 input deck and a PHOENIX input deck. The PHOENIX input deck outlines reactor parameters and provides burnup information, perturbation information, and isotope tally information.

PHOENIX begins operation by executing the provided MCNP6 input deck to gain material compositions and system parameters for the input model. Burnup and material tally information provided by the PHOENIX input file are added to the MCNP6 input deck, and the input deck is executed again to calculate one-group problem dependent cross-sections, neutron fluxes, and neutron flux spectrums for each material burned. The neutron flux spectrum and one-group interaction cross-sections provided by MCNP6 are input into COUPLE to create a problem dependent cross-section library used by ORIGEN-S for each material. COUPLE uses the neutron flux spectrum to create

neutron activation cross-sections for all isotopes (see Section 4.1.1). The neutron flux spectrum must be entered in either 44, 49, 200, or 238 groups. Tallying 27 or 238 neutron energy groups in MCNP6 for every material, for every time-step, adds significant computational time to the simulation. Therefore, an assumption is made that the neutron flux spectrum remains constant throughout burnup. A 44 group neutron energy tally is used in the initial time-step's MCNP6 input deck, and a standard five group energy tally is used in all subsequent time-steps. To maintain statistical consistency between the initial time-step with more numerous energy bins, and later time-steps with fewer energy bins, the number of source particles simulated for the initial time-step is multiplied by ten.

After COUPLE uses the 44 group neutron energy spectrum and one-group cross-sections to generate a binary cross-section library, ORIGEN-S deterministically solves depletion and decay problems using the neutron flux provided by MCNP6. At the end of an ORIGEN-S run the compositions for all materials are stored in a binary library format. In subsequent time-steps PHOENIX creates ORIGEN-S input decks that use material compositions from the previous time-step's composition library. For this reason a single composition file is created for every material at the initial time-step, and appended at every future time-step. Contrarily, a new ORIGEN-S cross-section library from COUPLE is created at every time-step. Previous versions of ORIGEN, like ORIGEN-2.2 used in MONTEBURNS 2.0, used pre-generated cross-section libraries of common reactor configuration. Since these cross-section libraries were not problem dependent, MONTEBURNS 2.0 added an additional predictor step to the initial time-

step of every simulation. The predictor step used by MONTEBURNS 2.0 to create an accurate cross-section library was derived from the predictor-corrector method. [34, 65] The predictor step entailed re-simulating the entire time-step which has the potential to create significant additional computational time. The predictor-corrector method is also used in PHOENIX, but to a lesser degree (See Section 4.5) It is important to note that although the number of simulated particles in the initial time-step of a PHOENIX run is multiplied by ten, re-simulating the entire first time-step in MONTEBURNS 2.0 has the capability to add more computational time, relative to the initial time-step in PHOENIX, if the input model is complex. A flow chart of how PHOENIX uses MCNP6, COUPLE, ORIGEN-S, and the predictor-corrector method can be seen in Figure 9.

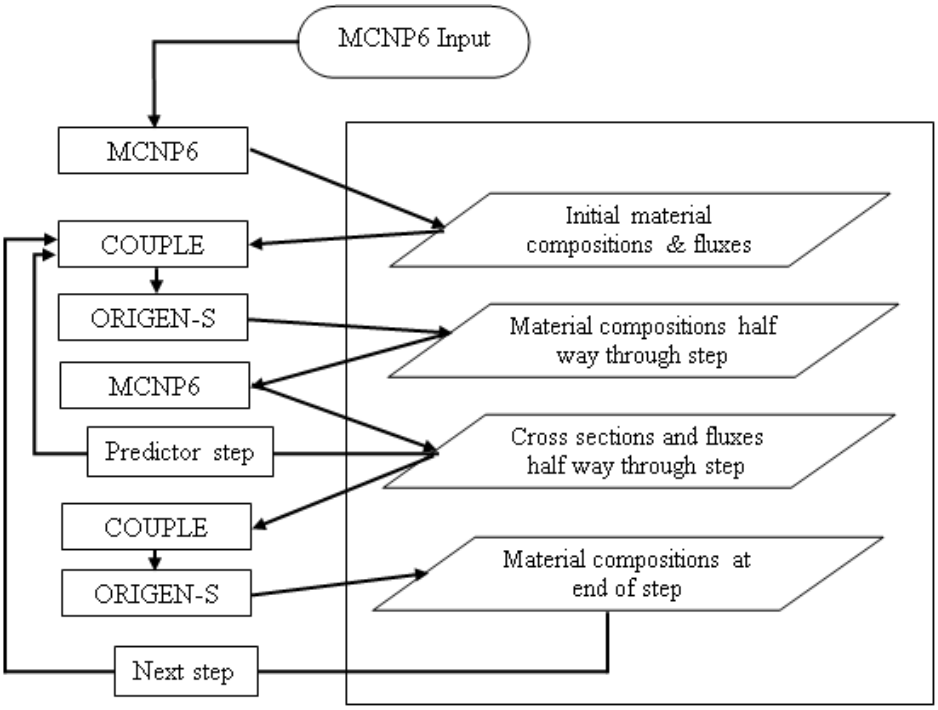

Figure 9. A flow chart of how PHOENIX uses MCNP6, COUPLE, ORIGEN-S, and the predictor-corrector method

4.1.1. Metastable Isotope Treatment

Accurately accounting for metastable isotopes in burnup software is a difficult process. Some isotopes have activation cross-sections with large uncertainties, others have half-lives that makes them difficult to track. In order to track every metastable isotope in previous linkage codes, a large number of additional tallies in MCNP6 would be required, and at least one predictor step at every burnup time-step would need to be performed. The first predictor step would be used to determine if isotopes are deemed important (See Section 4.5) in that particular time-step. Every one group cross-section calculated by MCNP has every activation level cross-section included within it, but not every activation level is available in the ORIGEN cross-section libraries. The predictor step is needed to determine which isotopes are deemed important for that time-step, and to discern what activation level cross-sections ORIGEN contains for that particular isotope. For every deemed important activation cross-section in ORIGEN, an additional interaction tally would be required in the full MCNP simulation of that time-step. Tallying activation cross-sections for every isotope, in every material, at every time-step adds significant computational time to the simulation. When comparing the additional computational time to the accuracy gained by quantifying every isotopic metastable state, the increased accuracy for the average user is not worth the time.

The advantage to using COUPLE to generate ORIGEN-S cross-section libraries in PHOENIX is that COUPLE calculates neutron activation cross-sections automatically. In PHOENIX, MCNP6 calculates the total interaction cross-section for a particular reaction type, including that reaction's activation cross-sections, at every time-

step. These total cross-sections and the 44 group neutron flux spectrum are used in COUPLE to create ORIGEN-S libraries containing activation cross-sections for every ORIGEN-S metastable state automatically. This method drastically improves the capability of quantifying metastable isotopes when compared to previous linkage codes, while minimizing computational costs.

4.2. Implementation of Uncertainty Quantification in PHOENIX

The component that sets PHOENIX apart from other reactor burnup codes is that it has the built-in ability to quantify systematic uncertainty. As mentioned in Section 3, PHOENIX quantifies systematic uncertainties by introducing and propagating perturbations to the initial fuel enrichment. In PHOENIX, the user can add a perturbation to the initial fuel's starting enrichment on the PHOENIX input deck. The user must enter the isotope they desire to be perturbed, as well as the amount (percentage of the initial starting weight percent) they would like to perturb it.

If a perturbation is entered on the PHOENIX input deck, an entirely new material in MCNP6 and ORIGEN-S is created for the perturbation before the initial burnup time-step. The isotopic compositions of the new materials are altered using the perturbation value from the PHOENIX input deck. If the isotope being perturbed exists in the material, the perturbed amount, as a percentage of the isotopes original weight percent in the system, is directly added (or subtracted) to the isotope's original weight percent:

$$x_{perturbed} = x_{unperturbed} + \frac{x_{unperturbed} * p}{100} \tag{9}$$

where $x_{perturbed}$ is the newly perturbed weight percentage for the isotope specified in the PHOENIX input deck, $x_{unperturbed}$ is the original weight percent of the isotope, and p is the perturbation value entered on the PHOENIX input deck. All other isotopes in the material are reduced (or increased) using a weighted average approach:

$$w_{perturbed} = w_{unperturbed} - \frac{\frac{x_{unperturbed} * p}{100} * w_{unperturbed}}{1 - x_{unperturbed}} \qquad (10)$$

where $w_{perturbed}$ is the isotope's perturbed weight percent and $w_{unperturbed}$ is the isotope's original weight percent.

To allow for multiple perturbations while running only a single simulation, the PERT and KPERT features are used in MCNP6. If a criticality problem in MCNP6 is selected (kcode run), the KPERT card is added to the MCNP6 deck which calculates the total change in system criticality due to the introduced perturbation. The PERT card allows MCNP to tally fluxes and interaction rates in the perturbed and unperturbed materials in the same simulation. Applied to burnup in PHOENIX, the fluxes and interaction rates from both the perturbed and unperturbed cases would be input into separate ORIGEN-S input decks. The depletion calculations on each of these cases would be performed individually, and the updated number densities for both cases would be put into the next time-step's MCNP deck. This process would be repeated until EOB was reached. This essentially allows unperturbed and perturbed burnup calculations to run in parallel in a single burnup simulation. More importantly, the use of the PERT card

not only provides a measure of uncertainty at each time-step, it also propagates that uncertainty through all of the remaining time-steps. A better representation of this process is seen in Figure 10.

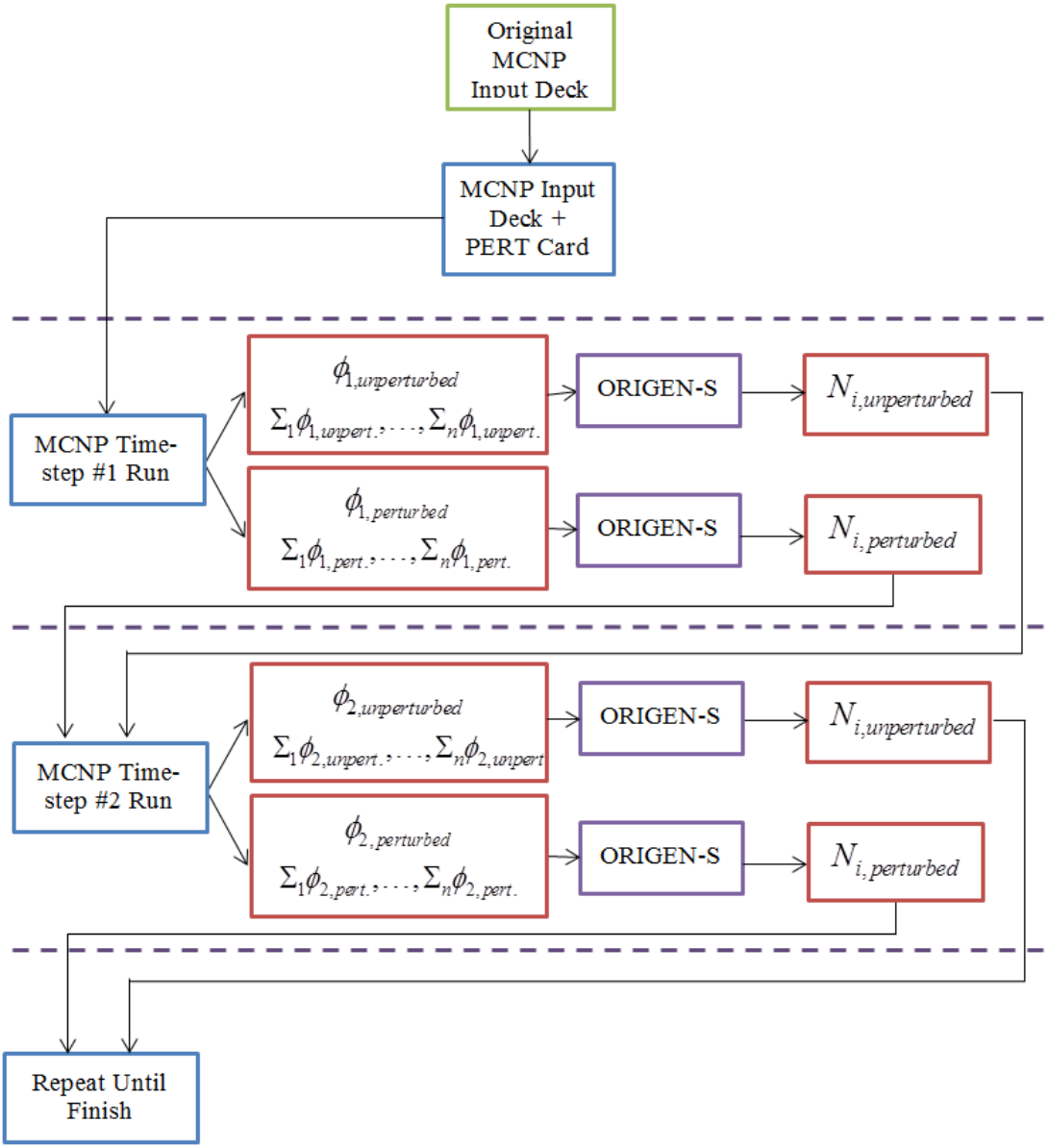

Figure 10. Proposed flow of PHOENIX operating using MCNP6's PERT card.

A linear regression analysis is also included in PHOENIX operation using unperturbed and perturbed gram quantities for each isotope of interest using Equation 8. The y-intercept ($y_{control}$ in Equation 8) and the slope (everything multiplied times $x_{desired}$ in Equation 8) for every isotope are printed in an additional output file with the extension ".regr". Using this file the user can interpolate gram quantities at every time-step for fuel perturbations up to the perturbation input by the user.

4.3. Calculated Values

The calculations performed by PHOENIX are very similar to those performed by MONTEBURNS 2.0 since similar versions of software are used by each package. [34] Calculations in PHOENIX are divided into six different categories: recoverable energy per fission, flux normalization, reactor physics constants, effective multiplication factor, power, and importance fraction.

4.3.1. Recoverable Energy per Fission

The user has two options when entering the recoverable energy per fission on the PHOENIX input deck. The first option is to enter a positive Q-value, at which case PHOENIX uses this Q-value as the average Q-value in the system for all calculations at every time-step throughout the burnup simulation. The second options is for the user to enter an estimated Q-value for U-235 (preceded by a negative sign), and have PHOENIX calculate an energy-dependent average Q-value at every time-step throughout the simulation. The energy-dependent Q-value is calculated using the Madland polynomial expansion, and the polynomial expansion coefficients seen in Table 1 are

from ENDF/B-VII MT=458 reactions. [66] The total amount of recoverable energy produce per fission is:

$$Q_{fiss} = |Q_{U-235}| * Q_{rat} \tag{11}$$

where Q_{fiss} is the total amount of recoverable energy produced per fission, Q_{U-235} is the recoverable energy per fission for U-235 input by the user, and Q_{rat} is the energy-dependent weighting factor to include recoverable fission energy for all actinides present:

$$Q_{rat} = \frac{\sum_{j=1}^{g}\sum_{i=1}^{n} f_{rat}(i)E_{rat}(j)(c_0(i) + c_1(i)E(j) + c_2(i)E(j)^2)}{Qr_{U-235}} \tag{12}$$

where g is the total number of energy groups in the system (5 or 44), n is the total number of actinides in the material (calculated by ORIGEN-S), $E(j)$ is the neutron energy at group j, c_0, c_1, c_2 are the Madland coefficients seen in Table 3 for isotope i, Qr_{U-235} is the actual recoverable energy from U-235 fission (193.4834 MeV), $E_{rat}(j)$ is the weighted neutron energy normalization for group j calculated using Equation 13, $f_{rat}(i)$ is the ratio of fissions resulting from isotope i to total number of fissions calculated using Equation 14:

$$E_{rat}(j) = \frac{\phi(j)}{\sum_{j=1}^{m} \phi(j)} \tag{13}$$

$$f_{rat}(i) = \frac{\sigma_f * n(i)}{\sum_{i=1}^{n} \left(\sigma_f * n(i)\right)} \tag{14}$$

where $\phi(j)$ is the neutron flux (n/cm^2-s-MeV) in energy group j (calculated by MCNP6), σ_f is the spectrum-averaged one-group microscopic fission cross-section of isotope i (calculated by MCNP6), and $n(i)$ is the number density of isotope i.

Using the above parameters we can calculate the average energy produced per fission for the entire system:

$$Q_{ave} = \frac{\sum_{k=1}^{m} \left(Q_{fiss}^{k} \phi^{k} \Sigma_f^{k} V^{k}\right)}{\sum_{k=1}^{m} \left(\phi^{k} \Sigma_f^{k} V^{k}\right)} \tag{15}$$

where Q_{ave} is the average recoverable energy per fission for the entire system (MeV), Q_{fiss}^{k} is the average recoverable energy per fission in material k (MeV), ϕ^{k} is the neutron flux in material k (calculated by MCNP6), Σ_f^{k} is the macroscopic fission cross-section in material k (cm^{-1}), V^{k} is the volume of all cells containing material k (cm^3), and m is the number of materials being analyzed (input by user).

Table 3. Madland Polynomial Expansion Coefficients (MeV) **[66]**

Isotope	c_0	c_1	c_2	Isotope	c_0	c_1	c_2
Th-227	1.823E+02			Pu-239	1.989E+02	-1.473E-01	-1.700E-03
Th-229	1.838E+02			Pu-240	1.995E+02		
Th-230	1.906E+02			Pu-241	2.020E+02		
Th-232	1.885E+02			Pu-242	2.016E+02		
Pa-231	1.856E+02	-1.146E+00	3.700E-03	Pu-244	1.993E+02	-1.340E+00	8.938E-03
Pa-233	1.857E+02	-1.124E+00	3.056E-03	Am-241	2.020E+02		
U-232	1.846E+02			Am-242	2.057E+02	-1.331E+00	2.333E-03
U-233	1.910E+02			Am-241m	2.057E+02	-1.330E+00	2.317E-03
U-234	1.918E+02			Am-243	2.036E+02		
U-235	1.934E+02	-3.790E-02		Cm-242	2.026E+02		
U-236	1.945E+02			Cm-243	2.040E+02		
U-237	1.878E+02	-1.153E+00	5.700E-04	Cm-244	2.084E+02		
U-238	1.978E+02	-4.210E-02	4.206E-03	Cm-245	2.052E+02		
U-240	1.981E+02			Cm-246	2.105E+02		
Np-237	1.964E+02			Cm-248	2.087E+02		
Np-238	1.996E+02			Cm-249	2.090E+02	-1.389E+00	8.968E-03
Pu-237	2.014E+02	-1.334E+00	6.797E-03	Cf-251	2.134E+02		
Pu-238	2.004E+02	-1.204E+00	1.662E-03	Es-254	2.223E+02		

4.3.2. Flux Tally Normalization

For every ORIGEN-S depletion or decay simulation, the neutron flux is required. The flux provided by MCNP6 is normalized per fission neutron in "kcode" problems, or per source neutron in "nps" problems. [34] The total neutron flux is:

$$\phi = \phi_n * C \tag{16}$$

where ϕ is the total neutron flux normalized to system power(n/cm^2-s), ϕ_n is the neutron flux tally normalized per fission or source neutron (provided by MCNP6), and C is the neutron source term calculated in Equation 17, or 18.

When a criticality source problem is run in MCNP6 (kcode), the flux is normalized per fission neutron, and the value of k_{eff} and its associated error are found in the MCNP6 output file. [34] In a criticality problem the neutron source term is:

$$C = \frac{\upsilon * P * 10^6(\frac{W}{MW})}{\left(1.603 * 10^{-13}\ \left(\frac{J}{MeV}\right)\right) * k_{eff} * Q_{ave}} \tag{17}$$

where υ is the average number of neutrons produced per fission (calculated by Equations 19), P is the total power (MW) of the system input by the user, and k_{eff} is the effective multiplication factor calculated by MCNP6. If the user opts to run an "nps" source definition, the neutron source term is:

$$C = \frac{src * P * 10^6(\frac{W}{MW})}{\left(1.603 * 10^{-13}\ \left(\frac{J}{MeV}\right)\right) * f_{loss} * Q_{ave}} \tag{18}$$

where src is the weight of source neutrons calculated by MCNP6, and f_{loss} is the weight of neutrons to fission calculated by MCNP6.

The neutron source term contains criticality information (k_{eff}, or $\frac{src}{f_{loss}}$) to modify the computed value of the neutron flux in systems that are not at critical. For a "kcode" problem, the flux calculated by MCNP6 is normalized per fission neutron, which assumes that the number of neutrons that cause fission in the system modeled are

representative of how many fissions occur to produce the given steady-state power level. However, if the system is subcritical, then the flux normalized per fission neutron is only a fraction of the flux produced at steady-state. Dividing by the criticality information increases the value of the flux appropriately to account for all neutrons in a steady-state system. Similarly, the relative number of neutrons produced in a supercritical system is greater than in a reactor at steady-state, so the flux must be reduced to accurately reflect power production. [34]

4.3.3. Reactor Physics Constants

The average number of neutrons produced per fission, υ, is calculated slightly differently for perturbations compared to previous linkage burnup software. Previous software utilized the MCNP6 calculated criticality (k_{eff}) and neutron source and loss terms (src and f_{loss} respectively) to calculate υ. The uncertainty quantification method implemented in PHOENIX utilizes the PERT and KPERT cards from MCNP6 which prevent us from using source and loss terms in perturbations. Therefore, PHOENIX makes use of the track length criticality estimate tally (FM -6 -7). The drawback to using this method is that PHOENIX assumes all fissionable material in the system is burned/depleted by PHOENIX. If fissionable material exists in the MCNP6 model but are not specified in the materials in the PHOENIX input deck, the average number of neutrons may be slightly smaller. The average number of neutrons produced per fission is:

$$\upsilon = \sum_{i=1}^{m} \frac{RR_{TLCE}(i) * n(i)}{RR_{fiss}(i) \sum_{j=1}^{m} n(j)} \tag{19}$$

where RR_{TLCE} is the reaction rate for the track length criticality estimate in material i provided by MCNP6, and RR_{fiss} is the fission reaction rate in material i provided by MCNP6.

The number of neutrons produced per fission can be used to calculate the number of neutrons produced per neutron destroyed:

$$\eta = \frac{\upsilon\sigma_f + 2.0 * \sigma_{n,2n}}{\sigma_\gamma + \sigma_f + \sigma_{n,2n}} \tag{20}$$

where η is the number of neutrons produced per neutron destroyed, σ_f is the microscopic fission cross-section calculated by MCNP6, σ_γ is the (n,γ) microscopic cross-section calculated by MCNP6, and $\sigma_{n,2n}$ is the (n,2n) microscopic cross-section calculated by MCNP6.

4.3.4. Effective Multiplication Factor

The value of the effective multiplication factor (k_{eff}) is provided by MCNP6 in a criticality ("kcode") calculation. Conversely, k_{eff} must be calculated for an "nps" problem:

$$k_{eff} = \frac{(fmult - 1)}{\left(fmult - \frac{1}{v}\right)} \tag{21}$$

where $fmult$ is the net multiplication in the system calculated by MCNP6. The relative error associated with the effective multiplication factor using an "nps" problem is:

$$\sigma = \frac{\frac{\left\{[fmult * (1 + err) - 1] - k_{eff}\right\}}{k_{eff}}}{\left[fmult * (1 + err) - \frac{1}{v}\right]} \tag{22}$$

where σ is the relative error associated with the effective multiplication factor, and err is the relative error associated with net multiplication in the system (calculated by MCNP6). [34]

For criticality calculations with perturbations, the differential change in the criticality due to the perturbation is provided by MCNP6 using the KPERT card. The total change in multiplication factor due to perturbation is simply the summation of these differential terms added to the original multiplication factor provided by MCNP6. The relative error term is propagated using Equation 3.2. At this time PHOENIX is not capable of calculating the multiplication factor for perturbations in "nps" problems.

4.3.5. Power

The power produced by each material is:

$$P^k = \frac{\left(Q_{ave}\phi^k\Sigma_f^k V^k * 1.60219 * 10^{-13}(\frac{J}{MeV})\right)}{10^6(\frac{W}{MW})} \quad (23)$$

where P^k is the power in material k (MW).

4.3.6. Importance Fraction

The importance fraction in PHOENIX is a term directly borrowed from MONTEBURNS 2.0. When running a Monte Carlo burnup simulation the user has to weigh increased computational time versus accuracy. In PHOENIX, one-group cross-sections are calculated for all isotopes deemed "important" by the user. These are isotopes input in the PHOENIX input deck under the automatic tally section. One component of burnup accuracy is determining which isotopes to calculate spectrum-averaged one-group cross-sections for. The burnup feature in MCNPX, for example, calculates a one-group cross-section for every single isotope in CINDER90's library. Unfortunately for MCNPX, calculating a one-group cross-section for every single isotope in CINDER90's library doesn't always translate to improved accuracy. Some isotopes play a marginal role in affecting the neutron flux and energy spectrum in the system. For this reason, PHOENIX includes an importance fraction for determining if isotopes are "important" to the neutron flux and energy spectrum.

If an isotope contributes a fraction to the system neutron absorption, fission, mass, or atom density higher than the importance fraction, then the isotope is deemed "important," and a spectrum-averaged one-group cross-section is calculated in MCNP6. If any of the values calculated by Equations 24-27 are greater than the importance

fraction entered by the user on the PHOENIX input deck, the isotope is deemed important and tallies are created in MCNP6. [34]

$$f(\sigma_a)_i = \frac{gad_i * \sigma_{ai}}{\sum_{i=1}^{n}(gad_i * \sigma_{ai})} \tag{24}$$

$$f(\sigma_f)_i = \frac{gad_i * \sigma_{fi}}{\sum_{i=1}^{n}(gad_i * \sigma_{fi})} \tag{25}$$

$$w_i = \frac{gad_i * A_i}{\sum_{i=1}^{n}(gad_i * A_i)} \tag{26}$$

$$a_i = \frac{gad_i}{\sum_{i=1}^{n}(gad_i)} \tag{27}$$

where n is the total number of isotopes in the system, $f(\sigma_a)_i$ is the fraction of absorption that isotope i contributes to the system, gad_i is the amount of isotope i in the system, σ_{ai} is the microscopic absorption cross-section of isotope i, $f(\sigma_f)_i$ is the fraction of fission that isotope i contributes to the system, σ_{fi} is the microscopic fission cross-section of isotope i, w_i is the weight fraction of isotope i, a_i is the atom fraction of isotope i, and A_i is the atomic weight of isotope i.

4.4. PHOENIX Operation

The primary module of PHOENIX is main.cpp. During the course of a burnup simulation, main.cpp calls 17 additional functions and is responsible for file manipulation. Below in Figure 11 is a flowchart of how these functions are used, followed by a detailed description of each function's purpose.

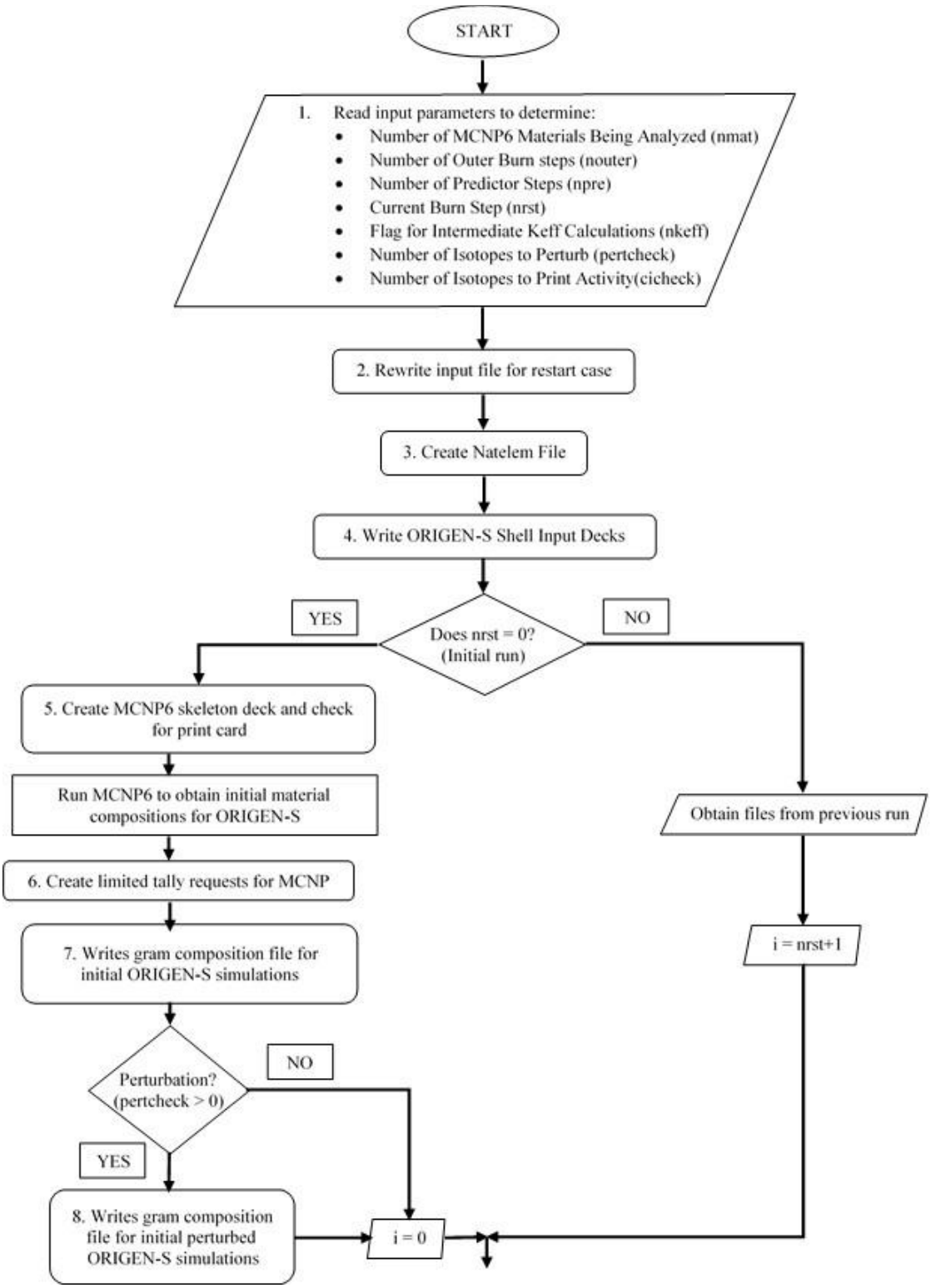

Figure 11. PHOENIX flow chart.

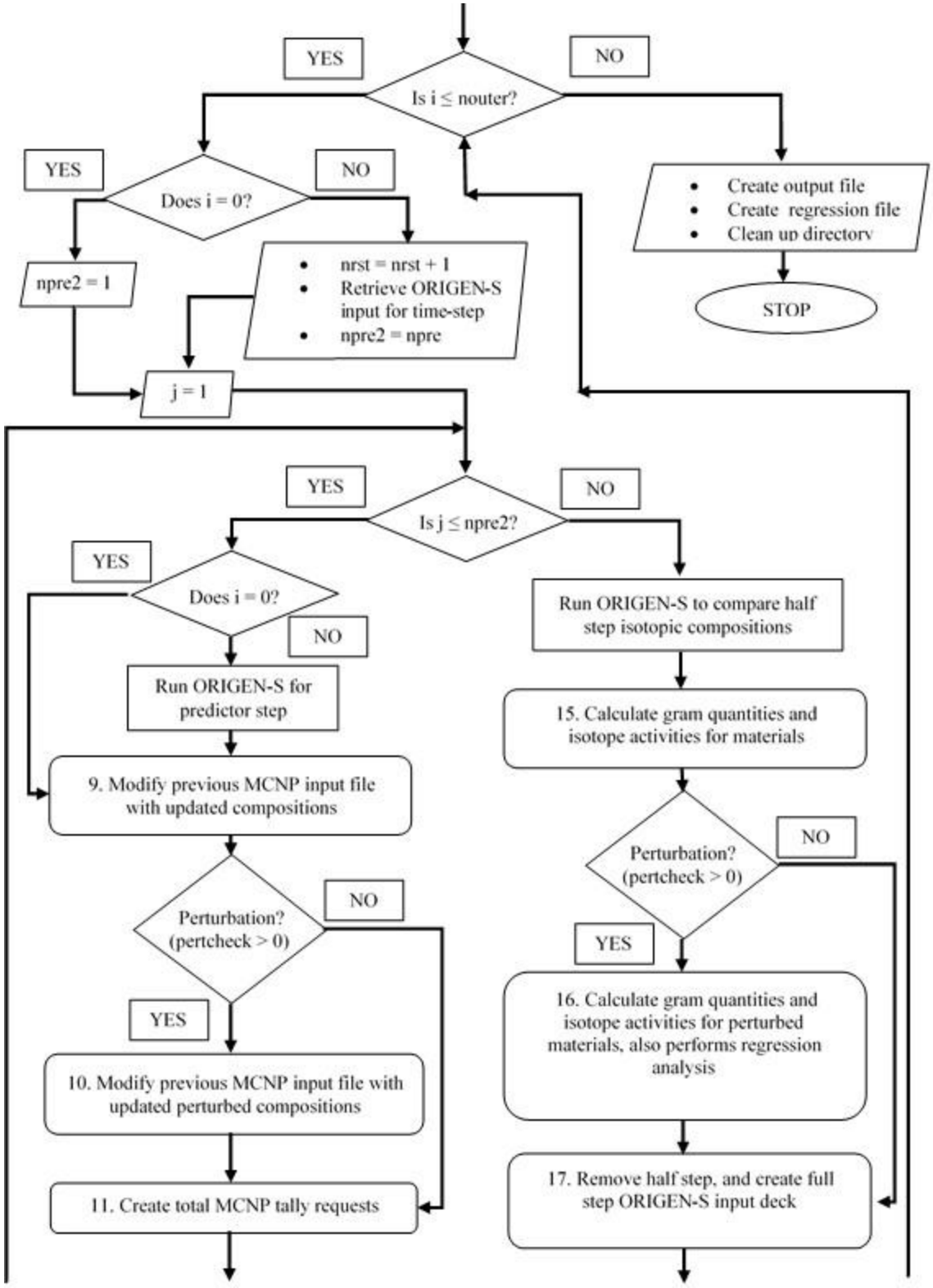

Figure 11. continued.

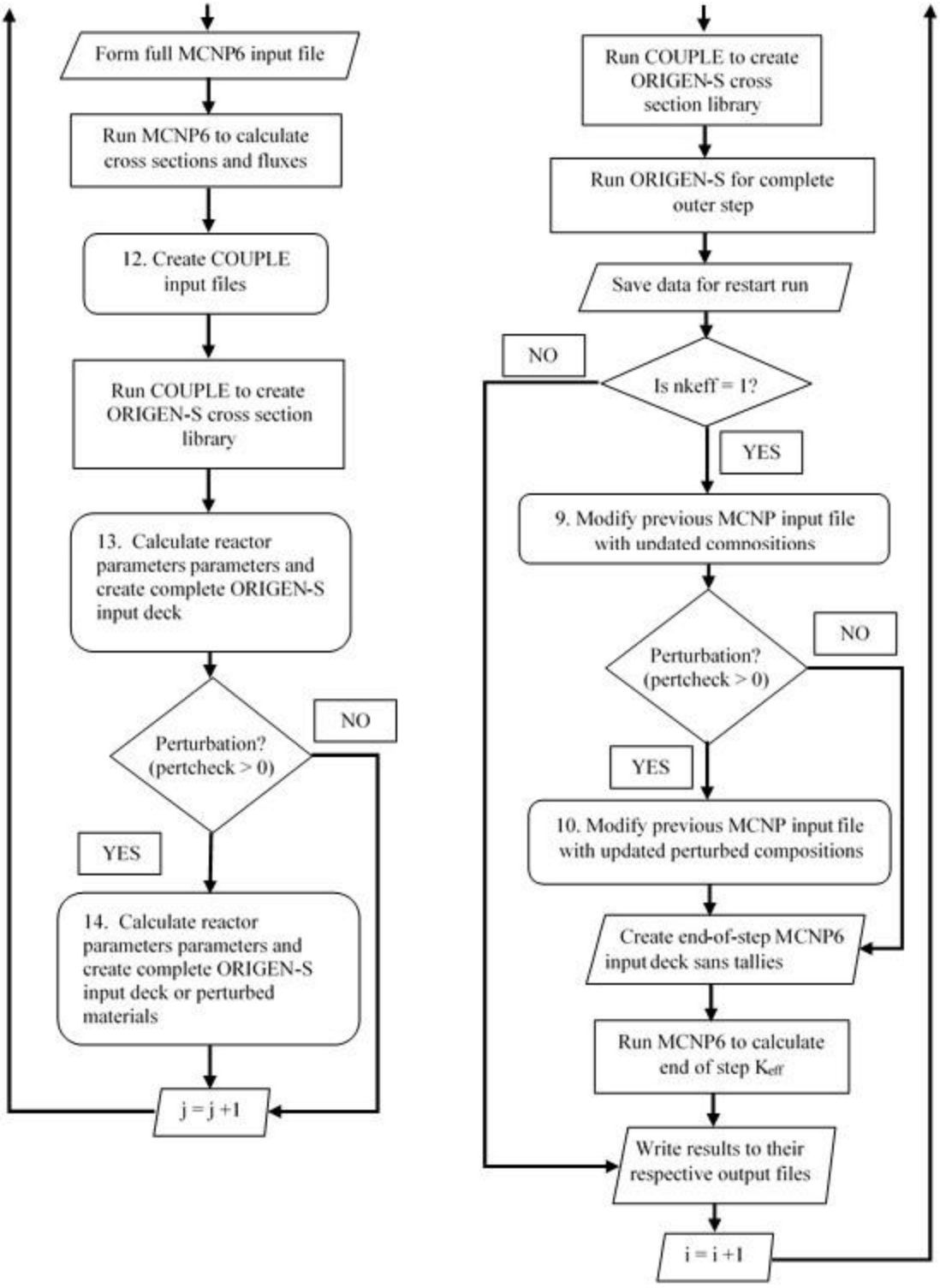

Figure 11. continued.

1. read input parameters,
2. rewrite input parameters to “phnx.inp” for a restart run,
3. create a file containing isotopic breakdowns for natural elements in MCNP6,
4. run MCNP6 once initially at the beginning of the program, this information is then used to create ORIGEN-S input files,
5. make sure a print card is present in MCNP6 input file, create a skeleton MCNP6 deck, create output files for PHOENIX output,
6. create limited tally requests for MCNP6,
7. write gram composition files for initial ORIGEN-S runs,
8. write gram composition files for initial ORIGEN-S perturbation runs,
9. modify MCNP6 input files with updated material compositions and densities,
10. modify MCNP6 input files with updated material compositions and densities for perturbed materials,
11. create total MCNP6 tally requests for all materials,
12. create COUPLE input decks for all materials,
13. use gram quantity and cross-section information to calculate important reactor parameters for use in ORIGEN-S,
14. use gram quantity and cross-section information to calculate reactor parameters in perturbed materials for use in ORIGEN-S,
15. calculate gram quantities and isotope activities for materials,
16. calculate gram quantities and isotopic activities for perturbed materials, also performs a regression analysis on perturbed and unperturbed gram quantities,

17. remove half burnup step in ORIGEN-S input decks and create full burn length input decks for the end of time-step ORIGEN-S simulations.

4.5. PHOENIX Input Files

4.5.1. PHOENIX Input

The following items are required on the PHOENIX input file:

- **Problem Description** - A single line with a problem description
- **Number of Materials to Burn in PHOENIX** – an integer giving the total number of MCNP6 materials to burn in PHOENIX
- **MCNP6 Material Number** - the MCNP6 material number of the material the user wants burned is input here. If the material number is entered as a negative integer, the material is not depleted in PHOENIX (although it is still decayed). For negative materials, PHOENIX calculates fluxes, flux spectrums, and interaction cross-sections at every time-step, but it does not deplete the material in ORIGEN-S. This is useful for calculating fluxes in regions not containing fissionable material, like a coolant channel. If a positive MCNP6 material number is entered, PHOENIX carries the material through depletion steps as well as MCNP6 transport calculations. An MCNP6 cross-section is also entered on the line (following the MCNP6 material number by a space). When a new material is deemed "important," PHOENIX opens the cross-section directory, "xslib," and searches for the "important" isotope at the specified cross-section. If that specific cross-section is not available in the cross-section directory, PHOENIX uses the first available cross-section for that isotope. If that cross-section for the "important" isotope is not in the cross-section directory, a

warning is issued notifying the user that the isotope was deemed important but not included due to lack of cross-section data.

- **MCNP6 Material Volume** - the volume of the MCNP6 materials being burned in PHOENIX is input here. If the volume is input as zero, the volume output from the initial time-step in MCNP6 for that material is included. If burning materials in a lattice, or a complex geometry exists such that MCNP6 does not calculate the volume, the volume must be calculated and entered in the PHOENIX input deck by the user.
- **Power of the System** – the total power of the system (in MWth).
- **Average Q-Value** – the average Q-value (in MeV) of the system. The user has two options when inputting the Q-value into a PHOENIX input deck. If the Q-value of the system being modeled is well understood by the user, the user may enter the total Q-value of the system by inputting the desired Q-value greater than zero. If the value is greater than zero, the Q-value entered will be used throughout the burnup simulation at every time-step to calculate the flux, power, and burnup in the problem. If the Q-value is not well understood by the user, the user may enter in an approximate Q-value as a negative number. PHOENIX will then use the flux spectrum and fission cross-sections in the system (provided by ORIGEN-S) to calculate an energy dependent system averaged Q-value via Equation 12.
- **Total Number of Days Burned** - the user has two options when entering the number of days burned. If the user would like a uniform burn, where the total number of days is divided evenly among burn steps, the user is asked to enter the

total number of days burned. If the user would like a non-uniform burn profile, or would like to include decay time-steps, the user is asked to enter in "0".

- **Total Number of Burn Steps** - if the number of days burned is greater than zero, then each burnup step is equal to the total number of days burned divided by the number of burnup steps.
- **Burnup Profile** - this section is only entered if the user decides to have a non-uniform burnup profile, or a decay time-step. If the number of days input by the user is equal to zero, the user is responsible for entering two pieces of information for every burnup step. The first is the number of days for that particular burnup step, and the second (separated by a space) is the total power fraction for that entire burnup step. If the user would like to operate the reactor at 100% of the power input by the user, the user should enter in the number of days burned at that particular step, followed by a space and then 1.0. Conversely, if the user strictly wants a decay step, a power fraction of 0.0 would be entered.
- **Total Number of Predictor Steps** - the number of predictor steps affects the problem accuracy. During the course of reactor operation, the isotopic compositions of the materials being burned change. To obtain the most accurate results, spectrum-averaged one-group cross-sections for a burn step should represent an average over the time interval. [34] To predict the cross-sections at the middle of the next time-step (where MCNP6 calculates fluxes and one-group cross-sections), ORIGEN-S uses the previous step's flux to solve the depletion equations halfway into the next time-step. Using these predicted isotopic compositions at the middle of the next

time-step, MCNP6 calculates fluxes and one group cross-sections that are taken as an average over the entire time-step. ORIGEN-S then uses these flux and cross-section values to solve the depletion equation over the length of the entire time-step. This method works well if the material isotopics and cross-sections predicted at the midpoint of the time-step are an accurate representation of the entire time-step. If the flux differs significantly between time-steps (affecting the predicted isotopics in the predictor ORIGEN-S run), or the length of time between time-steps is sufficiently long to have a large change in isotopic compositions, the results of the burnup simulation may be inaccurate. To increase accuracy, the user should reduce the length of burnup time-steps, which in most cases will avoid a large gradient in flux and isotopic compositions between time-steps.

The user also has the ability to add predictor steps in PHOENIX. If the initial cross-sections for a step are not accurate, then ORIGEN-S compositions halfway through the step may not be a good representation of the burn step. Thus, it is often beneficial to perform a "predictor" step to calculate cross-sections more than once at the midpoint of a time-step. The number of times a cross-section is calculated midway through the time-step is the number of predictor steps. [34, 65]

- **Step to Restart After** - if a PHOENIX simulation dies before completion, the user has the option to start another simulation using files previously generated by PHOENIX. The burnup time-step PHOENIX died on should be entered here. The user also has the ability to modify PHOENIX input files (such as MCNP6 and ORIGEN-S input decks) at a particular time-step after a run has completed. If the

user wants to simulate a change in cross-section or flux at a particular time-step, these values can be entered on their corresponding MCNP6 and COUPLE input decks. The user can enter the time-step on the PHOENIX input deck to start the simulation on (with the changed parameters), and PHOENIX will complete the run with the modified parameters. In order for this step to work correctly, all files created by the original PHOENIX simulation must be present in the same directory they were created in.

- **MCNP6 Executable** - this input line must contain the name and location of the MCNP6 executable. If the user decides to run MCNP6 in parallel, the corresponding number of processors selected by the user should be entered after the name and location. For example, to run an open-mpi job on MCNP6 with 10 processors the user should enter "`~/mcnp6.mpi 10`", where `~/` is the location of the MCNP6 executable, "`mcnp6.mpi`"is the name of the MCNP6 open-mpi executable, and 10 is the number of processors the user plans to run.
- **MCNP6 Data Location** - this input line is for the data path location of all MCNP6 data.
- **SCALE6.1 Executable** - this input line is for the location and executable name of SCALE6.1.
- **SCALE6.1 Data Location** - this input line is for the data path location of scale data.
- **Importance Fraction** - this value represents the lower limit for the importance of one isotope relative to the rest of the system based on results obtained from ORIGEN-S and MCNP6. [34] If an isotope's fraction of fission, absorption, mass, or

atom density is greater than the user entered importance fraction, the isotope is deemed "important." The "important" isotope is included in the next time-step's MCNP6 deck, and one-group cross-sections are calculated for that isotope. If the importance fraction input by the user is equal to zero, every isotope in ORIGEN-S with a corresponding MCNP6 reaction cross-section will be included in the next MCNP6 input deck. Conversely, if the importance fraction is set equal to one, only the elements specified by the user as "automatic tally" isotopes in the PHOENIX input deck will be tallied by MCNP6.

- **Flag for Intermediate Criticality Calculations** - this flag indicates whether end of time-step criticality calculations are performed. If a value of zero is entered, the only criticality calculation performed by MCNP6 is in the middle of the burnup time-step. If a value of one is input into the flag for intermediate criticality calculations, PHOENIX runs an additional MCNP6 calculation to find the criticality at the end of every burnup time-step. PHOENIX updates MCNP6 isotopic compositions using the corresponding end-of-step ORIGEN-S results from that time-step. In order to reduce the amount of time required by an additional MCNP6 simulation, and since cross-sections and fluxes are not needed at the end of a time-step, all tallies are removed from the MCNP6 input deck. The criticality is calculated in MCNP6 and output to the output file.
- **Number of Isotope Perturbations** - the total number of isotopes to perturb in the system.

- **Perturbation Information** - the user is responsible for entering two pieces of information for every perturbation. The first piece of information is the desired isotope to be perturbed. The input format for each isotope is in the MCNP format:

$$ZZZ * 100 + AAA \tag{28}$$

where ZZZ is the number of protons in the system, and AAA is the number of protons plus neutrons in the system. The user is also responsible for entering the total percentage to perturb the isotope (separated from the input isotope by a space). The percent entered on the PHOENIX input deck is entered as a function of the isotope's initial weight percent in a material (as seen in Section 4.2). The new isotopic compositions for each perturbed material are calculated via Equations 9 and 10. If the perturbation is large enough such that it forces the isotope's weight percent in the material to be greater than 100%, PHOENIX will warn the user and the perturbation will not be performed. Similarly, if the perturbation is small enough such that the density in the perturbed material changes by less than 1E-4 (grams/cm^3) relative to the unperturbed material, PHOENIX does not perform the perturbation.

- **Number of Printed Activities** - the total number of isotopes to print the activity (in Curies).
- **Isotopes to Print Activities** - the user enters the isotope in ORIGEN-S format:

$$(\mathrm{ZZZ} * 10{,}000 + \mathrm{AAA} * 100 + \mathrm{M}) \quad (29)$$

where M is the metastable state of the isotope (0 for ground level, 1 for first excited state, etc.).

- **Number and List of "Automatic Tally" Isotopes** - this integer represents the number of isotopes for which the user wants information about in the output file. The user must then enter each isotope in MCNP format (including cross-section) for that specific material. If an isotope is entered in the MCNP6 input deck, and specified as an "automatic tally" isotope, the cross-section provided on the MCNP6 input file will be used throughout the simulation. The process of entering the total number of isotopes to tally for a specific material, followed by which isotopes to "automatically tally," is repeated for all materials input by the user. Each isotope listed will be tallied in MCNP6, and cross-section and gram quantity information will be displayed in the output file.

4.5.2. Additional PHOENIX Input Files

After creating a PHOENIX input file and MCNP6 input, two additional files need to be located in the same directory to run PHOENIX without error. The first file is the cross-section file "xslib". This file contains cross-section information for MCNP6. This file is created by copying the "xsdir" file out of the MCNP data directory and renaming it to "xslib" in the simulation directory. Any set of MCNP cross-sections can be used by PHOENIX as long as the corresponding "xsdir" is renamed to "xslib," and placed inside the simulation directory. The second file PHOENIX needs in the

simulation directory is “amass.dat”. This file is provided with the PHOENIX source code and contains atomic masses for every isotope in MCNP6.

4.6. PHOENIX Output Files

After PHOENIX finishes execution, a file with the extension “.out” is created. This is the output file for the PHOENIX simulation and contains the results displayed below for each time-step:

- **PHOENIX MCNP k_{eff} Versus Time** - a list of all parameters affecting the simulation criticality. The first column is the time-step followed by the label “mid” or “end.” The label “mid” represents the parameters at the middle of the burnup time-step, and “end” represents parameters at the end of a time-step. This section also includes cumulative time in days, the multiplication factor (K_{eff}) and standard deviation, the burnup for the entire system (MWd/MT), υ (see Equation 19), and Q_{ave} (MeV - see Equation 15). If a perturbation is specified in the PHOENIX input deck, this section is repeated, and the corresponding results are displayed for every perturbation.
- **PHOENIX Transport History** – a list of important reactor parameters used in the solution to the burnup equations in ORIGEN-S. The calculated neutron flux (n/cm^2-s – see Equation 17 and 18), total fission cross-section for the material (cm^{-1}), the power produced in the material (MW – see Equation 23), the power density in the material (W/cc), and the burnup in each material (GWd/MTU). If a perturbation is specified in the PHOENIX input deck, this section is repeated and the corresponding results are displayed for every perturbation.

- **Neutron Information** – a list of all parameters representing neutron production and destruction in the simulation for every material. Neutron information is provided for both the total material, and the actinides alone. The microscopic cross-sections for radiative capture, fission, and (n,2n) are given (in barns), as well as the fission-to-capture ratio and η (see Equation 20).
- **Neutron Flux Spectrum** – a five group neutron flux spectrum is provided with energy groups between 0.1 eV, 1.0 eV, 100 eV, 100 KeV, 1 MeV, and 20 MeV.
- **PHOENIX One-group (n,γ) Cross-section** – a list of the One-group microscopic (n,γ) cross-section (barns). The number reported in this section is the total microscopic (n,γ) cross-section. This value is inserted into the COUPLE input file and is automatically separated into activation cross-sections if they exist.
- **PHOENIX One-group Fission Cross-sections** – a list of the one group microscopic fission cross-sections for every isotope (in barns).
- **PHOENIX Grams of Material at End-of-steps** – a list of the total gram quantities for every isotope at the end of burnup steps (in grams).
- **PHOENIX Activities (Ci) at End-of-steps** – if requested by the user in the PHOENIX input deck, this section lists the activities (in Ci) for the selected isotopes. It also lists the sum of the selected activities, as well as the total activity of the entire material.

An additional file with the extension ".regr" is generated if a perturbation is performed. The output file with the extension ".regr" contains information for reconstructing linear regression functions for gram concentrations at every burnup time-

step, for every isotope, for every material. If the user wishes to interpolate gram quantities for initial fuel perturbations up to the input PHOENIX perturbation, they simply need to multiply the "'X' Regression Coefficient" by the desired enrichment and add the value labeled "Y-intercept" as seen in Equation 8.

5. PHOENIX VALIDATION STRATEGY

The validation of PHOENIX was accomplished through code-to-code comparisons, validation to experimental data, and a perturbation and regression analysis. As mentioned in Section 3.0, PHOENIX was developed similar to MONTEBURNS 2.0. Both pieces of software "link" versions of MCNP to ORIGEN. The code-to-code validation of PHOENIX was performed by modeling four different reactor configurations in PHOENIX and MONTEBURNS 2.0. MONTEBURNS 2.0 was a good candidate for code-to-code comparisons because the accuracy of the software package has been well documented. [67, 68, 69, 70] To validate PHOENIX, the results of each reactor configuration's burnup simulation in PHOENIX and MONTEBURNS 2.0 were compared. A perturbation and regression analysis was also performed comparing results from simulations using the perturbation feature in PHOENIX. This section describes in detail the strategy behind our validation methodology and the parameters used to validate PHOENIX.

5.1. Code-to-Code Validation

Four different reactor configurations were simulated using both PHOENIX and MONTEBURNS 2.0:

1. The first configuration modeled was the GODIVA reactor provided by LANL as part of the MCNP6 benchmark suite. The GODIVA model consisted of a sphere of highly enriched uranium.

2. The second configuration modeled was a fuel pin from the heavy water moderated, CANDU-type, NRX research reactor. [71]
3. The third configuration was a fuel pin from the Takahama-3 PWR reactor from Japan. An additional advantage to modeling the Takahama-3 configuration was that experimental benchmark measurements already exist. [72]
4. The last configuration modeled was a full core Prototype Fast Breeder Reactor (PFBR). The PFBR core contained two different enrichments of MOX fuel surrounded by a natural uranium blanket. [73]

A detailed description of each of these reactor configurations is provided in Section 6.

5.1.1. Code-to-Code Validation Parameters

To validate the simulation results produced by PHOENIX, we selected key reactor parameters and isotopic compositions to compare to MONTEBURNS 2.0. A list of the reactor parameters and isotopes used for our validation analysis can be seen in Table 4.

Table 4. Code-to-Code Validation Parameters

Reactor Parameters	Isotopes	
k_{eff}	Ru-105	U-234
Flux (n/cm^2-s)	Sn-125	U-235
Burnup (GWd/MTU)	Sb-125	U-238
	I-135	Pu-239
	Xe-135	Pu-240
	Cs-133	Pu-241
	Cs-134	Am-241
	Cs-137	Am-242m
	Nd-148	Cm-242
	Sm-149	Cm-244
	Eu-154	

In our analysis we were interested in three primary reactor parameters that were related to overall reactor system properties: k_{eff}, flux, and burnup. The 21 isotopes from Table 4 were selected for a combination of reasons. Cs-137 and Nd-148 were included because they act as good burnup monitors. Both isotopes build up linearly with burnup regardless of reactor configuration. Xe-135 and Sm-149 were included to make sure PHOENIX correctly simulated strong absorber fission products. All of the actinides from Table 4 were included to validate the accuracy of the fission source and the ability to model complex buildup and decay chains. Ru-105 was included to validate how PHOENIX handled isotopes with short half-lives. Am-242m validated the treatment of metastable isotopes and traditionally Am-242m has been a difficult isotope to correctly model for many previous code systems. Lastly, Cm-242 and Cm-244 were included to validate how PHOENIX handled isotopes with extremely low gram quantity production and long buildup chains.

A comparison standard was set for each simulation parameter being evaluated based on the agreement typically seen in the literature for code-to-code comparisons. The k_{eff} in each simulation at every time-step between both burnup codes should be less than 1% different. The neutron flux and reactor burnup in PHOENIX at every time-step should be within 5% of the values provided by MONTEBURNS 2.0. All three of these reactor parameters are either provided directly by MCNP6, or are a direct result of calculations using information from MCNP6. Since there are minor differences between the way MCNP5 (used by MONTEBURNS 2.0) and MCNP6 calculate these parameters, we expect any deviation to be due only to the burnup modules, thus helping to isolate any source of error.

Since PHOENIX and MONTEBURNS 2.0 "link" different versions of the same software, we expect different results in isotopic composition even when simulating an identical problem. The sources of error for these differences are: (1) deviations in the cross-sections used by each code, (2) stochastic error in the Monte Carlo simulation, and (3) solution mechanism for metastable isotopes. The stochastic nature of flux and one-group cross-section calculations in Monte Carlo calculations also play a role in potential gram composition differences. As mentioned in Section 4.1.1, ORIGEN 2.2 also handles metastable isotopes differently than ORIGEN-S, and the degree of precision between ORIGEN 2.2 and ORIGEN-S is also different. ORIGEN 2.2 calculates gram quantities with only three digits of precision, where ORIGEN-S provides six digits of precision. All of these factors made it difficult to create a standard for direct comparison of isotopic compositions.

To resolve these issues, two separate categories were created for comparing gram compositions in PHOENIX and MONTEBURNS 2.0. The first category consisted of isotopes that are generally produced in relatively large quantities in burnup simulations and have smaller uncertainties in their interaction cross-sections and fission product yields. The gram compositions of isotopes in this category produced by PHOENIX are expected to be within 5% of those produced by MONTEBURNS 2.0. The second category consists of isotopes that have small half-lives, are produced in relatively small quantities, have relatively large uncertainties in their interaction cross-sections and fission product yields, or have complicated buildup and decay chains. All of these factors can contribute to a difference in isotopic gram quantities calculated by ORIGEN 2.2 and ORIGEN-S. Furthermore, the percent difference in the produced gram quantities for Category 2 isotopes between MONTEBURNS 2.0 and PHOENIX can vary depending on the type of reactor configuration modeled. Ideally we would like to see less than a 10% difference for Category 2 isotopes, but larger difference might be expected. A breakdown of which category each isotope belongs in can be seen in Table 5.

.

Table 5. Isotope Categories for Gram Composition Validation Analysis

CATEGORY 1	CATEGORY 2
< 5% Difference in Gram Comp.	Variable % Difference in Gram Comp.
I-135	Ru-105
Xe-135	Sn-125
Cs-133	Sb-125
Cs-134	Eu-154
Cs-137	Sm-149
Nd-148	Am-242m
U-234	Cm-242
U-235	Cm-244
U-238	
Pu-239	
Pu-240	
Pu-241	
Am-241	

5.1.2. Stochastic Uncertainty in Code-to-Code Validation

Stochastic uncertainties are inherent in any Monte Carlo calculation. When comparing the results from two separate Monte Carlo simulations, it is good practice to account for stochastic uncertainty. With regard to the validation standards introduced in the previous section, quantifying and removing the error introduced by stochastic uncertainties provided more comprehensive code-to-code validation. In our code-to-code validation analysis, statistical methods were used to quantify and remove stochastic uncertainties in the simulation results. As mentioned in Section 2.0, all Monte Carlo calculations are completed using random numbers. If a series of burnup simulations are started in PHOENIX or MONTEBURNS 2.0 which use different random numbers to calculate their results, the results produced by these simulations will be independent.

Therefore, in our validation analysis we performed seven identical simulations for each reactor configuration in both PHOENIX and MONTEBURNS 2.0. The only component that was changed in each simulation was which random numbers were used by MCNP6 and MCNP5 respectively. The results from these measurements were all independent, and could be treated as separate measurements. Statistical methods were used to calculate the mean and standard deviation for each reactor parameter and gram quantity calculated:

$$\bar{x} = \frac{1}{N}\sum_{i=1}^{N} x_i \tag{30}$$

$$\sigma = \frac{\sum_{i=1}^{N}(x_i - \bar{x})^2}{N-1} \tag{31}$$

where $\bar{x}$ is the mean from all seven samples, N is the total number of samples, x_i is the value of sample i, and σ is the standard deviation.

The accounting of stochastic uncertainties between the two simulations also helped to ensure the rigorousness of the PHOENIX code-to-code validation. For example, if only a single simulation was performed in both MONTEBURNS 2.0 and PHOENIX, and the stochastic uncertainty was large in each of these simulations, the validation conclusions that would be drawn from a comparison of these results may be incorrect. Quantifying and decreasing the stochastic uncertainty in our validation process reduced the inherent "random" nature created by using Monte Carlo software.

5.2 Experimental Validation

The results from PHOENIX and MONTEBURNS 2.0 burnup simulations from the code-to-code validation using the Takahama-3 reactor were compared to experimental values from the literature. For simplicity in the analysis, the same isotopes and parameters that were considered in the code-to-code validation were also used here.

5.3. Systematic Uncertainty Quantification Using Perturbations and Regression Analysis

The next portion of our validation analysis focused on the systematic uncertainty quantification component in PHOENIX. As mentioned in Section 2, PHOENIX uses a combination of perturbations and linear regression analysis to propagate and quantify the systematic uncertainties introduced by uncertainties in the starting fuel enrichment. To validate this methodology, a series of burnup simulations with perturbed initial fuel enrichments was conducted on each of the four reactor configurations. In this analysis two methods were used for perturbing the initial enrichment of the starting fuel. We refer to the first method as a "manual" perturbation of the fuel initial enrichment. This method involved manually changing the MCNP6 input deck in PHOENIX with a perturbed fuel enrichment before starting the burnup simulation. Using the enrichments entered via the "manual" method, PHOENIX would simulate burnup on the perturbed reactor configuration without using the PERT feature in MCNP6. The second method of modifying a fuel's initial enrichment was the "PERT" method. This method involved inserting the desired perturbation weight percentages into the PHOENIX input deck. PHOENIX would then create a new material for each perturbation and input the

perturbed isotopic compositions calculated using Equations 9-10. In both the "manual" and "PERT" perturbation cases, the perturbations were introduced at the initial time step and propagated through every burnup time-step.

To validate the perturbation feature implemented in PHOENIX, results from simulations using the "manual" method were compared to results from simulations using the "PERT" method. Similarly, to validate the linearity of our regression function discussed in Section 3, interpolated gram compositions using data from the "PERT" method were compared to gram compositions from "manual" simulations. At least four initial fuel enrichment perturbations were created for each of the four reactor configurations. This step led to five total fuel enrichments per reactor configuration: the initial unperturbed enrichment plus four additional perturbed enrichments. The goal behind our perturbation validation method was to prove that the reactor parameters and interpolated gram compositions from the "PERT" simulations matched the results from the "manual" simulations. Therefore, at least five simulations for each reactor configuration were performed in PHOENIX. To begin the validation process, a PHOENIX input package (MCNP6 + PHOENIX input deck) was created using the "PERT" method. Two of the four perturbed fuel enrichments were input into the PHOENIX input deck. The "PERT" simulation was executed, and reactor parameters and gram quantities were calculated for all three (unperturbed plus two additional perturbations) of the initial fuel enrichments. PHOENIX also calculated linear regression coefficients to interpolate gram compositions at every time-step. Since there were a total of three gram compositions available at every time-step (two perturbed plus the

original), PHOENIX used a three point linear regression. To create a standard for comparison, four additional PHOENIX input packages were created (one for each of the perturbed enrichments) using the "manual" method. These four input packages were simulated in PHOENIX, and the reactor parameters and gram quantities for each perturbation were compared to the interpolated results from the "PERT" simulations. It should be noted that for the first GODIVA configuration, an extra perturbation was performed which provided six different enrichments: the original unperturbed enrichment plus five additional perturbed enrichments. Both the isotope and fuel enrichment perturbations used in each reactor configuration can be seen in Table 6.

Table 6. Regression Validation Configuration Perturbations used in the "manual" method

Isotope	**wt% Perturbed**
Godiva	
U-235	1.067*
U-235	2.134
U-235	3.201*
U-235	4.268
U-235	5.336*
NRX	
U-235	3
U-235	5*
U-235	8
U-235	10*
Takahama-3	
U-235	3
U-235	5*
U-235	8
U-235	10*
PFBR	
Pu-239	3
Pu-239	5*
Pu-239	8
Pu-239	10*

*These isotopes and initial fuel enrichments were also perturbed using the "PERT" method.

6. PHOENIX VERIFICATION AND VALIDATION

6.1. GODIVA Reactor Configuration

The GODIVA Reactor configuration was provided as a benchmark simulation model from the MCNP6 package. During benchmark tests for MCNP, nine critical systems were analyzed to determine MCNP's ability to calculate the multiplication factor of a critical system. One of these systems was the GODIVA reactor configuration. [74] This section describes the GODIVA model in detail, and presents GODIVA simulation results relevant to PHOENIX validation.

6.1.1. GODIVA Model Description

The GODIVA reactor configuration consisted of a sphere of highly enriched U-235. In the MCNP6 input deck the sphere was placed inside of a vacuum with zero re-entry conditions. A "kcode" problem was run on this reactor simulation with 10,000 particles per cycle, an initial k_{eff} guess of 1.0, 20 inactive cycles, and 220 total cycles. A spherical source distribution was used to generate source point locations in MCNP6. Details about the reactor operating parameters and model characteristics can be seen in Table 7. The PHOENIX input package created to model the GODIVA reactor configuration is provided in Appendix A.

Table 7. GODIVA Model Characteristics

Parameter	Unit	Value
HEU Sphere Radius	cm	8.741E+00
HEU Sphere Volume	g/cm^3	2.797E+03
HEU Sphere Density	$atoms/cm^3$	4.798E-02
U-234 atom density	$atoms/cm^3$	4.918E-04
U-235 atom density	$atoms/cm^3$	4.499E-02
U-238 atom density	$atoms/cm^3$	2.498E-03

The GODIVA reactor configuration was not designed to be used in burnup simulations so some approximations were made when considering burnup parameters. The model was burned with a power of 0.5 MWth for 800 days. There were eight separate and equal burnup time-steps of 100 days each. An expected Q-value of 200 MeV was used for the simulation. Since the Q-value for the reactor configuration was not exactly known, a negative sign preceded the PHOENIX input, and PHOENIX calculated the value automatically at every time-step. One predictor step was used in every time-step. End-of-step criticality calculations were also requested on the PHOENIX input deck. An importance fraction of 1.0 was selected. The reason for selecting this value is because PHOENIX and MONTEBURNS 2.0 have different methods for deeming different isotopes "important." In order to preserve validation fidelity, both PHOENIX and MONTEBURNS 2.0 models needed to tally the exact same isotopes. The only way to ensure this occurred was to set an importance fraction equal to 1.0 in both input decks.

6.1.2. GODIVA Code-to-Code Validation

The validation results produced from the GODIVA model are presented below. All reactor parameters tested between MONTEBURNS 2.0 and PHOENIX passed the validation criteria of exhibiting less than 5% difference. However, all isotopic compositions measured did not pass the validation criteria. The reactor parameter and isotopic composition code-to-code validation results for the GODIVA model are provided in Figures 12-14 and Tables 8-11.

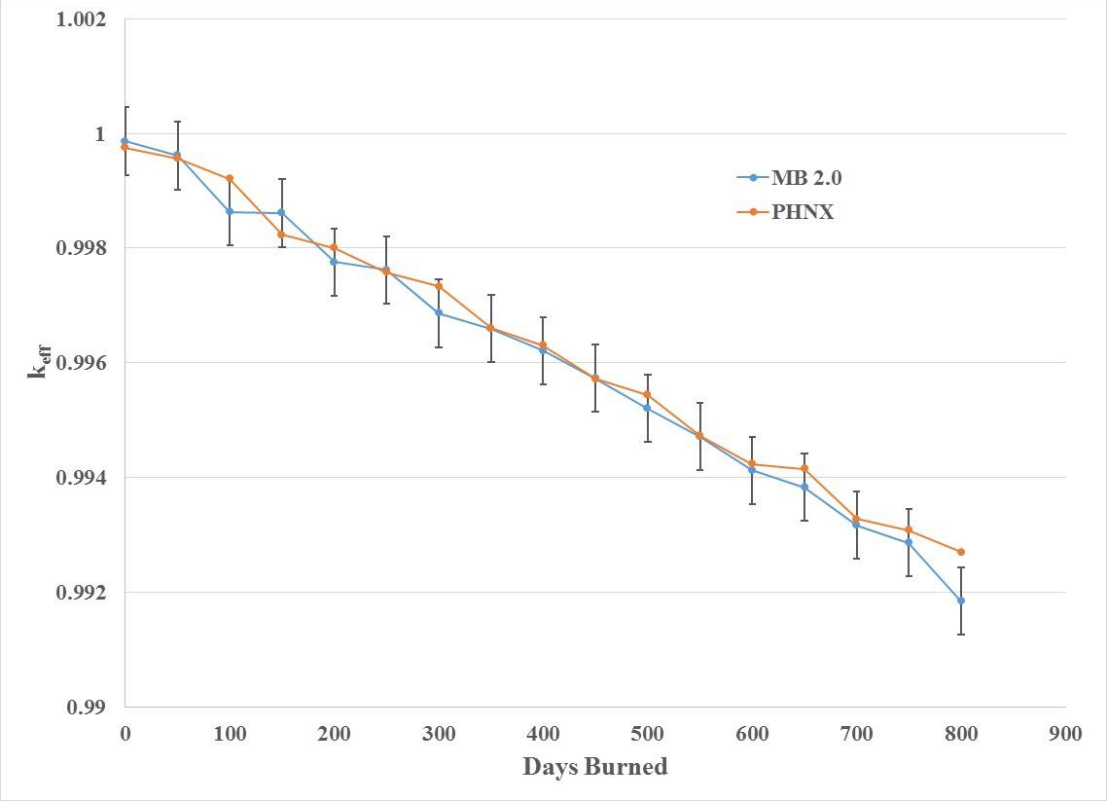

Figure 12. A comparison of k_{eff} produced by MONTEBURNS 2.0 and PHOENIX for every burnup time-step in the GODIVA model.

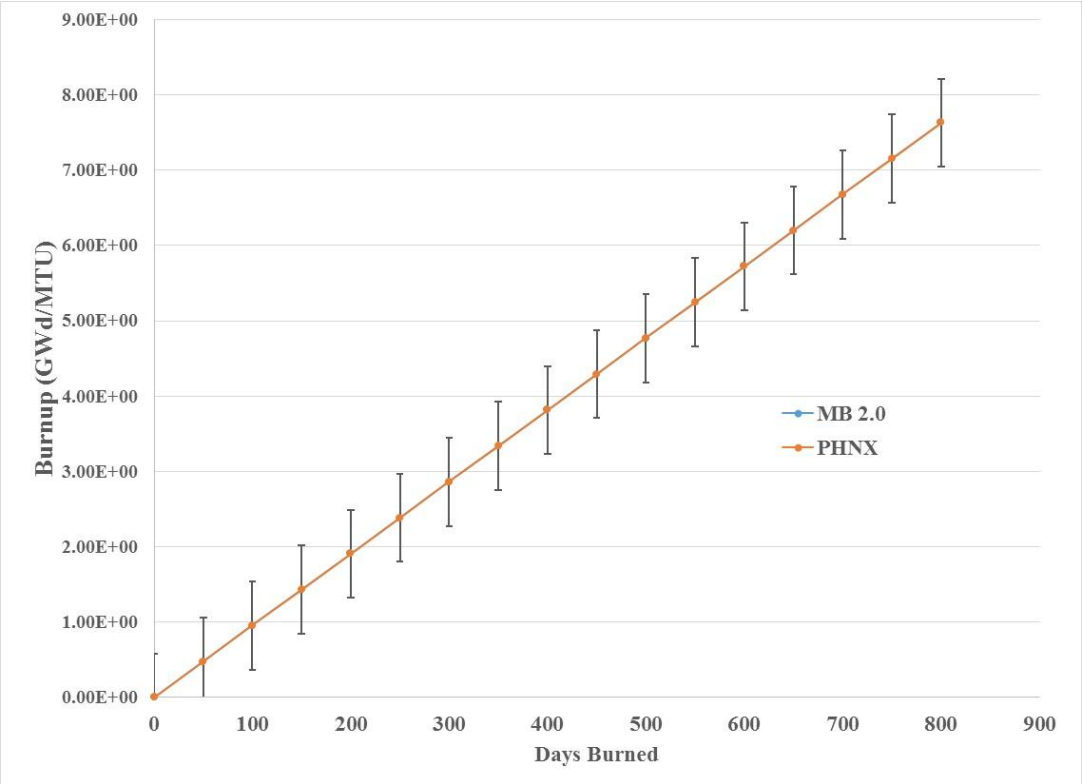

Figure 13. A comparison of burnup produced by MONTEBURNS 2.0 and PHOENIX for every burnup time-step in the GODIVA model.

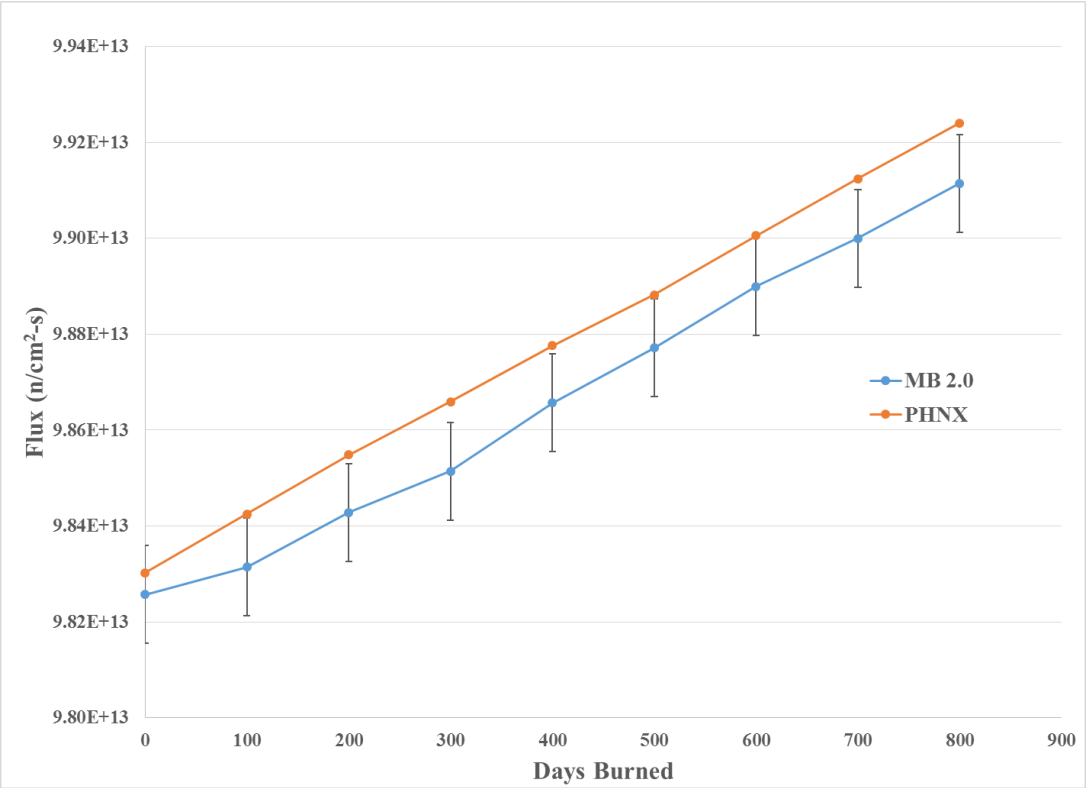

Figure 14. A comparison of the neutron flux produced by MONTEBURNS 2.0 and PHOENIX for every burnup time-step in the GODIVA model.

Table 8. k_{eff} Comparison Between MONTEBURNS 2.0 and PHOENIX for the GODIVA Model

Days	MB 2.0	PHNX	% Difference
0	1.000	1.000	0.01%
100	0.999	0.999	-0.06%
200	0.998	0.998	-0.02%
300	0.997	0.997	-0.05%
400	0.996	0.996	-0.01%
500	0.995	0.995	-0.02%
600	0.994	0.994	-0.01%
700	0.993	0.993	-0.01%
800	0.992	0.993	-0.09%

Table 9. Burnup Comparison Between MONTEBURNS 2.0 and PHOENIX for the GODIVA Model (GWd/MTU)

Days	MB 2.0	PHNX	% Difference
0	0	0	---
100	9.540E-01	9.538E-01	0.01%
200	1.908E+00	1.908E+00	0.02%
300	2.862E+00	2.862E+00	0.00%
400	3.815E+00	3.815E+00	0.00%
500	4.769E+00	4.769E+00	0.00%
600	5.723E+00	5.723E+00	0.00%
700	6.677E+00	6.677E+00	0.00%
800	7.631E+00	7.631E+00	0.00%

Table 10. Flux Comparison Between MONTEBURNS 2.0 and PHOENIX for the GODIVA Model (n/cm^2-s)

Days	MB 2.0	PHNX	% Difference
0	9.826E+13	9.830E+13	-0.05%
100	9.831E+13	9.843E+13	-0.11%
200	9.843E+13	9.855E+13	-0.12%
300	9.851E+13	9.866E+13	-0.15%
400	9.866E+13	9.878E+13	-0.12%
500	9.877E+13	9.888E+13	-0.11%
600	9.890E+13	9.901E+13	-0.11%
700	9.900E+13	9.912E+13	-0.13%
800	9.911E+13	9.924E+13	-0.13%

Table 11. Isotopic Gram Composition Comparisons Between PHOENIX and MONTEBURNS 2.0 at EOB for the GODIVA Model (grams)

Category 1 Isotopes	**MB 2.0**	**PHNX**	**% Difference**
I-135	7.084E-03	7.498E-03	-5.68%
Xe-135	1.040E-02	1.086E-02	-4.35%
Cs-133	1.520E+01	1.580E+01	-3.90%
Cs-134	3.809E-03	3.818E-03	-0.25%
Cs-137	1.430E+01	1.470E+01	-2.74%
Nd-148	4.430E+00	4.495E+00	-1.45%
U-234	5.330E+02	5.334E+02	-0.07%
U-235	4.870E+04	4.866E+04	0.08%
U-238	2.760E+03	2.757E+03	0.11%
Pu-239	1.730E+00	1.729E+00	0.08%
Pu-240	4.799E-04	2.146E-03	-126.90%
Pu-241	1.340E-07	8.006E-07	-142.65%
Am-241	3.637E-09	2.728E-08	-152.94%
Category 2 Isotopes			
Ru-105	7.206E-04	6.377E-04	12.20%
Sn-125	1.460E-03	4.648E-04	103.41%
Sb-125	2.180E-01	6.604E-02	107.00%
Eu-154	3.719E-03	7.332E-02	-180.69%
Sm-149	2.867E+00	2.885E+00	-0.61%
Am-242m	4.866E-13	2.551E-12	-135.93%
Cm-242	9.923E-13	9.150E-12	-160.87%
Cm-244	2.084E-17	2.893E-14	-199.71%

Excellent agreement is found between the PHOENIX and MONTEBURNS calculated values for k_{eff} and burnup. The neutron flux produced by PHOENIX passed the validation criteria, but a clear bias error exists between the MONTEBURNS and PHOENIX calculated flux values. This bias is due to the different mechanisms used to calculate the average Q-value in the problem. The PHOENIX produced average Q-value is energy dependent (as seen in Equation 12) and the MONTEBURNS 2.0 value is not.

This difference led MONTEBURNS 2.0 to have a slightly higher Q-value than PHOENIX at every time-step, which resulted in a lower neutron flux value from MONTEBURNS 2.0. As we continued the validation process through different models, we observed that the Q-value's effect on the flux was more pronounced in reactors with a hard neutron spectrum. It is also important to note that the flux value provided by MONTEBURNS 2.0 only has a precision of three significant figures, where PHOENIX's precision has six. The precision difference between the codes also played a minor role in the difference between the calculated neutron fluxes.

All of the Category 1 isotopes, with the exception of I-135 and the higher actinides, passed the validation criteria. Sm-149 was the lone Category 2 isotope that passed the validation criteria. The degree to which the gram quantities differed warranted additional research. The cause of the large discrepancy between the gram quantities resulted from a difference in precision between ORIGEN-S and ORIGEN 2.2. As mentioned previously, ORIGEN 2.2 outputs quantities with a smaller degree of precision than ORIGEN-S. In the GODIVA problem, a large majority of higher actinides are produced from capture reactions in U-238. In this reactor configuration, the neutron energy spectrum was exceedingly hard. The hard neutron energy spectrum reduced the number of U-238 capture reactions that occurred, which in turn resulted in low gram quantity production of plutonium, americium, and curium. Due to the differences in precision between the versions of ORIGEN used by MONTEBURNS 2.0 and PHOENIX, the low gram quantities output by ORIGEN 2.2 for these higher actinides were truncated at the initial time-step. The truncated gram quantities in ORIGEN 2.2

resulted in lower gram quantities throughout the burnup simulation. This result suggests that PHOENIX will have superior capability to MONTEBURNS in predicting low concentration isotopes in burnup simulations.

6.1.3. GODIVA Perturbation and Regression Analysis

In this validation analysis, a simulation in PHOENIX was performed using the "PERT" method with three U-235 input perturbations of 1.067 wt%, 3.201 wt%, and 5.336 wt%. Using data from this simulation, a four point linear regression function was calculated for reactor parameters and isotopic compositions. Reactor parameters and gram compositions were interpolated using this regression analysis for initial fuel perturbations of 1.067 wt%, 2.134 wt%, 3.201 wt%, 4.268 wt%, and 5.336 wt%. These interpolated values were compared to values computed from five separate "manual" simulations at identical enrichments. The differences between the interpolated values ("PERT" method) and the simulated values ("manual" method) can be seen in Tables 12-15 for all reactor parameters and gram compositions.

Table 12. Percent Difference Between the "PERT" and "manual" Method for Perturbation Validation Analysis of k_{eff} in the GODIVA Model

Days	1.067%	2.134%	3.201%	4.268%	5.336%
0	-0.09%	0.05%	0.04%	0.01%	-0.44%
100	0.08%	0.08%	0.05%	-0.01%	-0.42%
200	-0.02%	0.06%	0.02%	0.07%	-0.51%
300	0.01%	-0.03%	-0.04%	-0.03%	-0.40%
400	-0.07%	-0.09%	-0.13%	-0.07%	-0.36%
500	0.02%	0.05%	-0.01%	-0.06%	-0.37%
600	-0.05%	-0.03%	-0.07%	-0.07%	-0.36%
700	-0.02%	-0.09%	-0.07%	0.07%	-0.52%
800	-0.01%	-0.04%	-0.10%	0.06%	-0.50%

Table 13. Percent Difference Between the "PERT" and "manual" Method for Perturbation Validation Analysis of Burnup in the GODIVA Model

Days	1.067%	2.134%	3.201%	4.268%	5.336%
0	---	---	---	---	---
100	-0.02%	-0.02%	-0.01%	-0.05%	0.05%
200	-0.02%	-0.01%	-0.02%	-0.04%	0.04%
300	-0.02%	-0.01%	-0.02%	-0.04%	0.04%
400	-0.02%	-0.02%	-0.03%	-0.05%	0.05%
500	-0.01%	-0.02%	-0.03%	-0.04%	0.04%
600	-0.01%	-0.02%	-0.03%	-0.04%	0.04%
700	-0.01%	-0.02%	-0.02%	-0.04%	0.04%
800	-0.01%	-0.02%	-0.03%	-0.04%	0.03%

Table 14. Percent Difference Between the "PERT" and "manual" Method for Perturbation Validation Analysis of Neutron Flux in the GODIVA Model

Days	1.067%	2.134%	3.201%	4.268%	5.336%
0	0.07%	0.64%	1.19%	1.72%	2.27%
100	0.06%	0.64%	1.22%	1.74%	2.27%
200	0.05%	0.64%	1.21%	1.76%	2.30%
300	0.07%	0.62%	1.20%	1.74%	2.30%
400	0.03%	0.60%	1.17%	1.70%	2.26%
500	0.08%	0.63%	1.21%	1.77%	2.31%
600	0.07%	0.60%	1.19%	1.73%	2.30%
700	0.07%	0.64%	1.22%	1.74%	2.30%
800	0.07%	0.65%	1.19%	1.76%	2.29%

Table 15. Percent Difference Between the "PERT" and "manual" Method for Perturbation Validation Analysis of Gram Compositions in the GODIVA Model at EOB

	1.067%	2.134%	3.201%	4.268%	5.336%
Ru-105	-0.01%	0.01%	0.12%	0.08%	-0.09%
Sn-125	-0.01%	0.27%	0.92%	0.74%	-0.16%
Sb-125	-0.01%	0.17%	0.56%	0.43%	-0.12%
I-135	-0.01%	-0.02%	-0.03%	-0.03%	-0.05%
Xe-135	-0.01%	-0.02%	-0.02%	-0.03%	-0.05%
Cs-133	-0.01%	-0.08%	0.04%	0.01%	-0.05%
Cs-134	0.19%	0.21%	0.47%	0.44%	0.28%
Cs-137	-0.01%	-0.02%	-0.02%	-0.03%	-0.05%
Nd-148	-0.01%	0.34%	-0.33%	-0.28%	-0.05%
Sm-149	-0.01%	5.41%	-0.17%	-0.15%	-0.06%
Eu-154	-0.14%	13.56%	-19.28%	-15.56%	0.26%
U-234	0.00%	0.00%	0.00%	0.01%	0.03%
U-235	0.00%	0.00%	0.00%	0.00%	0.00%
U-238	0.00%	0.01%	0.00%	0.02%	0.04%
Pu-239	0.02%	-0.14%	-0.78%	-2.92%	-10.13%
Pu-240	-0.01%	31.17%	-18.32%	-17.30%	-12.38%
Pu-241	0.08%	33.43%	-19.78%	-20.79%	-24.16%
Am-241	0.09%	34.68%	-20.28%	-21.13%	-23.74%
Am-242m	0.17%	44.37%	-20.93%	-24.53%	-39.69%
Cm-242	0.15%	33.57%	-20.93%	-24.65%	-40.05%
Cm-244	0.17%	34.11%	-21.18%	-24.77%	-39.82%

Similar to Section 6.1.2, all reactor parameters passed the validation analysis of being less than 5% different. A large majority of the higher actinides at EOB in Table 15 did not pass the validation criteria of being less than 5% different. The large differences in gram quantities of higher actinides and fission products can again be attributed to the low number of U-238 absorptions, but for different reasons than described in Section 6.1.2. When using the PERT feature in MCNP6, the accuracy of perturbation results is dependent upon the amount an isotope is perturbed. [24] The MCNP6 user's manual suggests that perturbations be limited to less than 30 wt% of the starting isotopic composition. The perturbation of U-235 by 5.336 wt% was much less than 30%; however, the perturbed sample was an HEU mixture and contained other isotopes. The increase of 5.336 wt% in U-235 meant a drastic reduction in the starting quantity of U-234 and U-238 in the system. The exact percent of U-234 and U-238 that were removed initially due to U-235 perturbation can be seen in Table 16.

Table 16. Percent Difference in wt% Perturbations in U-234, U-235, and U-238 for the GODIVA Model

wt% U-235 Perturbation	wt% U-234 Perturbation	wt% U-238 Perturbation
1.07%	-17.28%	-17.28%
2.13%	-37.82%	-37.82%
3.20%	-62.65%	-62.65%
4.27%	-93.26%	-93.26%
5.34%	-131.96%	-131.96%

The perturbations in U-234 and U-238 were significantly over the advised 30% and resulted in a large degree of error in gram composition calculations between the "PERT" and "manual" method. This example was provided specifically so that users would be aware of this potential error and take it into consideration when using perturbations on their simulations.

6.2. NRX Reactor Configuration

The CANDU-type NRX reactor is a small, 40-MWth natural uranium (NatU) metal fueled research reactor. [71] The reactor is heavy-water moderated and light-water cooled. It contains 192 NatU metal fuel rods arranged with a triangular lattice pitch inside a heavy-water filled calandria tank which is surrounded radially by nuclear grade graphite. The natural uranium fuel is located inside an aluminum calandria tank which is surrounded by a radial graphite reflector, steel and light-water thermal shields above and below the core, and a concrete biological shield surrounding the complete structure. Penetrations are present for two large thermal columns, heavy-water moderator input and removal, light water coolant input and removal, as well as refueling penetrations through a shield door on top of the core. The upper and lower thermal shields are composed of stainless steel with channels for light water coolant. The upper thermal shield is 91.44 cm tall and the lower thermal shield is 127.00 cm tall. When homogenized as all one cell the thermal shields consist (by mass) of 89.06% stainless steel and 10.94% light water. A full list of NRX reactor characteristics can be seen in Table 17. These characteristics were used to create the MCNP6 model described in

Section 6.2.1. This section describes the NRX model in detail, and presents NRX simulation results relevant to PHOENIX validation.

Table 17. NRX Reactor Configuration Parameters

Parameter	Value
Number of fuel rods	1.920E+02
Number of central thimbles	1.000E+00
Number of shut-off rods	6.000E+00
Burnup (MWd/tU)	1.300E+03
Power (MWth)	4.000E+01
Fuel active length (cm)	3.061E+02
Specific power (MW/tU)	3.810E+00
Fuel OD (cm)	3.454E+00
Fuel temperature (K)	7.730E+02
Clad OD (cm)	3.658E+00
Clad temperature (K)	4.230E+02
Light water gap OD (cm)	4.216E+00
Light water coolant temperature (K)	3.680E+02
Pressure tube OD (cm)	4.420E+00
Air gap OD (cm)	5.715E+00
Calandria tube OD (cm)	6.033E+00
Moderator temperature (K)	3.530E+02
Fuel channel pitch (cm)	1.730E+01
Fuel channel arrangement	Triangular pitch
Calandria tank ID (cm)	2.667E+02
Calandria tank height (cm)	3.200E+02
Calandria tank thickness (cm)	6.350E-01
Air gap thickness between Calandria tank and graphite reflector (cm)	3.810E+00
Inner graphite reflector thickness (cm)	2.286E+01
J-annulus air gap thickness (cm)	6.350E+00
Outer graphite reflector thickness (cm)	6.096E+01

6.2.1. NRX Model Description

The MCNP6 input for the NRX reactor configuration modeled a single fuel pin infinite in the (axial) z-dimension and with reflecting boundaries on all six sides of the surrounding hexagon (which has an overall width of 17.304 cm). The width of the channel boundaries was increased slightly to maintain the fuel-to-moderator ratio in the core. The radial reflectivity, modified channel boundaries, and axial leakage of the fuel channel model provided a reasonably accurate representation of the conditions near the center of the core. The fuel, clad, light-water coolant, air gap, and heavy-water moderator were modeled explicitly. Dimensions used for the infinite pin cell model are shown in Figure 15. The properties of all materials used in the MCNP simulation are shown in Table 18. A "kcode" simulation was performed using 10,000 particles per cycle, an initial k_{eff} guess of 1.0, and a total of 220 cycles skipping 20 cycles before tallying. An "SDEF" distributed source was used to ensure source locations were spread appropriately throughout the pin. A "rand" card was included for adjusting the starting random number seed so the simulation's stochastic uncertainty could be quantified.

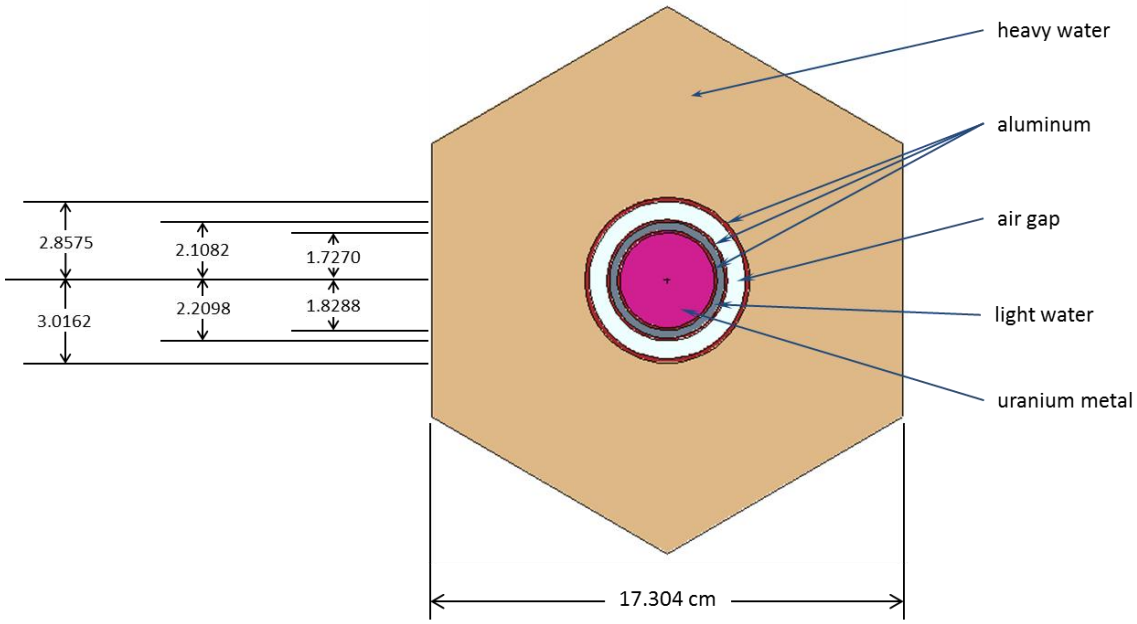

Figure 15. Radial cross-section of an individual NRX fuel channel modeled in MCNP (dimensions shown are in units of cm).

Table 18. Properties of the NRX Fuel Pin Modeled in MCNP6

Material	**Temperature (K)**	**Density (g/cm^3)**
Natural U Metal	6.000E+02	1.877E+01
Clad (Al)	2.930E+02	2.700E+00
H_2O Coolant	4.000E+02	9.827E-01
D_2O moderator	3.000E+02	1.092E+00
Coolant Tube (Al)	2.930E+02	2.700E+00
Air Gap	2.930E+02	2.790E-03
Graphite	3.000E+02	2.100E+00
Thermal Shield (89.06 w/o stainless steel 304 and 10.94 w/o light	2.930E+02	4.491E+00

The entire fuel pin was burned as a single material at a power of 0.20833 MWth. The initial guess for the Q-value for fission was set to -200 MeV and calculated by PHOENIX at every time-step. A fractional importance of 1.0 was again used because of

the differences in how each burnup code deems an isotope "important" (see Section 6.1.1). A single predictor step and an end-of-step criticality calculation were also added to the model. A total of six outer burn steps were used to burn the material 337 total days. Burnup time-step sizes of 0.395833, 19.6042, 79.0, 79.0, 79.0, and 80.0 days were used. The PHOENIX input package created to model the NRX reactor is provided in Appendix B.

6.2.2. NRX Code-to-Code Validation

The results provided during the code-to-code validation of PHOENIX to MONTEBURNS 2.0 for the NRX reactor configuration were well within the specified validation criteria. All reactor parameters and Category 1 isotopes calculated using PHOENIX were less than 5% different from values produced using MONTEBURNS 2.0. The reactor parameter and isotopic composition code-to-code validation results for the NRX reactor model are provided in Figures 16-18 and Tables 19-22.

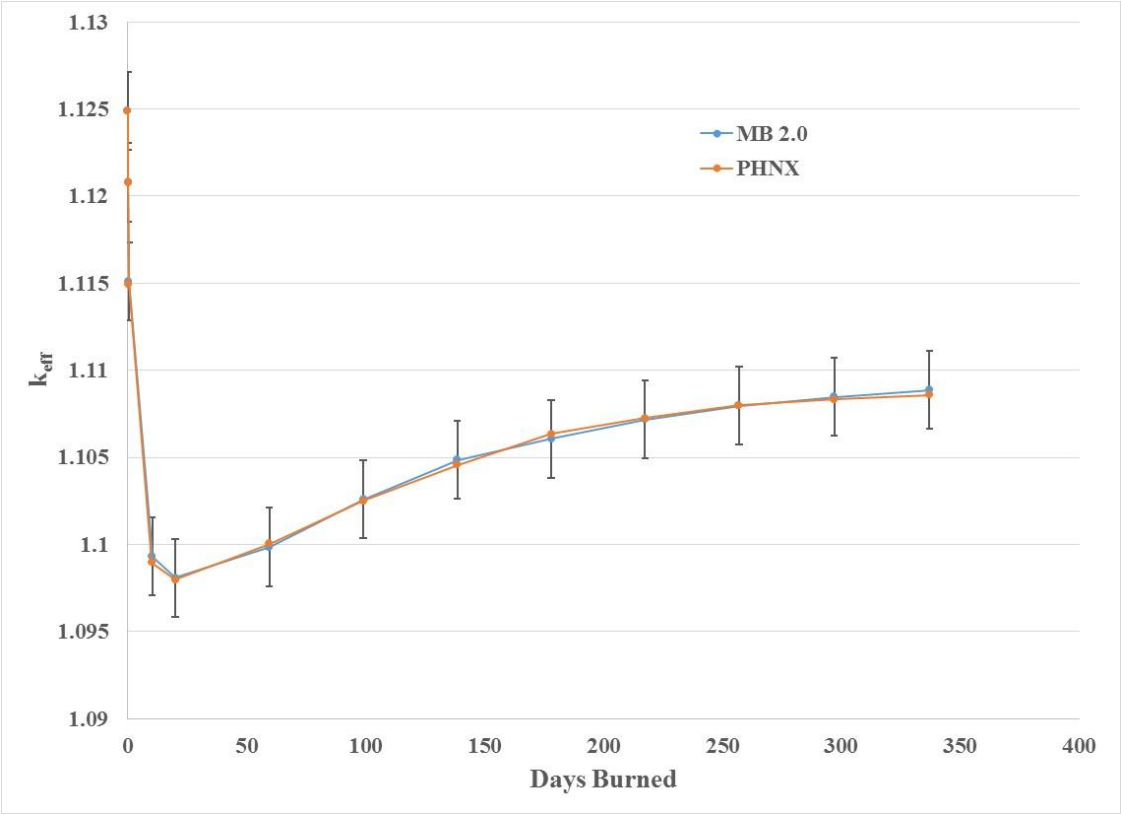

Figure 16. A comparison of k_{eff} produced by MONTEBURNS 2.0 and PHOENIX for every burnup time-step in the NRX model.

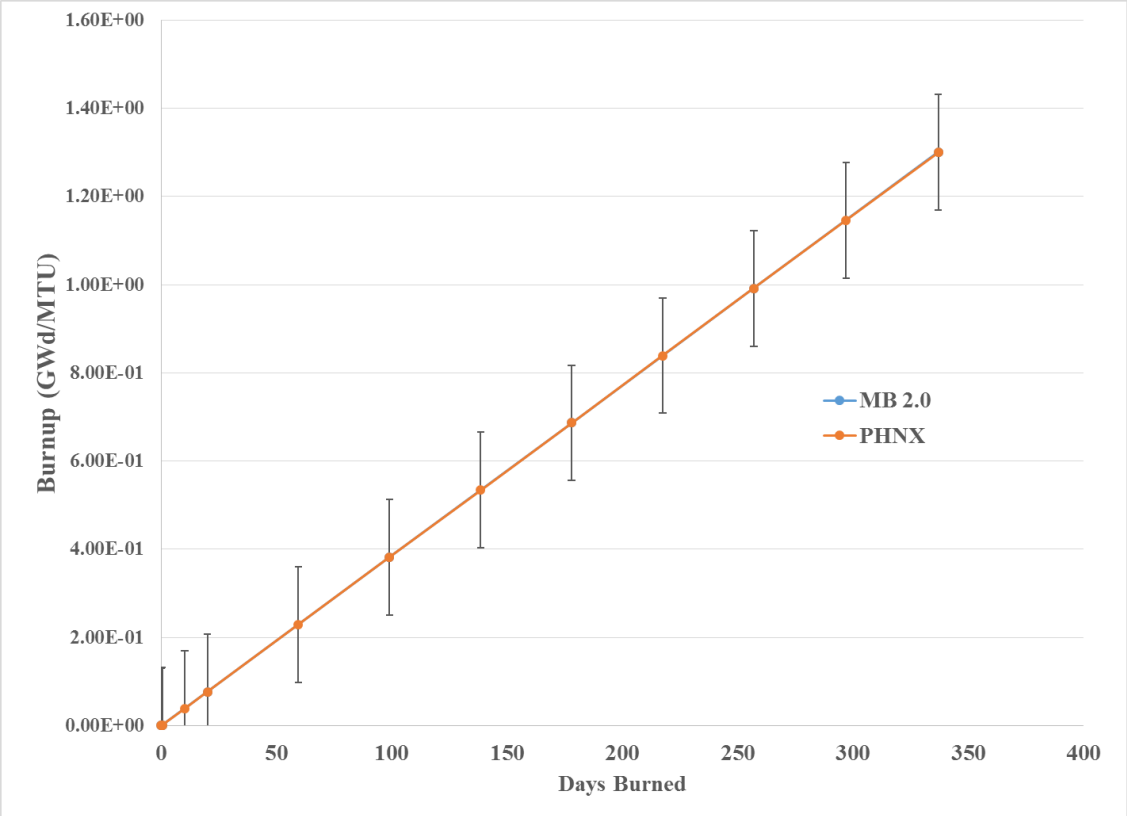

Figure 17. A comparison of burnup produced by MONTEBURNS 2.0 and PHOENIX for every burnup time-step in the NRX model.

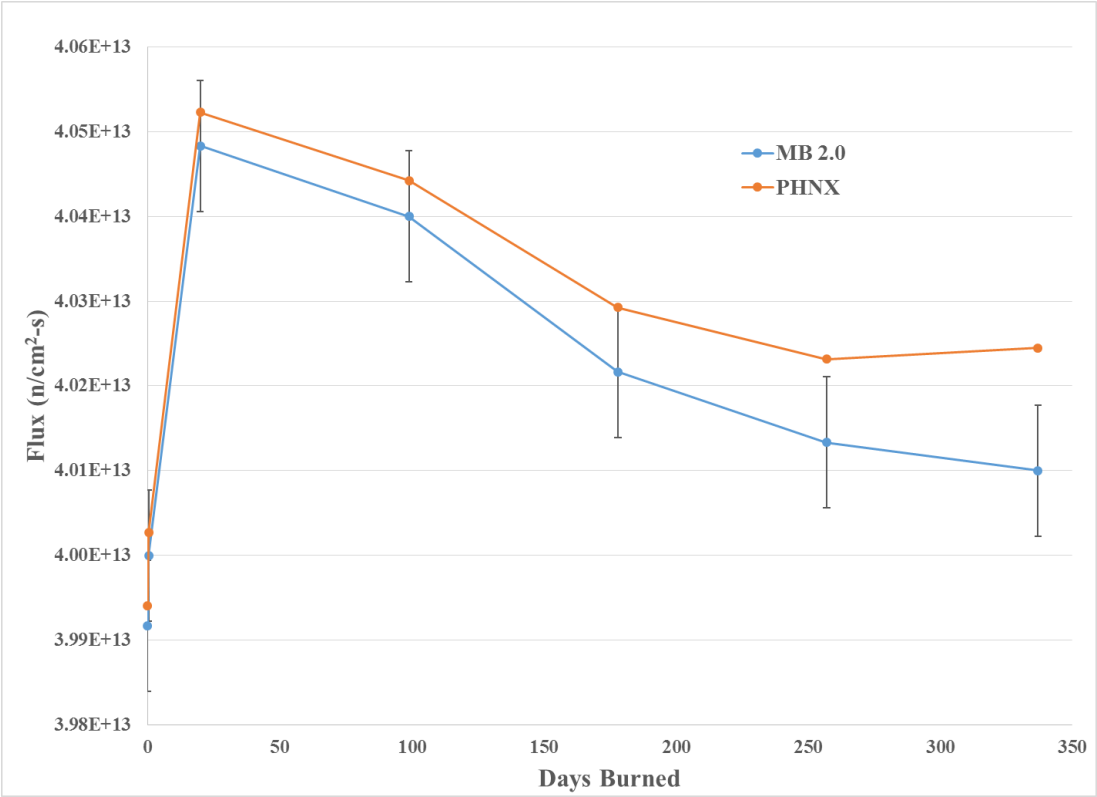

Figure 18. A comparison of neutron flux produced by MONTEBURNS 2.0 and PHOENIX for every burnup time-step in the NRX model.

Table 19. k_{eff} Comparison Between MONTEBURNS 2.0 and PHOENIX for the NRX Model

Days	MB 2.0	PHNX	% Difference
0	1.125	1.125	0.00%
0.4	1.115	1.115	0.02%
20	1.098	1.098	0.01%
99	1.103	1.103	0.01%
178	1.106	1.106	-0.03%
257	1.108	1.108	0.00%
337	1.109	1.109	0.03%

Table 20. Neutron Flux Comparison Between MONTEBURNS 2.0 and PHOENIX for the NRX Model (n/cm^2-s)

Days	MB 2.0	PHNX	% Difference
0	3.992E+13	3.994E+13	-0.06%
0.4	4.000E+13	4.003E+13	-0.07%
20	4.048E+13	4.052E+13	-0.10%
99	4.040E+13	4.044E+13	-0.10%
178	4.022E+13	4.029E+13	-0.19%
257	4.013E+13	4.023E+13	-0.25%
337	4.010E+13	4.024E+13	-0.36%

Table 21. Burnup Comparison Between MONTEBURNS 2.0 and PHOENIX for the NRX Model (GWd/MTU)

Days	MB 2.0	PHNX	% Difference
0	0.000E+00	0.000E+00	---
0.4	1.527E-03	1.527E-03	0.03%
20	7.718E-02	7.717E-02	0.01%
99	3.820E-01	3.820E-01	0.00%
178	6.869E-01	6.868E-01	0.01%
257	9.918E-01	9.914E-01	0.03%
337	1.301E+00	1.300E+00	0.06%

Table 22. Isotopic Gram Composition Comparisons Between PHOENIX and MONTEBURNS 2.0 at EOB for the NRX Model (grams)

Category 1 Isotopes	**MB 2.0**	**PHNX**	**% Difference**
I-135	3.127E-03	3.156E-03	-0.93%
Xe-135	1.730E-03	1.737E-03	-0.42%
Cs-133	2.710E+00	2.711E+00	-0.03%
Cs-134	1.848E-02	1.851E-02	-0.16%
Cs-137	2.600E+00	2.621E+00	-0.80%
Nd-148	7.948E-01	7.958E-01	-0.13%
U-234	2.790E+00	2.792E+00	-0.08%
U-235	3.120E+02	3.121E+02	-0.02%
U-238	5.350E+04	5.355E+04	-0.09%
Pu-239	4.910E+01	4.918E+01	-0.17%
Pu-240	3.350E+00	3.368E+00	-0.54%
Pu-241	2.808E-01	2.840E-01	-1.13%
Am-241	3.247E-03	3.303E-03	-1.72%
Category 2 Isotopes			
Ru-105	5.353E-04	5.422E-04	-1.28%
Sn-125	5.450E-04	3.131E-04	54.06%
Sb-125	2.668E-02	1.581E-02	51.18%
Eu-154	1.240E-02	5.158E-03	82.50%
Sm-149	2.047E-02	1.977E-02	3.44%
Am-242m	2.557E-05	1.306E-05	64.75%
Cm-242	1.015E-04	1.173E-04	-14.47%
Cm-244	9.263E-07	6.082E-07	41.47%

The difference in the neutron flux between MONTEBURNS 2.0 and PHOENIX at later time steps can again be contributed to the calculated Q-value. Towards EOB, more Pu-239 is present in the system. Fissions occurring in Pu-239 increase the average energy of the neutron spectra in the NRX reactor. The harder spectrum affects the Q-value and neutron flux calculated by MONTEBURNS 2.0 via the methods described in Section 6.1.2. The difference in Category 2 gram compositions can be attributed to the

different ORIGEN cross-section libraries used by PHOENIX and MONTEBURNS 2.0. The reduced precision of ORIGEN 2.2 also affects the difference in Category 2 gram production. As outlined by the tables and figures above, all of the validation criteria for reactor parameters and gram compositions for code-to-code validation of PHOENIX to MONTEBURNS 2.0 in the NRX model were successfully achieved.

6.2.3. NRX Perturbation and Regression Analysis

The results from the perturbation validation analysis on the NRX reactor met all validation criteria. In this analysis, a simulation in PHOENIX was performed using the "PERT" method with two U-235 input perturbations of 5 wt%, and 10 wt%. Using data from this simulation, a three point linear regression function was calculated for reactor parameters and isotopic compositions. Reactor parameters and gram compositions were interpolated using this regression analysis for initial fuel perturbations of 3 wt%, 5 wt%, 8 wt%, and 10 wt%. These interpolated values were compared to values computed from four separate "manual" simulations at identical starting enrichments. The percent differences between the interpolated values ("PERT" method) and the simulated values ("manual" method) can be seen in Tables 23-26 for all reactor parameters and gram compositions. All the percent differences shown in Tables 23-26 meet the validation criteria for the perturbation validation analysis of the NRX reactor configuration.

Table 23. Percent Difference Between the "PERT" and "manual" Method for Perturbation Validation Analysis of k_{eff} in the NRX Model

Day	3%	5%	8%	10%
0	-0.73%	-0.07%	-0.01%	-0.01%
0.4	-0.83%	-0.17%	-0.18%	-0.20%
20	-0.78%	-0.06%	-0.13%	-0.04%
99	-0.77%	-0.16%	-0.10%	-0.11%
178	-0.60%	0.01%	0.00%	0.06%
257	-0.60%	-0.02%	-0.03%	-0.02%
337	-0.63%	-0.01%	-0.03%	0.00%

Table 24. Percent Difference Between the "PERT" and "manual" Method for Perturbation Validation Analysis of Burnup in the NRX Model

Day	3%	5%	8%	10%
0	---	---	---	---
0.4	-0.36%	-0.48%	-0.79%	-0.95%
20	-0.48%	-0.57%	-0.78%	-1.04%
99	-0.40%	-0.49%	-0.77%	-0.95%
178	-0.37%	-0.51%	-0.74%	-0.96%
257	-0.37%	-0.50%	-0.73%	-0.92%
337	-0.36%	-0.49%	-0.69%	-0.89%

Table 25. Percent Difference Between the "PERT" and "manual" Method for Perturbation Validation Analysis of Neutron Flux in the NRX Model

Day	3%	5%	8%	10%
0	0.00%	-0.04%	-0.22%	-0.34%
0.4	0.07%	0.05%	-0.15%	-0.31%
20	-0.08%	-0.09%	-0.13%	-0.38%
99	0.02%	0.02%	-0.16%	-0.29%
178	-0.01%	-0.12%	-0.21%	-0.42%
257	0.02%	-0.09%	-0.19%	-0.17%
337	0.01%	-0.04%	-0.10%	-0.15%

Table 26. Percent Difference Between the "PERT" and "manual" Method for Perturbation Validation Analysis of Gram Compositions at EOB in the NRX Model

	3%	**5%**	**8%**	**10%**
Ru-105	-0.23%	-0.38%	-0.55%	-0.88%
Sn-125	-0.24%	-0.41%	-0.60%	-0.97%
Sb-125	-0.22%	-0.34%	-0.58%	-0.82%
I-135	-0.22%	-0.37%	-0.47%	-0.70%
Xe-135	-0.16%	-0.20%	-0.36%	-0.44%
Cs-133	-0.24%	-0.37%	-0.58%	-0.78%
Cs-134	-0.06%	-0.53%	-1.02%	-0.91%
Cs-137	-0.23%	-0.37%	-0.58%	-0.78%
Nd-148	-0.23%	-0.36%	-0.57%	-0.77%
Sm-149	-0.19%	-0.05%	-0.41%	-0.42%
Eu-154	-0.17%	-0.22%	-0.81%	-1.42%
U-234	0.02%	-0.01%	0.04%	-0.03%
U-235	0.05%	0.09%	0.13%	0.16%
U-238	0.00%	0.00%	0.00%	0.00%
Pu-239	-0.11%	-0.19%	-0.27%	-0.38%
Pu-240	-0.33%	-0.46%	-0.93%	-1.52%
Pu-241	0.50%	0.22%	0.06%	-0.03%
Am-241	0.50%	0.16%	-0.19%	-0.56%
Am-242m	0.34%	-0.15%	-0.63%	-1.57%
Cm-242	0.34%	-0.21%	-0.88%	-1.87%
Cm-244	0.24%	-0.36%	-1.06%	-2.38%

6.3. Takahama-3 PWR Configuration

The Takahama-3 reactor is a PWR with a rated power of 2,652 MWth which operates with a 17x17 fuel assembly design. The active core consists of 157 fuel assemblies. Each assembly contains 14 integral burnable gadolinia-bearing fuel rods containing 2.6 wt% U-235 and 6.0 wt% gadolinia, while the fuel rods possess a standard PWR fuel enrichment of 4.11 wt% U-235. The assemblies also have 25 water-filled guide tubes. A summary of the Takahama-3 reactor parameters is provided in Table 27.

[44, 75] These characteristics were used to create the MCNP6 model described in Section 6.3.1.

Table 27. Takahama-3 Core Characteristics

Parameter	Data
Takahama-3 Reactor Data	
Operating Power (MWth)	2.652E+03
Core diameter (m)	3.040E+00
Active core height (m)	3.660E+00
Number of assemblies	1.570E+02
Inlet coolant temperature (℃)	2.840E+02
Outlet coolant temperature (℃)	3.210E+02
Fuel Assembly Design Data	
Lattice	17x17
Number of fuel rods	2.640E+02
Number of fuel rods containing burnable poisons	1.400E+01
Number of guide tubes	2.500E+01
Assembly fuel mass, kg U	~4.600E+01
Assembly pitch, cm	2.140E+01
Total assembly length, m	4.060E+00
Fuel Rod Data	
Fuel material	UO_2
Enrichment, wt % U-235	4.110E+00
Fuel theoretical density g/cm^3	1.096E+01
Fuel density, g/cm^3	95 % TD
Fuel temperature, K	9.000E+02
Rod pitch, cm	1.259E+00
Fuel diameter, cm	8.050E-01
Rod OD, cm	9.500E-01
Rod ID, cm	8.220E-01
Active fuel length, cm	3.648E+02
Total fuel rod length, cm	4.038E+02
Clad material	Zircaloy-4
Clad density, g/cm^3	6.440E+00
Estimated clad temperature, K	5.700E+02

The Takahama-3 reactor is a well-known burnup benchmark experiment that has been used to validate burnup codes and burnup calculation methodologies. Three fuel rods, designated SF95, SF96, and SF97, from different locations in a Takahama-3 reactor assembly were destructively analyzed to determine isotopic composition and burnup for each sample. Two of the fuel rods, SF95 and SF97, were located on the periphery of the fuel assembly, and SF96 was located directly adjacent to a water guide tube. Five fuel samples were taken from various axial locations on each of the three fuel rods. The fuel samples from different axial locations in the core covered a wide burnup range from, from 7.8 GWd/MTU to 47.3 GWd/MTU. This section describes a fuel channel modeled in PHOENIX for one of the Takahama-3 benchmark samples described above. This section also provides the Takahama-3 simulation results for code-to-code and experimental validation of PHOENIX.

6.3.1. Takahama-3 Model Description

In order to provide code-to-code validation with MONTEBURNS 2.0, and experimental validation with the results provided by the JAERI, the SF95 fuel pin described in the previous section was modeled. Fuel rod SF95 was selected because it was physically furthest from water guide tubes and burnable poison fuel elements. Figure 19 shows the location of all three fuel rods in the Takahama-3 PWR assembly. [76]

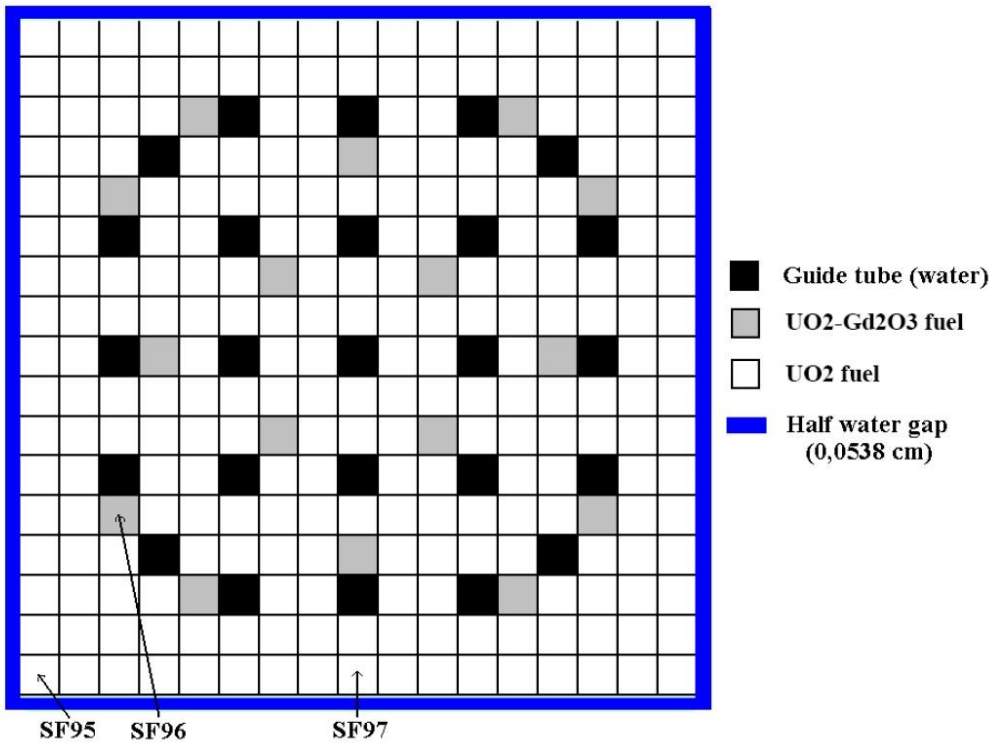

Figure 19. Locations of the fuel rods SF95, SF96, and SF97 in the Takahama-3 fuel assembly.

The MCNP6 input for the SF95 fuel channel consisted of a single fuel pin infinite in the (axial) z-dimension, with reflecting boundaries on the x- and y-dimensions of the fuel channel. The width of the channel boundaries was increased slightly to maintain the fuel-to-moderator ratio in the core. The radial reflectivity, modified channel boundaries, and axial leakage of the fuel channel model provided a reasonably accurate representation of the conditions near the center of the core. The fuel, clad, and light-water coolant were modeled explicitly. The properties of all materials used in the MCNP6 simulation are shown in Table 28. A "kcode" simulation was performed using 10,000 particles per cycle, an initial k_{eff} guess of 1.0, and a total of 220 cycles skipping

20 cycles before tallying. An “SDEF” distributed source was used to ensure source locations were spread appropriately throughout the pin. A “rand” card was included for adjusting the starting random number seed so the simulation’s stochastic uncertainty could be quantified.

Table 28. SF95 MCNP6 Model Characteristics

Parameter	**Data**
Fuel material	UO_2
Enrichment, wt % U-235	4.110E+00
Fuel density, g/cm^3	1.041E+01
Fuel temperature, K	9.000E+02
Active fuel length, cm	3.648E+02
Clad material	Zircaloy-4
Clad density, g/cm^3	6.531E+00
Estimated clad temperature, K	5.700E+02
Borated water density, g/cm^3	7.490E-01
Borated water temperature, K	5.700E+02

The entire fuel pin was burned as a single material at a power of 0.0725 MWth. The initial guess for the Q-value for fission was set to -200 MeV and calculated by PHOENIX at every time-step. A fractional importance of 1.0 was used for the reasons discussed in Section 6.1.1. A single predictor step and an end-of-step criticality calculation were also added to the model.

In the experimental analysis of the SF95 fuel rod performed by JAERI, five separate samples were taken at different axial locations. From bottom to top, these samples had burnup quantities of 14.3 GWd/MTU, 24.35 GWd/MTU, 35.42

GWd/MTU, 36.69 GWd/MTU, and 30.4 GWd/MTU respectively. Creating different input packages for five different axial locations to match these burnups was time intensive. For simplification purposes, a single experimental axial location with a burnup of 35.42 GWd/MTU was selected and the entire fuel pin was burned to that value. With the average power and reactor operating timeline of the fuel pin known from experimental measurements, a simulation power profile was created for the pin such that it would reach the desired burnup at the end of the simulation. In this simulation we created a burnup profile to match the central SF95 fuel pin sample burnup of 35.42 GWd/MTU. Thirty-one separate time steps were used to burn the fuel pin a total of 787 days. A decay step of 88 days was also introduced into the middle of the simulated operating history. The full burnup profile for all 32 time-steps can be seen in Table 29. The PHOENIX input package created to model the Takahama-3 reactor to a burnup of 35.42 GWd/MTU is provided in Appendix C.

Table 29. Takahama-3 SF95 Burnup Profile to Reach 35.42 GWd/MTU

Time-step	Days Burned/Decayed	Power Fraction
1	12	0.307
2	8	1.227
3	27	1.228
4	35	1.233
5	28	1.221
6	21	1.214
7	35	1.209
8	35	1.190
9	28	1.191
10	27	1.184
11	49	1.167
12	15	1.151
13	37	1.136
14	19	1.124
15	9	1.118
16	88	0.000
17	10	0.263
18	11	1.059
19	20	1.069
20	23	1.074
21	28	1.072
22	28	1.070
23	28	1.068
24	35	1.066
25	28	1.064
26	34	1.061
27	43	1.057
28	28	1.047
29	28	1.037
30	35	1.031
31	15	1.027
32	8	1.025

6.3.2. Takahama-3 Code-to-Code Validation

The results provided during the code-to-code validation of PHOENIX to MONTEBURNS 2.0 for the Takahama-3 fuel pin configuration were well within the specified validation criteria. All reactor parameters and Category 1 isotopes calculated using PHOENIX were less than 5% different from values produced using MONTEBURNS 2.0, with the exception of Nd-148. The reactor parameter and isotopic composition code-to-code validation results for the Takahama-3 fuel pin configuration are provided in Figures 20-22 and Tables 30-33.

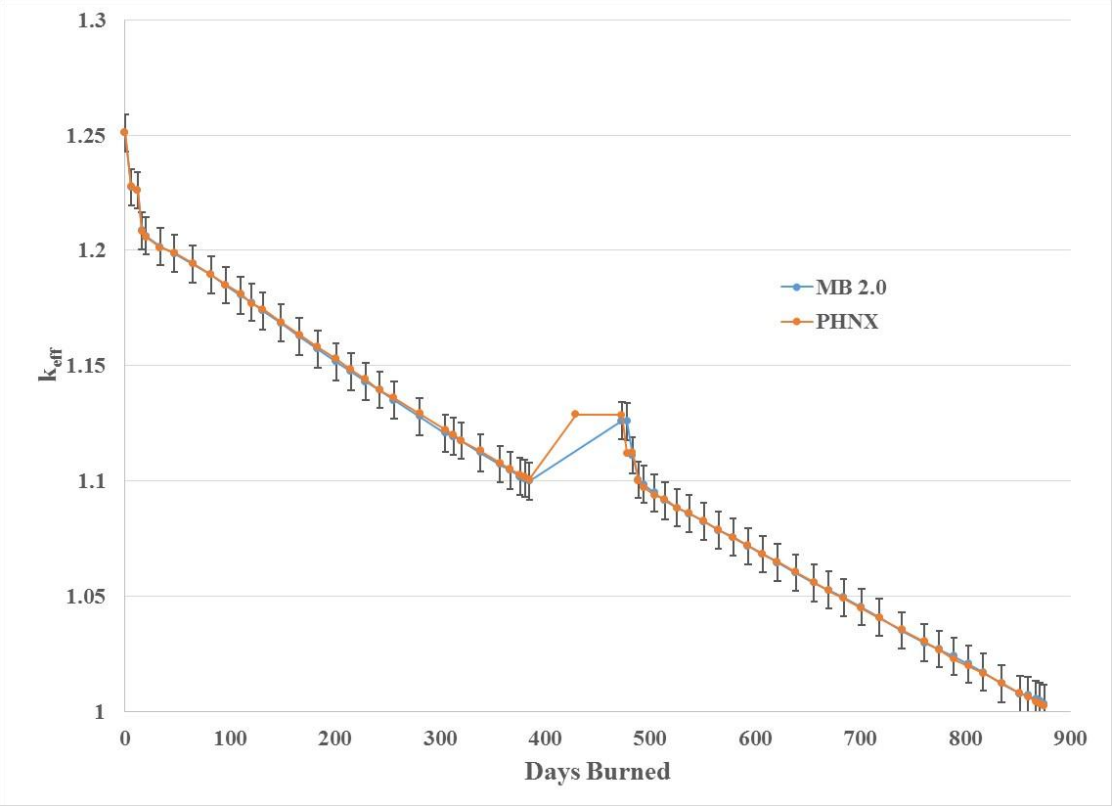

Figure 20. A comparison of k_{eff} produced by MONTEBURNS 2.0 and PHOENIX for every burnup time-step in the Takahama-3 fuel pin model.

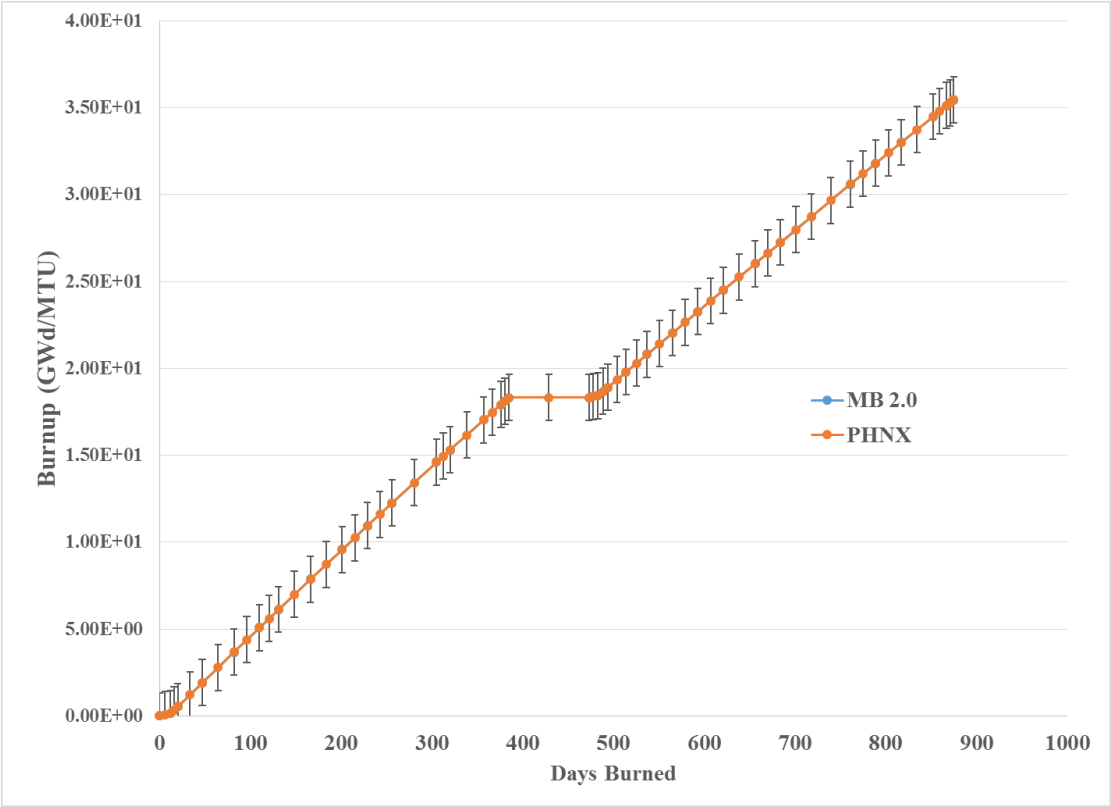

Figure 21. A comparison of burnup produced by MONTEBURNS 2.0 and PHOENIX for every burnup time-step in the Takahama-3 fuel pin model.

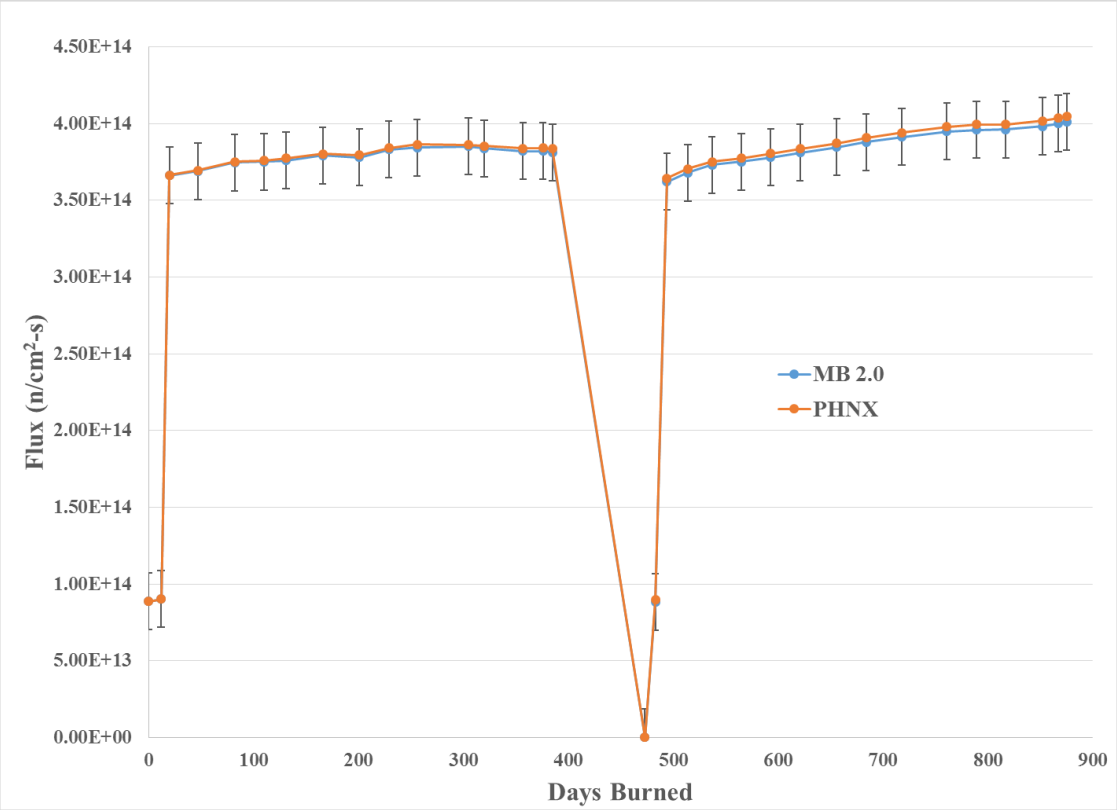

Figure 22. A comparison of neutron flux produced by MONTEBURNS 2.0 and PHOENIX for every burnup time-step in the Takahama-3 fuel pin model.

Table 30. k_{eff} Comparison Between MONTEBURNS 2.0 and PHOENIX for the Takahama-3 Fuel Pin Model

Days	MB 2.0	PHNX	% Difference
0	1.251	1.251	0.00%
12	1.226	1.226	0.01%
20	1.206	1.206	0.04%
47	1.199	1.199	-0.03%
82	1.189	1.189	-0.01%
110	1.181	1.180	-0.05%
131	1.174	1.174	-0.05%
166	1.163	1.163	-0.06%
201	1.153	1.152	-0.11%
229	1.144	1.143	-0.09%
256	1.136	1.135	-0.10%
305	1.122	1.121	-0.13%
320	1.117	1.117	0.01%
357	1.108	1.107	-0.05%
376	1.103	1.102	-0.08%
385	1.101	1.100	-0.06%
473	1.129	1.126	-0.24%
483	1.112	1.111	-0.12%
494	1.097	1.098	0.11%
514	1.092	1.091	-0.05%
537	1.086	1.086	-0.02%
565	1.079	1.079	-0.01%
593	1.072	1.072	-0.03%
621	1.065	1.064	-0.05%
656	1.056	1.056	0.00%
684	1.049	1.049	0.03%
718	1.040	1.041	0.02%
761	1.030	1.030	-0.06%
789	1.023	1.024	0.12%
817	1.017	1.024	0.72%
852	1.008	1.007	-0.02%
867	1.004	1.005	0.11%
875	1.002	1.003	0.09%

Table 31. Burnup Comparison Between MONTEBURNS 2.0 and PHOENIX for the Takahama-3 Fuel Pin Model (GWd/MTU)

Days	MB 2.0	PHNX	% Difference
0	0.000E+00	0.000E+00	---
12	1.510E-01	1.511E-01	0.05%
20	5.538E-01	5.541E-01	0.06%
47	1.913E+00	1.913E+00	0.01%
82	3.684E+00	3.683E+00	-0.01%
110	5.086E+00	5.087E+00	0.01%
131	6.131E+00	6.132E+00	0.02%
166	7.867E+00	7.868E+00	0.00%
201	9.577E+00	9.577E+00	0.00%
229	1.094E+01	1.094E+01	0.00%
256	1.226E+01	1.225E+01	-0.02%
305	1.460E+01	1.460E+01	0.01%
320	1.531E+01	1.531E+01	0.01%
357	1.704E+01	1.703E+01	-0.01%
376	1.791E+01	1.791E+01	0.00%
385	1.833E+01	1.832E+01	-0.01%
473	1.833E+01	1.832E+01	-0.01%
483	1.843E+01	1.843E+01	0.00%
494	1.891E+01	1.891E+01	0.01%
514	1.979E+01	1.979E+01	0.02%
537	2.080E+01	2.080E+01	0.00%
565	2.204E+01	2.203E+01	-0.01%
593	2.327E+01	2.326E+01	-0.01%
621	2.450E+01	2.449E+01	0.00%
656	2.603E+01	2.602E+01	-0.01%
684	2.725E+01	2.725E+01	-0.02%
718	2.873E+01	2.873E+01	-0.02%
761	3.060E+01	3.060E+01	-0.02%
789	3.181E+01	3.180E+01	-0.03%
817	3.300E+01	3.299E+01	-0.04%
852	3.448E+01	3.447E+01	-0.05%
867	3.512E+01	3.510E+01	-0.05%
875	3.545E+01	3.544E+01	-0.04%

Table 32. Neutron Flux Comparison Between MONTEBURNS 2.0 and PHOENIX for the Takahama-3 Fuel Pin Model (n/cm^2-s)

Days	MB 2.0	PHNX	% Difference
0	8.870E+13	8.869E+13	-0.01%
12	9.020E+13	9.027E+13	0.07%
20	3.661E+14	3.664E+14	0.07%
47	3.690E+14	3.696E+14	0.16%
82	3.746E+14	3.752E+14	0.16%
110	3.751E+14	3.760E+14	0.22%
131	3.760E+14	3.775E+14	0.39%
166	3.791E+14	3.801E+14	0.26%
201	3.780E+14	3.794E+14	0.37%
229	3.830E+14	3.842E+14	0.31%
256	3.843E+14	3.863E+14	0.52%
305	3.850E+14	3.861E+14	0.28%
320	3.837E+14	3.854E+14	0.44%
357	3.820E+14	3.838E+14	0.46%
376	3.820E+14	3.840E+14	0.52%
385	3.813E+14	3.835E+14	0.57%
473	0.000E+00	0.000E+00	---
483	8.816E+13	8.968E+13	1.71%
494	3.620E+14	3.643E+14	0.64%
514	3.680E+14	3.706E+14	0.71%
537	3.730E+14	3.751E+14	0.57%
565	3.751E+14	3.775E+14	0.64%
593	3.780E+14	3.806E+14	0.68%
621	3.810E+14	3.837E+14	0.70%
656	3.847E+14	3.871E+14	0.62%
684	3.880E+14	3.908E+14	0.71%
718	3.911E+14	3.942E+14	0.78%
761	3.949E+14	3.980E+14	0.79%
789	3.959E+14	3.994E+14	0.88%
817	3.961E+14	3.994E+14	0.83%
852	3.983E+14	4.018E+14	0.87%
867	3.999E+14	4.034E+14	0.89%
875	4.009E+14	4.045E+14	0.91%

Table 33. Isotopic Gram Composition Comparisons Between PHOENIX and MONTEBURNS 2.0 at EOB for the Takahama-3 Fuel Pin Model (grams)

Category 1 Isotopes	**MB 2.0**	**PHNX**	**% Difference**
I-135	1.100E-03	1.135E-03	3.14%
Xe-135	3.603E-04	3.690E-04	2.39%
Cs-133	2.130E+00	2.129E+00	-0.07%
Cs-134	2.330E-01	2.337E-01	0.28%
Cs-137	2.284E+00	2.323E+00	1.69%
Nd-148	7.100E-01	7.557E-01	6.24%
U-234	4.160E-01	4.140E-01	-0.47%
U-235	2.190E+01	2.176E+01	-0.62%
U-238	1.650E+03	1.654E+03	0.24%
Pu-239	9.183E+00	9.181E+00	-0.02%
Pu-240	3.699E+00	3.742E+00	1.17%
Pu-241	2.247E+00	2.266E+00	0.84%
Am-241	5.170E-02	5.234E-02	1.23%
Category 2 Isotopes			
Ru-105	3.220E-04	3.341E-04	3.70%
Sn-125	2.540E-04	1.746E-04	-37.07%
Sb-125	2.540E-02	1.517E-02	-50.45%
Eu-154	5.313E-02	6.895E-02	25.92%
Sm-149	5.084E-03	4.100E-03	-21.44%
Am-242m	9.284E-04	8.576E-04	-7.93%
Cm-242	2.259E-02	2.332E-02	3.20%
Cm-244	4.227E-02	2.131E-02	-65.93%

The failure of Nd-148 to pass the validation criteria is troublesome. Nd-148, in theory, should be one of the best modeled of the Category 1 isotopes. It is stable, has a relatively large fission yield, and is only produced as a result of fission reactions. Therefore, it should be one of the most well modeled isotopes in each of our simulations. In the previous two reactor configurations, we saw differences of less than 1.5% Nd-148 between MONTEBURNS 2.0 and PHOENIX. The reason for the failure of PHOENIX

to model the Nd-148 gram compositions within five percent of MONTEBURNS warranted additional research.

During the code-to-code validation process, the importance fraction feature in both PHOENIX and MONTEBURNS 2.0 was disabled (importance fraction set equal to 1.0 on the PHOENIX input deck). If the importance fraction were enabled, each burnup software would deem different isotopes "important." These "important" isotopes would effect cross-section tallies, which would in-turn effect the criticality of the system. In order to have a true code-to-code comparison, the importance fraction feature was disabled and identical isotopes in each burnup software were tallied. The differences in Nd-148 gram compositions were the result of not including Nd-147 in the tallied isotopes. For a PWR flux spectrum, the (n,γ) cross-section produced by COUPLE to use in ORIGEN-S was 140 barns. In the ORIGEN2.2 "PWRU" library, the Nd-147 (n,γ) cross-section is listed at 20 barns. If Nd-147 was added to the MCNP6 deck to be tallied in PHOENIX, its MCNP6 calculated effective one-group cross-section would be 31.84 barns. Not including Nd-147 in the automatically tallied isotopes, as well as disabling the importance fraction, erroneously increased the Nd-148 gram production in PHOENIX due to the high (n,γ) cross-section of Nd-147. For this reason, it is strongly advised that the user not disable the importance fraction feature in order to avoid similar errors. A better representation of Nd-148 production in the Takahama-3 simulation is presented in the following subsection, where the importance fraction feature is enabled.

6.3.3. Takahama-3 Experimental Validation

Another advantage to modeling the SF95 Takahama-3 fuel pin was that we had the ability to benchmark PHOENIX burnup simulations to experimental data. The benchmark isotopic gram compositions of the SF95 fuel pin provided by JAERI were normalized to the weight of the starting uranium in the fuel pin. This method made it easy to compare simulated gram quantities to the experimental data, without actually knowing the gram quantities present in the experiment. The Takahama-3 SF95 fuel pin was modeled in PHOENIX and burned to 35.42 GWd/MTU. A comparison was made using the ratio of the computed-to-experimental result (C/E Ratio) for each isotope's concentration (grams of isotope per gram of initial heavy metal). If the gram compositions from the PHOENIX simulation directly matched those provided by JAERI, an experimental difference ratio of 1.0 would be achieved. If a ratio of greater than 1.0 were to occur, it would mean that PHOENIX predicted a larger gram content for that particular isotope when compared to the experimental data. For these simulations alone, an entirely new isotope suite was selected to match those provided by JAERI. The C/E ratios for PHOENIX and other burnup software for the Takahama-3 SF95 fuel pin can be seen in Table 34.

Table 34. Experimental Validation of PHOENIX and Other Burnup Software to Takahama-3 SF95 Data at 35.42 GWd/MTU

	PHNX	**MB 2.0**	**SAS2H**	**HELIOS**
U-234/Total U	1.25	1.25	1.28	1.27
U-235/Total U	0.98	0.98	0.98	1.02
U-236/Total U	0.99	0.99	1	1.01
U-238/Total U	1.00	1.00	1	1
Am-241	1.05	1.03	1.13	1.19
Am-242m	0.75	0.79	1.03	1.03
Am-243	1.01	0.98	1.16	0.99
Ce-144	0.97	0.95	0.96	0.92
Cm-242	0.72	0.71	0.6	0.83
Cm-243	0.97	0.00	0.81	0.81
Cm-244	1.05	1.00	0.98	0.92
Cm-245	1.16	1.07	0.63	0.93
Cm-246	0.99	0.92	0.91	0.86
Cs-134	0.95	0.94	0.86	0.76
Cs-137	0.97	0.96	0.99	0.97
Eu-154	1.07	1.57	0.98	1.09
Nd-142	0.84	0.87	0.85	N/A
Nd-143	0.97	0.96	0.97	0.98
Nd-144	1.01	1.00	1.01	0.99
Nd-145	1.01	1.01	1	0.99
Nd-146	1.02	1.01	1.01	1
Nd-148	1.01	1.01	0.99	1
Nd-150	0.99	0.99	0.98	0.99
Pu-238	1.02	1.01	0.97	1
Pu-239	0.99	0.98	0.98	1.06
Pu-240	1.01	1.00	1.02	1.01
Pu-241	0.98	0.96	0.95	1.01
Pu-242	1.00	0.98	1.01	0.92
Ru-106	1.29	1.27	1.26	1.23
Sb-125	2.35	3.97	2.13	2.69

On average the simulation results provided by PHOENIX compare well to the SF95 fuel pin experimental results. Compared to MONTEBURNS 2.0, PHOENIX had the better C/E ratios for important isotopes like Cs-137, Eu-154, and Pu-239. The C/E for Cs-137 and Nd-148, which are the isotopes that are most prevalent for determining

reactor operating history, are very close to unity. The closeness to unity of these isotopes is a great indication that PHOENIX and MONTEBURNS 2.0 are modeling burnup correctly. Comparing the Nd-148 C/E in Table 34 to the percent differences in Nd-148 shown in Table 33, it is evident that enabling the importance fraction feature increased the accuracy of Nd-148 predictions. More code-to-code validations should be performed on this configuration in the future to validate that PHOENIX and ORIGEN-S are calculating Nd-148 for the Takahama-3 configuration correctly. It is also important to note that the Cs-137 C/E ratio for MONTEBURNS 2.0 is slightly lower than the one calculated by PHOENIX. In all of the simulations performed by PHOENIX in our code-to-code validation analysis, PHOENIX had slightly larger Cs-137 gram concentrations when compared to MONTEBURNS 2.0. Therefore, we can assert that PHOENIX is more accurate at predicting Cs-137 gram quantities when compared to MONTEBURNS 2.0

Certain isotopes like Ru-106 and Sb-125 are hard to verify comparing simulated to experimental data. Ru-106 is difficult to quantify experimentally due to its short half-life. Sb-125 is hard to simulate because of the complicated decay chain that leads to its production. Therefore, it is no surprise that the C/E ratio for both of these isotopes in Table 34 is large in every burnup software. U-234 is also hard to quantify experimentally using mass spectrometry, so the large differences in C/E are also justified. The most important aspect when looking at the U-234 C/E ratios is that all of the burnup codes used to simulated the Takahama-3 fuel pin share an equal error. Due to the similarities

between the PHOENIX simulations and the SF95 experimental benchmarking results, we can consider PHOENIX validated experimentally for this reactor configuration.

6.3.4. Takahama-3 Perturbation and Regression Analysis

The results from the perturbation validation analysis on the Takahama-3 fuel pin configuration met all validation criteria. In this analysis, a simulation in PHOENIX was performed using the "PERT" method with two U-235 input perturbations of 5 wt%, and 10 wt%. Using data from this simulation, a three point linear regression function was calculated for reactor parameters and isotopic compositions. Reactor parameters and gram compositions were interpolated using this regression analysis for initial fuel perturbations of 3 wt%, 5 wt%, 8 wt%, and 10 wt%. These interpolated values were compared to values computed from four separate "manual" simulations at identical starting enrichments. The percent differences between the interpolated values ("PERT" method) and the simulated values ("manual" method) can be seen in Tables 35-38 for all reactor parameters and gram compositions. All of the percent differences shown in Tables 35-38 meet the validation criteria for the perturbation validation analysis of the Takahama-3 fuel pin configuration.

Table 35. Percent Difference Between the "PERT" and "manual" Method for Perturbation Validation Analysis of k_{eff} in the Takahama-3 Fuel Pin Model

Day	3%	5%	8%	10%
0	-0.08%	0.01%	-0.01%	1.65%
12	-0.05%	-0.13%	-0.01%	1.63%
20	-0.04%	-0.08%	-0.10%	1.57%
47	-0.09%	-0.08%	0.01%	1.58%
82	-0.06%	-0.03%	0.03%	1.60%
110	0.06%	0.03%	0.08%	1.63%
131	-0.14%	-0.07%	-0.10%	1.51%
166	0.05%	-0.01%	0.07%	1.52%
201	-0.03%	-0.04%	0.04%	1.45%
229	-0.04%	0.03%	0.12%	1.59%
256	-0.01%	-0.02%	0.02%	1.52%
305	-0.01%	0.01%	0.17%	1.45%
320	0.14%	0.12%	0.24%	1.60%
357	0.09%	0.18%	0.26%	1.49%
376	0.07%	0.01%	0.15%	1.39%
385	0.09%	0.13%	0.16%	1.46%
473	0.03%	0.09%	0.05%	1.27%
483	0.04%	0.03%	0.13%	1.36%
494	0.03%	0.10%	0.13%	1.32%
514	0.15%	0.16%	0.34%	1.53%
537	0.18%	0.18%	0.27%	1.45%
565	-0.03%	0.10%	0.11%	1.31%
593	0.15%	0.22%	0.36%	1.41%
621	0.19%	0.20%	0.29%	1.25%
656	0.16%	0.40%	0.50%	1.55%
684	0.04%	0.19%	0.26%	1.22%
718	0.13%	0.32%	0.38%	1.24%
761	0.09%	0.25%	0.46%	1.17%
789	0.22%	0.22%	0.37%	1.05%
817	0.23%	0.33%	0.48%	1.14%
852	0.23%	0.28%	0.50%	1.08%
867	0.25%	0.42%	0.53%	1.05%
875	0.19%	0.33%	0.48%	0.96%

Table 36. Percent Difference Between the "PERT" and "manual" Method for Perturbation Validation Analysis of Burnup in the Takahama-3 Fuel Pin Model

Day	3%	5%	8%	10%
0	---	---	---	---
12	0.56%	-0.55%	-0.88%	-1.18%
20	0.62%	-0.59%	-0.98%	-1.17%
47	0.63%	-0.56%	-0.99%	-1.26%
82	0.65%	-0.55%	-0.99%	-1.25%
110	0.61%	-0.56%	-0.95%	-1.18%
131	0.60%	-0.55%	-0.93%	-1.16%
166	0.60%	-0.59%	-0.93%	-1.18%
201	0.61%	-0.59%	-0.94%	-1.19%
229	0.63%	-0.60%	-0.94%	-1.18%
256	0.60%	-0.58%	-0.93%	-1.16%
305	0.60%	-0.57%	-0.92%	-1.16%
320	0.59%	-0.57%	-0.92%	-1.15%
357	0.58%	-0.56%	-0.91%	-1.15%
376	0.58%	-0.56%	-0.91%	-1.14%
385	0.58%	-0.56%	-0.90%	-1.14%
473	0.58%	-0.56%	-0.90%	-1.14%
483	0.58%	-0.56%	-0.90%	-1.14%
494	0.58%	-0.56%	-0.90%	-1.14%
514	0.57%	-0.55%	-0.89%	-1.12%
537	0.57%	-0.54%	-0.89%	-1.11%
565	0.56%	-0.54%	-0.88%	-1.10%
593	0.56%	-0.54%	-0.88%	-1.10%
621	0.57%	-0.55%	-0.89%	-1.11%
656	0.56%	-0.54%	-0.88%	-1.10%
684	0.56%	-0.54%	-0.88%	-1.10%
718	0.56%	-0.53%	-0.88%	-1.10%
761	0.56%	-0.53%	-0.88%	-1.10%
789	0.57%	-0.54%	-0.89%	-1.11%
817	0.56%	-0.53%	-0.88%	-1.11%
852	0.56%	-0.54%	-0.88%	-1.10%
867	0.56%	-0.53%	-0.88%	-1.10%
875	0.56%	-0.54%	-0.88%	-1.10%

Table 37. Percent Difference Between the "PERT" and "manual" Method for Perturbation Validation Analysis of Neutron Flux in the Takahama-3 Fuel Pin Model

Day	3%	5%	8%	10%
0	-0.04%	-0.20%	-0.24%	-1.36%
12	0.05%	0.06%	-0.09%	-1.23%
20	-0.04%	-0.06%	-0.20%	-1.17%
47	-0.06%	0.01%	-0.24%	-1.22%
82	0.03%	-0.08%	-0.12%	-1.14%
110	-0.02%	-0.01%	-0.15%	-1.11%
131	0.09%	-0.07%	-0.15%	-1.09%
166	-0.12%	-0.20%	-0.27%	-1.31%
201	-0.01%	-0.10%	-0.28%	-1.11%
229	-0.12%	-0.09%	-0.31%	-1.21%
256	0.05%	-0.05%	-0.21%	-1.08%
305	-0.13%	-0.16%	-0.30%	-1.13%
320	0.00%	-0.08%	-0.32%	-1.01%
357	0.01%	-0.17%	-0.30%	-0.93%
376	-0.10%	-0.15%	-0.39%	-0.93%
385	0.01%	-0.18%	-0.41%	-1.09%
473	---	---	---	---
483	-0.15%	-0.19%	-0.35%	-0.96%
494	-0.15%	-0.26%	-0.38%	-1.01%
514	-0.01%	-0.13%	-0.29%	-0.80%
537	-0.13%	-0.23%	-0.33%	-0.89%
565	-0.12%	-0.34%	-0.51%	-0.85%
593	-0.30%	-0.31%	-0.57%	-0.89%
621	-0.12%	-0.22%	-0.50%	-0.72%
656	-0.27%	-0.26%	-0.64%	-0.91%
684	-0.14%	-0.36%	-0.60%	-0.82%
718	-0.18%	-0.41%	-0.60%	-0.62%
761	-0.32%	-0.48%	-0.66%	-0.55%
789	-0.25%	-0.43%	-0.78%	-0.56%
817	-0.33%	-0.47%	-0.79%	-0.55%
852	-0.27%	-0.53%	-0.84%	-0.46%
867	-0.32%	-0.44%	-0.69%	-0.23%
875	-0.27%	-0.45%	-0.78%	-0.25%

Table 38. Percent Difference Between the "PERT" and "manual" Method for Perturbation Validation Analysis of Gram Compositions at EOB in the Takahama-3 Fuel Pin Model

	3%	**5%**	**8%**	**10%**
Ru-105	-0.48%	-0.67%	-1.19%	-3.38%
Sn-125	-0.45%	-0.71%	-1.18%	-3.76%
Sb-125	-0.31%	-0.51%	-0.89%	-2.78%
I-135	-0.47%	-0.61%	-1.03%	-1.43%
Xe-135	0.48%	0.55%	0.74%	-5.18%
Cs-133	-0.30%	-0.47%	-0.80%	-1.28%
Cs-134	-0.45%	-0.89%	-1.34%	-0.20%
Cs-137	-0.33%	-0.54%	-0.89%	-1.18%
Nd-148	-0.36%	-0.59%	-0.90%	-1.10%
Sm-149	0.58%	0.58%	1.00%	-6.00%
Eu-154	-0.48%	-0.77%	-0.05%	-3.61%
U-234	0.00%	0.15%	0.32%	0.20%
U-235	0.79%	1.27%	1.83%	-1.23%
U-238	0.00%	0.01%	0.01%	0.15%
Pu-239	0.26%	0.37%	0.64%	-9.61%
Pu-240	-1.30%	-2.00%	-3.32%	-11.68%
Pu-241	0.55%	0.92%	1.57%	-3.87%
Am-241	1.00%	1.50%	2.43%	-4.88%
Am-242m	1.18%	1.74%	2.74%	-5.08%
Cm-242	0.49%	0.68%	0.94%	-1.69%
Cm-244	0.45%	0.60%	0.84%	-1.42%

Observing the results from Tables 35-38, as the initial fuel enrichment perturbation increases, so does the difference between the "PERT" and "manual" method. This result indicates that a 10 wt% perturbation on this system is approaching the recommended perturbation boundaries. If a large enough perturbation is introduced by the user, the true shape of the regression function may switch from linear to quadratic. At that point the interpolated values produced by a linear regression function may be inaccurate. An example of this is illustrated by the Pu-239 percent difference in

Table 38. The percent difference in Pu-239 gram compositions when comparing wt% perturbations of 8 wt% and 10 wt% increases from 0.64% different to -9.61%. Observations like this are a good indication that the linear regression function is a poor fit for initial fuel perturbations of 10 wt% or higher.

6.4. PFBR Configuration

The PFBR is a 500 MWe, sodium cooled, pool type, MOX fueled reactor. [76] The active core consists of 181 fuel subassemblies, of which 85 are in the inner enrichment zone with 21% PuO_2 content and 96 are in the outer enrichment zone with 28% PuO_2 content. Two rows of depleted UO_2 radial blanket subassemblies surround the active core, followed by one row of steel reflector. Surrounding the steel reflector are boron carbide subassemblies, outside of which are the internal fuel storage locations and then the radial bulk shielding subassemblies of steel and boron carbide. [77]

Inside the core are twelve absorber rods. Nine of these rods constitute the primary control and safety rod system and three constitute the diverse safety rod system. Each fuel subassembly consists of 217 helium bonded fuel pins of 6.6 mm outer diameter, incased in 20% cold worked D9 alloy cladding. [77] The cladding is surrounded by helically wound spacer wires giving a triangular pin pitch of 0.825 mm and a subassembly pitch of 135 mm. [79] Each fuel pin has a 1000 mm column of MOX fuel pellets and 300 mm each of upper and lower blanket columns. The maximum linear power in the fuel pin is 450 W/cm and the initial peak fuel burnup is limited to 200 GWd/MTU. Outside of the fuel zones are 114 radial blanket subassemblies. Each of these radial blanket subassemblies contain 61 pins with an outer diameter of 14.33 mm,

a radial blanket pin triangular pitch of 15.53 mm, and blanket assembly rod length of 1600 mm. [80]

The average neutron flux inside of the PFBR is on the order 10^{15} n/cm^2-s which is two orders of magnitude higher than a typical thermal reactor. Along with an increased neutron flux, the PFBR will also see higher average operating temperatures compared to most thermal reactors. Under steady state operation conditions, the fuel clad will experience temperatures between 400°C and 700°C with transient temperature conditions rising up to 1000°C. [81] The core is cooled using liquid sodium which is circulated through the core using two primary sodium pumps. The sodium enters the core at 397°C and leaves at 547°C. At these temperatures the corresponding densities of the fuel, blanket, and sodium coolant are 11.08, 11.509, and 0.903 g/cm^3 respectively.

The fuel handling is done at 180 effective full power days (EFPD) in a reactor shutdown condition with the sodium coolant at a temperature of 200°C. [80] There are two initial startup core configurations, both burned for 180 EFPD, before the core reaches an "equilibrium" core configuration. Upon reaching an "equilibrium" core configuration, the PFBR core maintains a composition of one-third fresh fuel assemblies, one-third once burned fuel assemblies, and one-third twice burned fuel assemblies. [80] The radial blankets are reloaded in a similar manner. The outer most ring of the radial blanket sees three full 180 EFPD burn cycles, and the inner ring has a split reload configuration. 7/8ths of the inner radial blanket are reloaded every 180 EFPDs, and 1/8th are twice burned and reloaded every 360 EFPDs. The axial blankets are replaced with fresh depleted UO_2 anytime its fuel assembly is reloaded.

A list of general PFBR reactor properties is provided in Table 39. The values in Table 39 are primarily taken from Ref. [80] with additional information from Ref. [79]. A detailed description of the PFBR can be found in Refs. [76] through [81]. The characteristics from Table 39 were used to create the MCNP6 model described in Section 6.3.1. This section describes the PFBR model in detail, and presents PFBR simulation results relevant to PHOENIX validation.

Table 39. PFBR Configuration Parameters

Core parameter	**Value**
Thermal power	1250 MWt
Fuel pellet diameter	5.330 mm
Gap thickness	0.185 mm
Clad thickness	0.450 mm
Pin OD	6.6 mm
Density of fuel	11.08 g/cc
Clad materials	20% CW D9
Clad OD	0.45mm
Equivalent core diam	1990 mm
Active core height	1000 mm
Axial blanket thickness (each)	300 mm
# of pins per fuel subassembly	217
Fuel pin triangular pitch	8.25 mm
Subassembly pitch	135 mm
Radial blanket height	1600 mm
Radial blanket triangular-pitch	15.53 mm
Pins per radial blanket subassembly	61
Plutonium isotopic ratios: Pu-239,240,241,242	68.8/24.6/5.3/1.3 (%)
Core Pu enrichments, inner core / outer core	20.7/27.7 (%)
Primary inlet/outlet temperature (°C)	397/547
Fuel average temperature (°C)	1289
Fuel cycle (EFPD)	180

6.4.1. PFBR Model Description

In the previous three reactor configurations discussed, only a single fuel pin channel was modeled. To show the capabilities of PHOENIX, the entire PFBR core was modeled for this reactor configuration. The MCNP6 input file for this simulation contained three levels of modeling: a PFBR fuel channel, an assembly configuration consisting of multiple fuel channels arranged in a lattice configuration, and the entire core consisting of multiple assembly configurations. In the fuel channel model, the fuel, gap, clad, liquid sodium coolant, axial blanket, plenum, and B_4C top reflector were modeled extensively. The stainless steel shielding above and below was made infinite in the axial direction. This approach models an infinite lattice of fuel pins but allows for axial leakage. An example of the fuel pin channel with its accompanying dimensions is shown in Figure 23. The material characteristics used in the MCNP6 input deck are provided in Table 40.

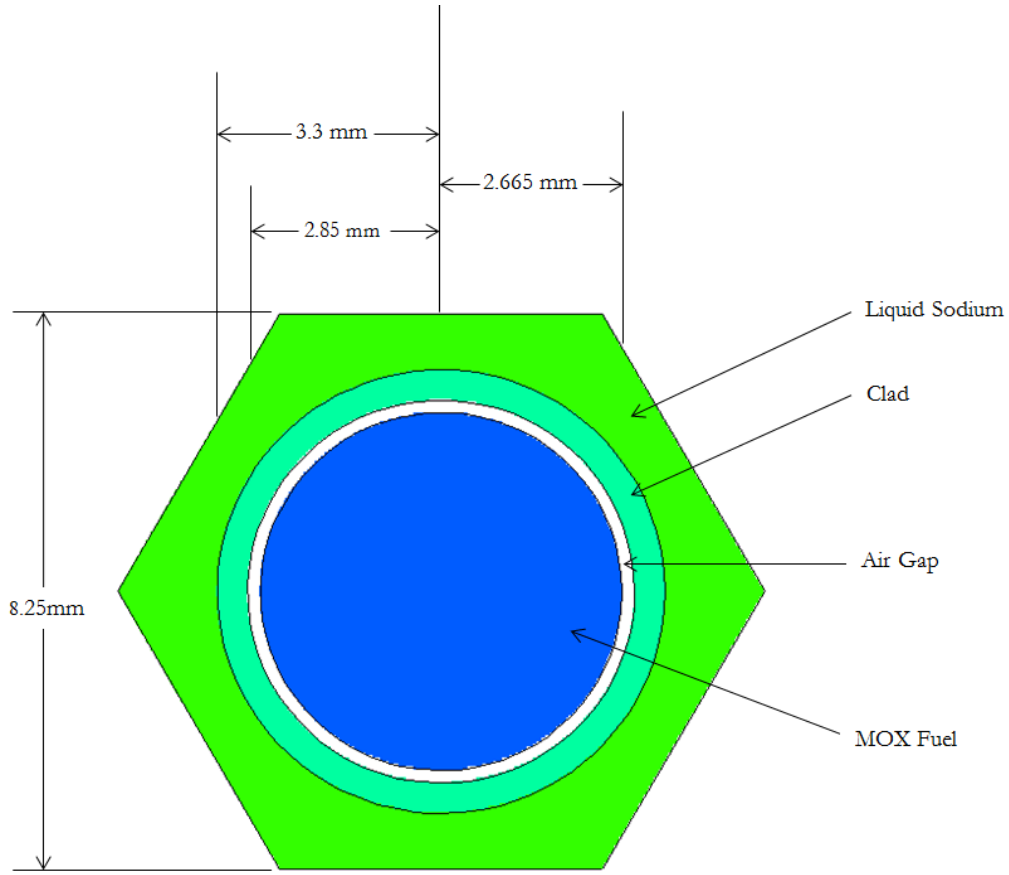

Figure 23. Radial cross-section of individual PFBR fuel channel modeled in MCNP.

Table 40. PFBR MCNP6 Material Characteristics

Material	**Temperature (K)**	**Density (g/cc)**
MOX UO_2-PuO_2 20.7% enrichmen	1200	10.84223
MOX UO_2-PuO_2 27.7% enrichmen	1200	10.87653
Blanket UO_2	1200	11.51
D9 Alloy Cladding	600	8
Liquid Sodium	600	0.90304
Gap He-4	600	0.0001785
CSR and DSR B_4C	600	2.4
Core Stainless Steel	600	4.34

The fuel channels described above were replicated multiple times within a hexagonal lattice that modeled the full PFBR core. The core radial peripheral materials were added and a no-return boundary condition (vacuum boundary condition) was used outside the outer stainless steel reflector. As mentioned previously, three separate core configurations are loaded into a PFBR during its first three 180 EFPD burns before equilibrium conditions are reached. At this time one-third of the fuel assemblies are fresh, one-third of the assemblies are once burned (180 EFPD), and one-third of the assemblies are twice burned (360 EFPD). Since exact core 1 and core 2 configurations are unknown, an equilibrium configuration was used in our full core model. [79] The equilibrium configuration has 97 inner core assemblies (PuO_2 content in MOX is 20.7%), 90 outer core assemblies (PuO_2 content in MOX is 27.7%), 3 DSR, 9 CSR, and 114 radial blanket (Depleted UO_2) assemblies. A cross-sectional view of the equilibrium core configuration can be seen in Figure 24. [79]

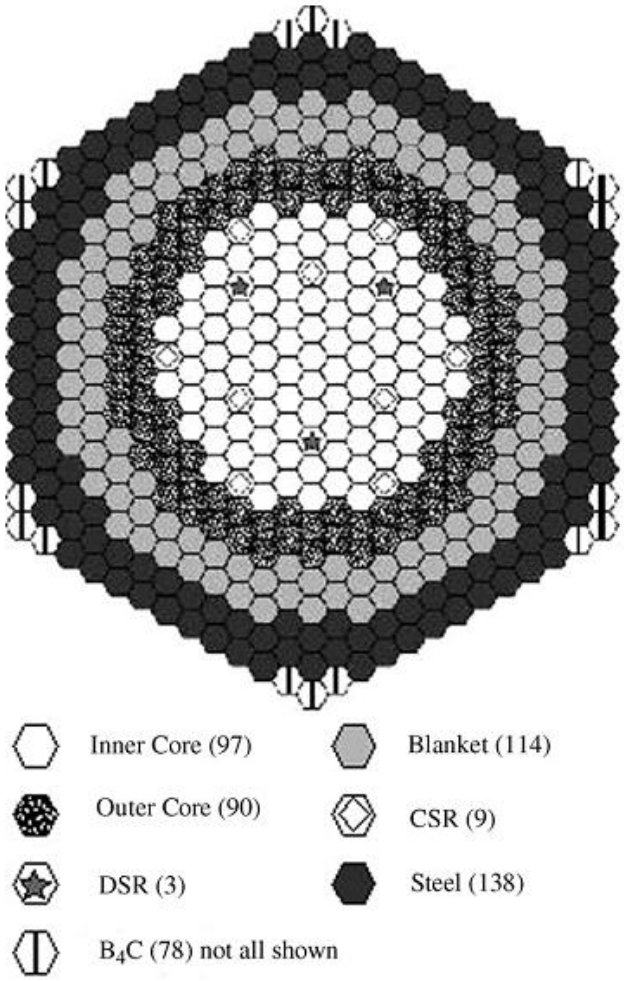

Figure 24. Equilibrium core configuration for a PFBR.

The equilibrium core configuration input deck was created in MCNP6 and can be seen with the PFBR PHOENIX input package in Appendix D. Six total materials were burned in PHOENIX: one material for MOX fuel zone one, another for MOX fuel zone two, one for the natural uranium radial blanket, another for the natural uranium axial blanket, and two separate materials for DSR homogenizations. A radial cutout of the PFBR core modeled in MCNP6 is shown in Figure 25. The properties of all materials used in the full core MCNP6 simulation are shown in Table 40. A “kcode” simulation

was performed using 5,000 particles per cycle, an initial k_{eff} guess of 1.0, and a total of 150 cycles skipping 25 cycles before tallying. An "SDEF" distributed source was used to ensure source locations were spread appropriately throughout the core. A "rand" card was included for adjusting the starting random number seed so the simulation's stochastic uncertainty could be quantified.

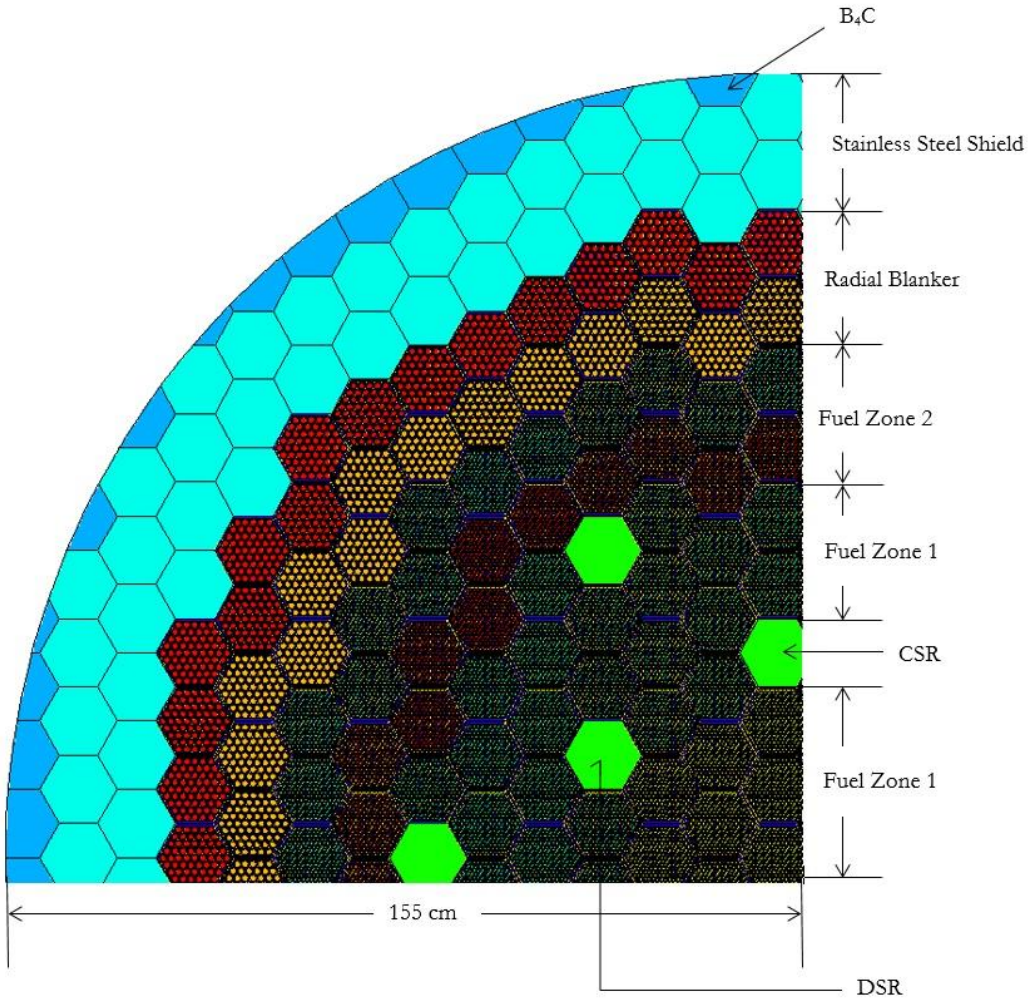

Figure 25. Cross-sectional view of the PFBR core modeled in MCNP6.

The PFBR core was separated into six materials and simulated with a power level of 1250 MWth. The initial guess for the Q-value for fission was set to -196 MeV and calculated by PHOENIX at every time-step. A fractional importance of 1.0 was again used for the reasons expressed in Section 6.1.1. A single predictor step and an end-of-step criticality calculation were also added to the model. A total of seven outer burn steps were used to burn the material 180 total days. The exact location of fuel reloading after the first burnup cycle of 180 days was unknown. Therefore, only the first operating period of 180 days was modeled. Burnup time-step sizes of 0.395833, 29.6042, 30.0, 30.0, 30.0, 30.0 and 30.0 days were used. An additional 45-day decay only step was also included.

6.4.2. PFBR Code-to-Code Validation

The code-to-code validation of PHOENIX to MONTEBURNS 2.0 on the PFBR configuration was performed for two different sections of the PFBR. Since the entire PFBR core was modeled, separate gram composition validations were performed on the homogenized core containing both MOX fuel zones and a homogenized natural uranium blanket. For the purposes of reactor parameter validation, a volume averaged neutron flux was calculated for the entire core. The results for the reactor parameter code-to-code validation can be seen in Figures 26-28 and Tables 41-43. The isotopic gram composition validations for the core and blanket are shown in Table 44 and Table 45, respectively.

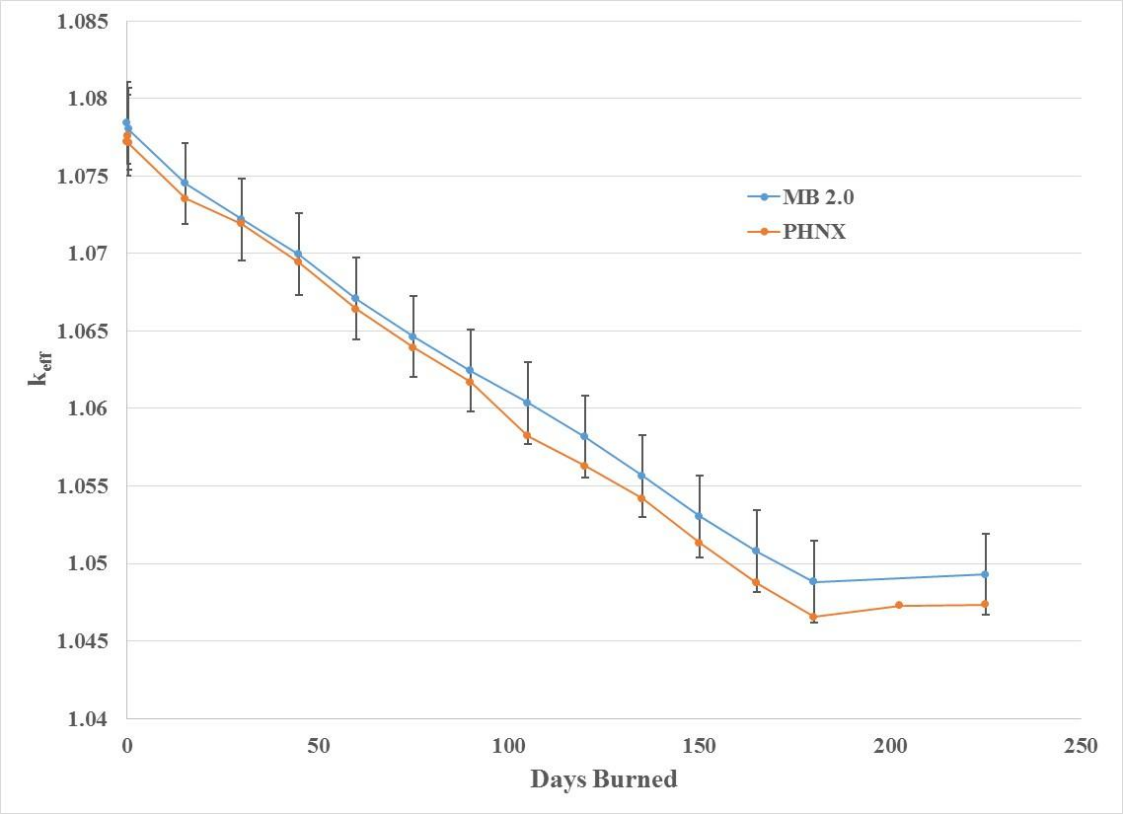

Figure 26. A comparison of k_{eff} produced by MONTEBURNS 2.0 and PHOENIX for every burnup time-step in the PFBR core.

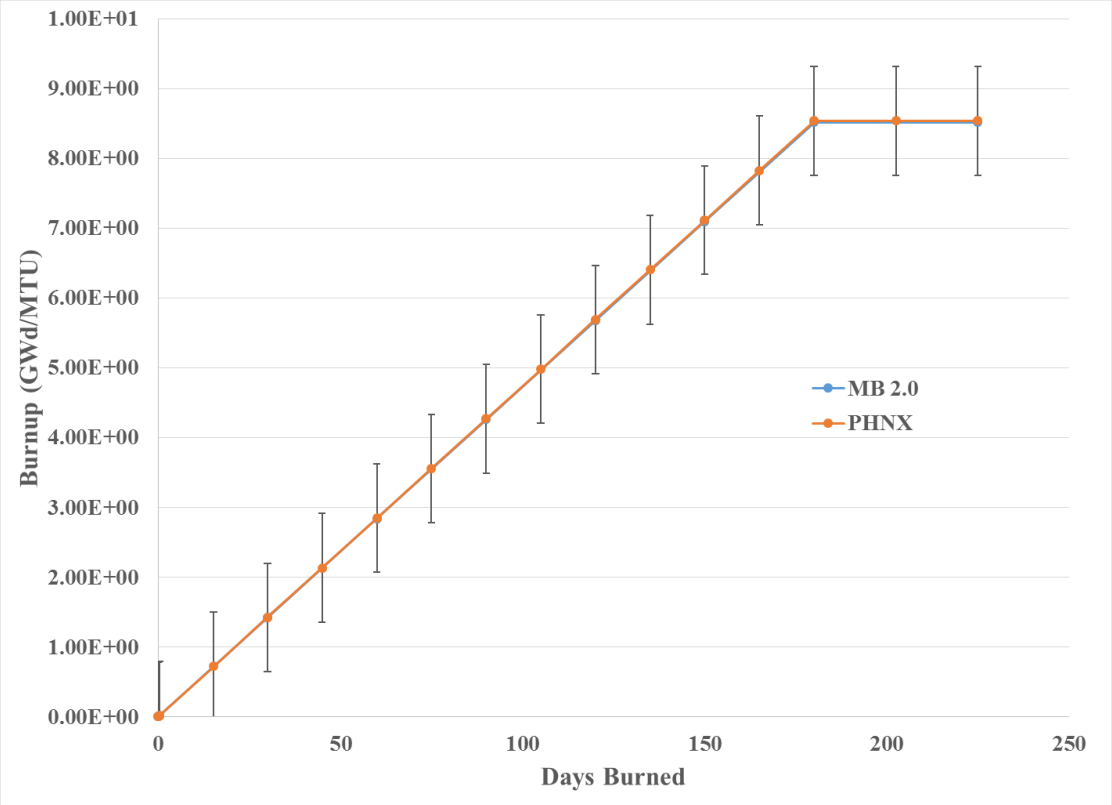

Figure 27. A comparison of burnup produced by MONTEBURNS 2.0 and PHOENIX for every burnup time-step in the PFBR core.

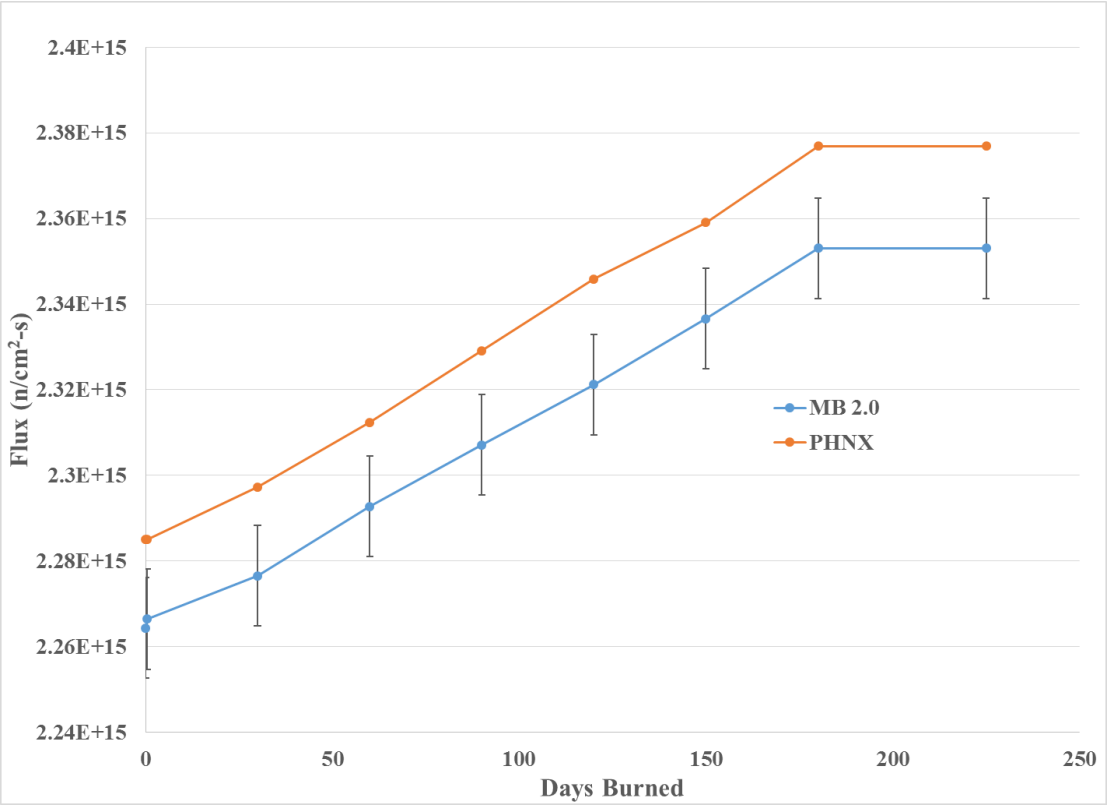

Figure 28. A comparison of the volume averaged neutron flux produced by MONTEBURNS 2.0 and PHOENIX for every burnup time-step in the PFBR core.

Table 41. k_{eff} Comparison Between MONTEBURNS 2.0 and PHOENIX for the PFBR

Days	PHNX	MB 2.0	% Difference
0	1.074	1.077	-0.28%
0.4	1.074	1.077	-0.28%
30	1.069	1.072	-0.28%
60	1.063	1.066	-0.28%
90	1.059	1.062	-0.28%
120	1.053	1.056	-0.28%
150	1.048	1.051	-0.29%
180	1.044	1.047	-0.29%
225	1.044	1.047	-0.29%

Table 42. Volume Averaged Neutron Flux Comparison Between MONTEBURNS 2.0 and PHOENIX for the PFBR (n/cm^2-s)

Days	PHNX	MB 2.0	% Difference
0	2.285E+15	2.264E+15	0.90%
0.4	2.285E+15	2.266E+15	0.82%
30	2.297E+15	2.277E+15	0.91%
60	2.312E+15	2.293E+15	0.86%
90	2.329E+15	2.307E+15	0.95%
120	2.346E+15	2.321E+15	1.06%
150	2.359E+15	2.337E+15	0.96%
180	2.377E+15	2.353E+15	1.01%
225	2.377E+15	2.353E+15	1.01%

Table 43. Burnup Comparison Between MONTEBURNS 2.0 and PHOENIX for the PFBR (GWd/MTU)

Days	PHNX	MB 2.0	% Difference
0	0.000E+00	0.000E+00	0.00%
0.4	1.875E-02	1.872E-02	0.21%
30	1.422E+00	1.419E+00	0.25%
60	2.845E+00	2.838E+00	0.24%
90	4.268E+00	4.258E+00	0.26%
120	5.692E+00	5.677E+00	0.26%
150	7.115E+00	7.096E+00	0.27%
180	8.539E+00	8.515E+00	0.28%
225	8.539E+00	8.515E+00	0.28%

Table 44. Isotopic Gram Composition Comparison between MONTEBURNS 2.0 and PHOENIX for the MOX Fuel Segment in the PFBR at EOB (grams)

Category 1 Isotopes	**MB 2.0**	**PHNX**	**% Difference**
I-135	0.000E+00	2.313E-09	---
Xe-135	0.000E+00	6.984E-06	---
Cs-133	8.167E+03	7.883E+03	-3.54%
Cs-134	1.246E+02	1.290E+02	3.49%
Cs-137	7.910E+03	8.144E+03	2.91%
Nd-148	2.420E+03	2.554E+03	5.40%
U-234	1.623E+00	1.711E+00	5.29%
U-235	1.211E+04	1.207E+04	-0.32%
U-238	5.790E+06	5.793E+06	0.05%
Pu-239	1.214E+06	1.209E+06	-0.42%
Pu-240	4.870E+05	4.909E+05	0.80%
Pu-241	9.458E+04	9.505E+04	0.49%
Am-241	2.700E+03	2.606E+03	-3.54%
Category 2 Isotopes			
Ru-105	0.000E+00	1.868E-14	---
Sn-125	2.347E-01	2.348E+00	163.65%
Sb-125	2.210E+02	1.117E+02	-65.72%
Eu-154	4.123E+01	5.067E+01	20.53%
Sm-149	1.757E+03	1.518E+03	-14.59%
Am-242m	2.880E+01	1.547E+01	-60.19%
Cm-242	6.597E+01	8.784E+01	28.44%
Cm-244	3.108E+01	5.736E+03	197.84%

Table 45. Isotopic Gram Composition Comparison Between MONTEBURNS 2.0 and PHOENIX for the Blanket Segment in the PFBR at EOB (grams)

Category 1 Isotopes	**MB 2.0**	**PHNX**	**% Difference**
I-135	0.000E+00	1.445E-10	---
Xe-135	0.000E+00	4.285E-07	---
Cs-133	3.828E+02	3.874E+02	1.19%
Cs-134	3.092E+00	3.211E+00	3.79%
Cs-137	3.542E+02	3.718E+02	4.85%
Nd-148	1.256E+02	1.318E+02	4.79%
U-234	3.738E-01	3.980E-01	6.26%
U-235	4.120E+04	4.119E+04	-0.04%
U-238	1.775E+07	1.773E+07	-0.11%
Pu-239	1.093E+05	1.094E+05	0.08%
Pu-240	1.319E+03	1.350E+03	2.31%
Pu-241	1.875E+01	1.970E+01	4.97%
Am-241	2.260E-01	2.368E-01	4.67%
Category 2 Isotopes			
Ru-105	0.000E+00	8.773E-16	---
Sn-125	2.487E-02	8.653E-02	110.69%
Sb-125	1.844E+01	4.330E+00	-123.93%
Eu-154	3.958E-01	7.640E-01	63.49%
Sm-149	9.075E+01	7.540E+01	-18.48%
Am-242m	3.528E-04	3.973E-04	11.86%
Cm-242	8.688E-04	2.501E-03	96.88%
Cm-244	6.579E-07	4.424E-03	199.94%

The flux produced by MONTEBURNS 2.0 was more than one standard deviation away from the neutron flux produced in PHOENIX. This was caused by the difference in Q-value of the two simulations as a result of the harder neutron spectrum. In both the core and the blanket, there were Category 1 elements that did not pass the validation criteria. The failure to pass the validation criteria can be attributed to the difference in precision between ORIGEN-S and ORIGEN 2.2, how PHOENIX handles metastable

isotopes compared to MONTEBURNS 2.0, how each software calculates neutron flux, stochastic uncertainty in calculated values, and the different cross-section libraries used by PHOENIX and MONTEBURNS 2.0. The effects of the software differences were present in the three previous fuel channel validation analyses; however, when extrapolated to a core-wide analysis, the differences in values produced by MONTEBURNS 2.0 and PHOENIX were much more pronounced.

In both the core and the blanket, Category 1 actinides are simulated well; however, Category 2 actinides between the two codes have large differences. The large differences in these Category 2 actinides can be attributed to the way ORIGEN-S and ORIGEN 2.2 calculate them. The flux is different in each of these simulations due to the difference in Q-value, and that affects how isotopes are calculated. The difference in flux and Q-value are not strong enough to cause differences of greater than 5% gram compositions for well modeled Category 1 isotopes, but they do create large differences in the Category 2 isotopes. Since these Category 2 isotopes are not present in large quantities in the reactor, their significant percentage differences do not affect reactor parameters like k_{eff} and burnup. Similar to the Takahama-3 model, Nd-148 does not pass the Category 1 validation criteria in the core because the importance fraction feature was disabled. In order to verify that the correct Nd-148 gram compositions are being simulated, Nd-147 needs to be added to the automatic tally isotopes, or the importance fraction feature needs to be enabled. Ultimately, the validation of PHOENIX to MONTEBURNS 2.0 can be confirmed in this case, but due to large differences between some Category 1 isotopes, and all Category 2 isotopes, additional code-to-code

simulations need to be performed. Furthermore, if experimental data existed for this reactor configuration, simulated data should be compared for validation purposes.

6.4.3. PFBR Perturbation and Regression Analysis

The results from the perturbation validation analysis on the PFBR configuration were mixed. A majority of the validation conditions were met successfully. The validation conditions that failed were the result of how υ was calculated in the "PERT" method. In the PFBR validation analysis, a simulation in PHOENIX was performed using the "PERT" method with two Pu-239 input perturbations of 5 wt%, and 10 wt%. Using data from this simulation, a three point linear regression function was calculated for reactor parameters and isotopic compositions. Reactor parameters and gram compositions were interpolated using this regression analysis for initial fuel perturbations of 3 wt%, 5 wt%, 8 wt%, and 10 wt%. These interpolated values were compared to values computed from four separate "manual" simulations at identical starting enrichments. The percent differences between the interpolated values ("PERT" method) and the simulated values ("manual" method) can be seen in Tables 46-50 for all reactor parameters and gram compositions.

Table 46. Percent Difference Between the "PERT" and "manual" Method for Perturbation Validation Analysis of k_{eff} in the PFBR Model

Day	3%	5%	8%	10%
0	-0.13%	-0.08%	-0.09%	-0.04%
0.39583	-0.21%	-0.18%	-0.14%	-0.20%
30	-0.07%	-0.13%	0.00%	-0.13%
60	-0.08%	-0.02%	-0.08%	-0.05%
90	0.03%	0.03%	0.12%	0.15%
120	-0.14%	-0.06%	-0.08%	0.17%
150	-0.19%	-0.06%	-0.06%	0.00%
180	-0.10%	-0.16%	-0.09%	-0.06%
225	0.02%	0.03%	0.00%	-0.02%

Table 47. Percent Difference Between the "PERT" and "manual" Method for Perturbation Validation Analysis of Burnup in the PFBR Model

Day	3%	5%	8%	10%
0	---	---	---	---
0.39583	2.86%	1.75%	0.08%	-1.10%
30	2.69%	1.56%	-0.07%	-1.16%
60	2.57%	1.53%	-0.01%	-1.02%
90	2.40%	1.44%	0.00%	-0.96%
120	2.26%	1.35%	-0.02%	-0.92%
150	2.14%	1.24%	-0.06%	-0.93%
180	2.06%	1.19%	-0.07%	-0.92%
225	2.06%	1.19%	-0.07%	-0.92%

Table 48. Percent Difference Between the "PERT" and "manual" Method for Perturbation Validation Analysis of Volume Average Neutron Flux in the PFBR Model

Day	3%	5%	8%	10%
0	3.03%	1.89%	-0.02%	-1.33%
0.39583	2.97%	1.98%	-0.06%	-1.45%
30	2.72%	1.78%	-0.02%	-1.44%
60	2.35%	1.34%	-0.17%	-1.28%
90	2.09%	1.38%	0.25%	-1.14%
120	2.07%	1.31%	-0.09%	-0.98%
150	1.82%	0.99%	-0.18%	-0.92%
180	1.78%	0.87%	-0.16%	-1.18%
225	---	---	---	---

Table 49. Percent Difference Between the "PERT" and "manual" Method for Perturbation Validation Analysis of Isotopic Gram Compositions for the MOX Fuel Segment in the PFBR Model

	3%	**5%**	**8%**	**10%**
Ru-105	1.41%	0.97%	0.17%	-0.60%
Sn-125	0.55%	-0.21%	-0.20%	1.28%
Sb-125	1.12%	0.20%	-0.01%	1.16%
I-135	1.47%	0.99%	0.20%	-0.56%
Xe-135	1.44%	0.97%	0.18%	-0.57%
Cs-133	1.02%	0.53%	0.29%	2.27%
Cs-134	2.75%	1.81%	0.56%	1.53%
Cs-137	1.75%	1.15%	0.25%	-0.40%
Nd-148	4.42%	3.30%	1.57%	-7.52%
Sm-149	39.24%	18.46%	43.15%	-28.16%
Eu-154	-2.73%	1.67%	-19.94%	-34.53%
U-234	2.58%	0.78%	3.01%	6.72%
U-235	-0.35%	-0.24%	-0.05%	0.08%
U-238	-0.05%	-0.03%	-0.01%	0.01%
Pu-239	-0.14%	-0.07%	0.00%	0.04%
Pu-240	0.12%	0.06%	0.02%	-0.05%
Pu-241	-0.04%	-0.03%	-0.02%	0.00%
Am-241	-0.15%	-0.11%	-0.03%	0.04%
Am-242m	-0.43%	-1.11%	-1.57%	3.01%
Cm-242	1.60%	1.24%	0.33%	-0.90%
Cm-244	-20.25%	-2.53%	-31.55%	-29.52%

Table 50. Percent Difference Between the "PERT" and "manual" Method for Perturbation Validation Analysis of Isotopic Gram Compositions in the Blanket for the PFBR Model

	3%	**5%**	**8%**	**10%**
Ru-105	3.45%	2.29%	5.19%	1.94%
Sn-125	4.07%	2.99%	6.26%	2.51%
Sb-125	3.29%	2.62%	5.12%	1.59%
I-135	2.92%	1.75%	4.36%	1.41%
Xe-135	2.96%	1.80%	4.43%	1.44%
Cs-133	2.27%	1.69%	3.76%	1.11%
Cs-134	5.49%	4.75%	8.95%	4.40%
Cs-137	3.00%	2.34%	4.72%	1.28%
Nd-148	5.63%	4.70%	7.97%	1.54%
Sm-149	30.06%	30.47%	32.26%	-0.55%
Eu-154	16.94%	12.85%	24.98%	5.69%
U-234	-2.29%	-2.01%	-1.94%	-0.07%
U-235	-0.13%	-0.08%	-0.22%	0.03%
U-238	-0.01%	-0.01%	-0.02%	0.00%
Pu-239	1.63%	1.04%	2.89%	-0.43%
Pu-240	12.51%	10.94%	16.86%	3.22%
Pu-241	18.48%	17.73%	27.77%	16.51%
Am-241	18.98%	18.11%	30.70%	16.13%
Am-242m	27.10%	25.07%	43.22%	27.06%
Cm-242	27.46%	25.67%	43.72%	27.10%
Cm-244	-24.32%	-31.22%	-5.54%	34.42%

The relatively large percent differences in Tables 46-50 can be attributed directly to each perturbation method's calculation of υ. As mentioned in Section 4, υ plays an important role in flux calculations. The "manual" method gets the "true" υ output directly from the MCNP6 output file. The "PERT" method calculates υ by tallying the number of fission events in every material input by the user. The "PERT" method has to calculate υ because MCNP6 does not list this parameter for perturbed values in its output

file. When the "PERT" method is used and every fissionable material is not tallied in PHOENIX, or poor sampling statistics exist, the value of υ calculated by PHOENIX may be inaccurate. For this specific example, the "manual" method calculated an average υ value of 2.93. The "PERT" method calculated an average υ of 2.71. This nearly 8% difference in υ is carried into neutron flux calculations, which in turn affect gram quantity calculations by ORIGEN-S. To reduce this error, it is suggested that the user burn all materials containing fissionable actinides in their model, as well as ensure a sufficient number of particles are simulated to have low stochastic uncertainty in the MCNP6 tallies. Taking into account the difference in υ values between the "manual" and "PERT" method, the perturbation validation analysis for the PFBR configuration was successful.

7. CONCLUSIONS AND FUTURE WORK

The intent behind the development of PHOENIX was twofold: to create accurate and time efficient burnup software using modern neutron transport and depletion codes and to implement a new method of uncertainty quantification for burnup simulations using perturbations. Both of these goals were achieved and verified through a rigorous validation analysis on four separate reactor configurations. PHOENIX provides a powerful computational package that is easy to use and provides excellent results. In developing and testing PHOENIX, we have identified the following limitations and areas for future work that might be considered:

1. During the author's process of developing PHOENIX, ORNL began updating SCALE6.1 to SCALE6.2. Included in SCALE6.2 is a completely different version of ORIGEN-S. In the future, PHOENIX should be upgraded to be compatible with SCALE6.2 software in order to continue using the most modern software.
2. Software development is an ongoing process. PHOENIX has been benchmarked to the Takahama-3 Pin Cell measurements, but more benchmarking is needed. [72] At this time PHOENIX is intended for burnup simulations of nuclear reactors. Over time different users may find different applications for PHOENIX, so the output file should also be modified to add more or less information based on user needs.

3. Another potential improvement in PHOENIX is to research more advanced numerical techniques for predicting isotopic quantities at the middle of a burnup time-step. PHOENIX currently uses the predictor-corrector method. This method is simple and accurate, but time consuming. If another numerical technique were developed, the computational time in PHOENIX could be reduced significantly.
4. A current limitation in PHOENIX is that it does not have the ability to add or remove materials during reactor operation. If the user wanted to simulate refueling a reactor, they would have to create two separate PHOENIX runs and use some of the ORIGEN-S composition files in the folder "decks" created by PHOENIX. ORIGEN-S has the ability to add or remove material during depletion or decay steps, so adding this feature to PHOENIX is possible.
5. One assumption that PHOENIX makes is that the neutron flux spectrum does not change significantly over time. Currently PHOENIX tallies a 44 group neutron flux spectrum at the initial time-step, and uses this spectrum in COUPLE to create activation libraries at every future time-step. If the flux spectrum in the system changes over time, the results provided by PHOENIX may be inaccurate. To resolve the potential for neutron flux spectrum inaccuracies, PHOENIX should ask the user if they would like a 44, 49, 200, or 238 group calculation to be performed at every time-step.

There are also limitations imposed on perturbation calculations in PHOENIX. When performing perturbed criticality calculations using an "nps" source definition, PHOENIX cannot calculate a perturbed k_{eff} due to the nature of the PERT card in

MCNP6. Without a k_{eff}, many of the calculations in Section 2.3 cannot be performed. The nature of the PERT card also affects how υ is calculated in perturbed simulations. Because υ is not provided for perturbations in the MCNP6 output file, the only method to calculate it is to use tallies. The total υ value for perturbed systems ends up being a weighted average of all the materials tallied. If there are fissionable materials that are not tallied, the total calculated υ for the system may not be an accurate representation of the "true" υ value.

REFERENCES

[1] D. R. Olander, Fundamental aspects of nuclear reactor fuel elements, Oak Ridge: Energy Research and Developement Administration, 1976.

[2] J. Martinez, O. Cabellos and C. Diez, "Methodologies for an improved prediction of the isotopic content in high burnup samples.," *Annals of Nuclear Energy,* vol. 57, pp. 199-208, 2013.

[3] E. Schneider, M. Deinert and K. Cady, "Cost analysis of the US spent nuclear fuel reprocessing facility," *Energy Economics,* vol. 31, pp. 627-634, 2009.

[4] "Background for position statement 55: nonproliferation background information," American Nuclear Society, LaGrange Park, 2009.

[5] A. Walter, Radiation and modern life, Amherst, New York: Prometheus Books, 2004.

[6] "A special report: protection and management of plutonium," American Nuclear Society, LaGrange Park, 1995.

[7] "Technological opportunities to increase the proliferation resistance of global civilian nuclear power systems (TOPS)," TOPS Task Force of the Nuclear Energy Research Advisory Committee, 2001.

[8] C. Bathke, "The attractiveness of materials in advanced fuel cycles for various proliferation and theft scenarios," in *Global 2009*, Paris, 2009.

[9] R. A. Bari, "Proliferation resistance and physical protection (PR&PP) evaluation

methodology: objectives, accomplishments, and future directions," in *Global 2009*, Paris, 2009.

[10] G. Peter and E. Jones, "Explosive properties of various types of plutonium," in *Managing the Plutonium Surplus; Applications and Technical Options*, Dordrecht, Kluwer, 1994, pp. 23-25.

[11] D. E. Beller and R. A. Krakowski, "Burnup dependence of proliferation attributes of plutonium from spent LWR fuel," Los Alamos National Laboratory, Los Alamos, 1999.

[12] M. Khan, Aslam and N. Ahmad, "Proliferation resistance potential and burnup characteristics of an equilibrium core of novel natural uranium fueled nuclear research reactor," *Annals of Nuclear Energy,* vol. 32, pp. 612-620, 2005.

[13] United States Nuclear Regulator Commision, "US Nuclear Regulatory Commision," December 2013. [Online]. Available: http://www.nrc.gov/reading-rm/doc-collections/fact-sheets/bg-high-burnup-spent-fuel.html. [Accessed 15 July 2014].

[14] A. Isotalo and P. Aarnio, "Higher order methods for burnup calculations with Bateman solutions," *Annals of Nuclear Energy,* vol. 38, pp. 1987-1995, 2011.

[15] B. El Bakkari, T. El Bardouni, B. Nacir, C. El Younoussi, Y. Boulaich, O. Meroun, M. Zoubair and E. Chakir, "Accuracy assessment of a new Monte Carlo based burnup computer code," *Annals of Nuclear Energy,* vol. 45, pp. 29-36, 2012.

[16] F. Leszczynski, "Detailed burnup calculations for testing nuclear data," in *American*

Institute of Physics, 2005.

[17] D. Calic, M. Kromar and A. Trkov, "Use of Monte Carlo and deterministic codes for calculation of plutonium radial distribution in a fuel cell," in *Nuclear Energy for New Europe 2011*, Bovec, 2011.

[18] M. S. Fisher, Software verification and validation an engineering and scientific approach, Springer, 2010.

[19] Y. Jarraya, A. Soeanu, L. Alawneh, M. Debbabi and F. Hassaine, "Synergistic verification and validation of systems and software engineering models," *Inernational Journal of General Systems,* vol. 38, no. 7, pp. 719-746, 2009.

[20] J. D. Arthur and M. K. Groner, "Verification and validation of operational software: A process methodology critique," *Software Process Improvement and Practice,* vol. 9, pp. 157-171, 2004.

[21] C. Ceresio, O. Cabellos, J. Martinez and C. Diez, "Importance of nuclear data uncertainties in criticality calculations," in *2nd Workshop on Neutron Cross Section Covariances,* 2012.

[22] K. Hadad, N. Ayobian and A. Piroozmand, "Quantitative accuracy analysis of burnup calculations for BNPP fuel assemblies using FFTBM method," *Progress in Nuclear Energy,* vol. 51, pp. 170-176, 2009.

[23] Z. Xu, J. Rhodes and K. Smith, "Satistical implications in Monte Carlo depletions," in *Physor 2010 - Advances in Reactor Physics to Power the Nuclear Renaissance,* Pittsburgh, 2010.

[24] "MCNP - A general Monte Carlo N-particle transport code, Version 5," Los Alamos National Laboratory, Los Alamos, 2005.

[25] "Origen 2.2: Isotopic generation and depletion code matrix exponential method," Oak Ridge National Laboratory, Oak Ridge, 2002.

[26] T. O. Mock, Tandem use of Monte Carlo and deterministic methods for analysis of large scale heterogeneous radiation systems, Thesis, Gainsville, Florida: University of Florida, 2007.

[27] J. Leppanen, "Development of a New Monte Carlo Reactor Physics Code," 18 June 2007. [Online]. Available: https://aaltodoc.aalto.fi/bitstream/handle/123456789/2743/isbn9789513870195.pdf?sequence=1. [Accessed 24 June 2014].

[28] J. C. Spall, "Simulation and Monte Carlo some general principles," Johns Hopkins University Applied Physics Laboratory, September 2007. [Online]. Available: http://www.google.com/url?sa=t&rct=j&q=&esrc=s&source=web&cd=2&ved=0CCcQFjAB&url=http%3A%2F%2Fwww.jhuapl.edu%2FISSO%2FPDF-txt%2FSMC_Intro_000.ppt&ei=VKprVPP4G4OrgwS3i4CoDg&usg=AFQjCNGaOfxuZt--5yNWSrazrnoVKe_cXQ&sig2=WKj_38JvO6YhOK3aB3KkpA. [Accessed 15 July 2014].

[29] W. Terry, H. Gougar and A. Ougouag, "Direct deterministic method for neutronics analysis and computation of asymptotic burnup distribution in a recirculating pebble-bed reactor," *Annals of Nuclear Energy*, vol. 29, pp. 1345-1364, 2002.

[30] B. Merk, "On the influence of spatial discretization in LWR-burnup calculations with HELIOS 1.9 - part I: uranium oxide (UOX) fuel," *Annals of Nuclear Energy,* vol. 36, pp. 151-167, 2009.

[31] "HELIOS 2.0 methods," Studsvik Scandpower, Oslo, 2010.

[32] D. Rochman, A. Koning, S. van der marck and C. Sciolla, "Nuclear data uncertainty propagation: perturbation vs. Monte Carlo," *Annals of Nuclear Energy,* vol. 38, pp. 942-952, 2011.

[33] A.-M. Barragan-Martinez, C. Martin-del-Campo, J.-L. Francois and G. Espinosa-Paredes, "MCNPX and HELIOS-2 comparison for the neutronics calculations of a supercritical water reactor HPLWR," *Annals of Nuclear Energy,* vol. 51, pp. 181-188, 2013.

[34] "MONTEBURNS 2.0," Los Alamos National Laboratory, Los Alamos, 2002.

[35] J. Cetnar, "General solution of Bateman equations for nuclear transmutations," *Annals of Nuclear Energy,* vol. 33, pp. 640-645, 2006.

[36] J. E. Turner, Atoms, radiation, and radiation protection second edition, Toronto: John Wiley & Sons, Inc., 1995.

[37] D. B. Pelowitz, "MCNPX user's manual version 2.7.0," Los Alamos National Laboratory, LA-CP-11-00438, Los Alamos, 2011.

[38] C. M. Read Jr., T. W. Knight and K. S. Allen, "Using a modified CINDER90 routine in MCNPX2.6.0 for the prediction of helium production in minor actinide targets," *Nuclear Engineering Data,* vol. 241, pp. 5033-5038, 2011.

[39] W. Wilson, "CINDER90 code for transmutation calculations," in *International Conference on Nuclear Data for Science and Technology*, Trieste, 1997.

[40] Y. Cao, Y. Gohar and C. H. Broeders, "MCNPX Monte Carlo burnup simulations of the isotope correlation experiments in the NPP Obrigheim," *Annals of Nuclear Energy,* vol. 37, pp. 1321-1328, 2010.

[41] X. Ma, L. Wang, Y. Chen, W. Zhong and F. An, "Uncertainties analysis of fission fraction for reactor antineutrino experiments using DRAGON," North China Electric Power University, Beijing, 2014.

[42] G. Marleau, A. Hebert and R. Roy, "A user guide for DRAGON V4," Institut de g´enie nucl´eaire, Montreal, 2014.

[43] G. Marleau, "DRAGON theory manual part 1: collision probability calculations," Institut de g'enie nucl'eaire, Montreal, 2001.

[44] C. E. Sanders and I. C. Gauld, "Isotopic analysis of high-burnup PWR spent fuel samples from the Takahama-3 reactor," Oak Ridge National Laboratory, Oak Ridge, 2003.

[45] C. Jones, "The Takahama-3 benchmark: validating DRAGON for nonproliferation and neutrino oscillations," in *Applied Antineutrino Physics,* Vienna, 2011.

[46] I. D. Hau, W. Russ and F. Bronson, "MCNP HPGe detector benchmark with previously validated Cyltran model," *Applied Radiation and Isotopes,* vol. 2009, pp. 711-715, 2009.

[47] D. P. Gierga, Electron photon calculations using MCNP, Boston: Master's Thesis,

Massachusetts Institue of Technology, 1998.

[48] J. T. Goorley, M. L. Fensin and G. W. Mckinney, "MCNP6 user's manual version 1.0," Los Alamos National Laboratory, Los Alamos, 2013.

[49] Oak Ridge National Laboratory, "SCALE: A comprehensive modeling and simulation suite for nuclear safety analysis and design," Oak Ridge National Laboratory, Oak Ridge, 2011.

[50] I. C. Gauld, "ORIGEN-S: Depletion module to calculate neutron activation, actinide transmutation, fission product generation, and radiation source terms," Oak Ridge National Laboratory, Oak Ridge, 2011.

[51] I. C. Gauld and D. Wiarda, "COUPLE: A nuclear decay and cross section data processing code for creating ORIGEN-S llibraries," Oak Ridge National Laboratory, Oak Ridge, 2011.

[52] J. Helton, "Uncertainty and sensitivity analysis in the presence of stochastic and subjective uncertainty," *Journal of Statistical Computation and Simulation,* vol. 57, no. 1-4, pp. 3-76, 2007.

[53] B. T. Mervin, "Uncertainty underprediction in Monte Carlo eigenvalue calculations," *Nuclear Science and Engineering,* vol. 173, pp. 276-292, 2013.

[54] H. J. Shim, "Real variance estimation using an intercycle fission source correlation for Monte Carlo eigenvalue calculations," *Nuclear Science and Engineering,* vol. 162, pp. 98-108, 2009.

[55] M. Sternat and W. S. Charlton, "Monte-Carlo burnup calculation uncertainty

quantification and propagation determination," in *International Conference on Mathematics and Computation Methods Applied to Nuclear Science and Engineering*, Rio de Janeiro, Brazil, 2011.

[56] K. P. Kumar and J. Sobandari, "Estimation of uncertainties in absolute neutron cross-section measurement," *Annals of Nuclear Energy,* vol. 4, pp. 229-233, 1993.

[57] H. J. Park, H. J. Shim and C. H. Kim, "Uncertainty propagation in Monte Carlo depletion analysis," *Nuclear Science and Engineering,* vol. 167, pp. 196-208, 2011.

[58] T. Takeda, N. Hirokawa and T. Noda, "Estimation of error propagation in Monte-Carlo burnup calculations," *Nuclear Science and Technology,* vol. 36, p. 738, 1999.

[59] M. Tohjoh, E. Tomohiro, M. Watanabe and A. Yamamoto, "Effect of error propagation of nuclide number densities on Monte Carlo burn-up calculations," *Annals of Nuclear Energy,* vol. 33, pp. 1424-1436, 2006.

[60] N. Garcia-Herranze, O. Cabellos, J. Sanz, J. Juan and J. C. Kuijper, "Propagation of statistical and nuclear data uncertainties in Monte Carlo burn-up calculations," *Annals of Nuclear Energy,* vol. 35, pp. 714-730, 2008.

[61] International Nuclear Data Commitee, "Method of estimating the sensitivity of a calculated nuclide vector to deviations in initial data," International Atomic Energy Agency, INDC(CCP)-418, Vienna, 1998.

[62] Q. T. Newell, Quantification of stochastic uncertainty propagation for Monte Carlo depletion methods in reactor analysis, Las Vegas: Master's Thesis, University of Nevada, 2011.

[63] "A summary of error propagation," Fall 2007. [Online]. Available: http://ipl.physics.harvard.edu/wp-uploads/2013/03/PS3_Error_Propagation_sp13.pdf. [Accessed 5 September 2013].

[64] H. R. Trellue, "Development of MONTEBURNS: A code that Links MCNP and ORIGEN2 in an automated fashion for burnup calculations," Los Alamos National Laboratory, Los Alamos, 1998.

[65] C. F. Gerald and P. O. Wheatley, Applied numerical analysis, 5th ed., Massachusetts: Addison-Wesley Publishing Co., 1994.

[66] A. Trkov, M. Herman and D. A. Brown, ENDF-6 formats manual, Upton: Brookhaven National Laboratory, 2012.

[67] W. S. Charlton, W. D. Stanbro and R. Perry, "Comparisons of HEILIOS, ORIGEN2, and MONTEBURNS calculated 241Am and 243Am concentrations to measuerd values for PWR, BWR, and VVER spent fuel," *Nuclear Science and Technology,* vol. 37, no. 7, pp. 615-623, 2000.

[68] A. Talamo, W. Ji, J. Cetnar and W. Gudowski, "Comparison of MCB and MONTEBURNS Monte Carlo burnp," *Annals of Nuclear Energy,* vol. 33, pp. 1176-1188, 2006.

[69] E. Bomboni, N. Cerullo, E. Fridman, G. Lomonaco and E. Shwageraus, "Comparison among MCNP-based depletion codes applied to burnup calculations of pebble-bed HTR lattices," *Nuclear Engineering and Design,* vol. 240, pp. 918-924, 2010.

[70] J. Lebenhaft and H. Trellue, "Mathmatics and computation," [Online]. Available: http://mathematicsandcomputation.cowhosting.net/MC03/Papers/046.pdf. [Accessed 20 June 2013].

[71] E. Larson, "A general description of the NRX reactor," Atomic Energy of Canada Limited, Chalk River, 1961.

[72] Y. Nakahara, K. Sukayama, J. Inagawa, S. Kurosawa, N. Kohno, M. Onuki and H. Mochizuki, "Nuclide composition benchmark for verifying burn-up codes on light water reactor fuels," *Nuclear Technology,* vol. 135, pp. 111-126, 2002.

[73] S. Chetal, V. Balasubramaniyan, P. Chellapandi, P. Mohanakrishnan, P. Puthiyavinayagam, C. Pillai, S. Raghupathy, T. K. Shanmugham and C. S. Pillai, "The design of the Prototype Fast Breeder Reactor," *Nuclear Engineering and Design,* vol. 236, pp. 852-860, 2006.

[74] D. J. Whalen, D. A. Cardon, J. L. Uhle and J. S. Hendricks, "MCNP: neutron benchmark problems," Los Alamos National Laboratory, Los Alamos, 1991.

[75] H. M. Dalle, "Monte Carlo burnup simulation of the Takahama-3 benchmark experiment," in *International Nuclear Atomic Conference*, Rio de Janeiro, 2009.

[76] K. Devan, A. Riyas, M. Alagan and P. Mohanakrishnan, "A new physics design of control safety rods for prototype fast breeder reactors," *Annals of Nuclear Energy,* vol. 35, no. 8, pp. 1484-1491, 2008.

[77] S. M. Lee, S. Govindarajan, R. Indira, T. John, P. Mohanakrishnan, R. S. Singh and S. Bhoje, "Conceptual design of PFBR core," India Gandhi Centre for Atomic

Research, Kalpakkam, 1995.

[78] S. S. Chirayath, G. Hollenbeck, J. Ragusa and P. Nelson, "Neutronic and nonproliferation characteristics of (PuO2-UO2) and (PuO2-ThO2) as fast reactor fuels," *Nuclear Engineering and Design,* vol. 239, pp. 1916-1924, 2009.

[79] A. Glaser and M. V. Ramana, "Weapon-grade plutonium production potential in the Indian Prototype Fast Breeder Reactor," *Science and Gloabal Security,* vol. 15, pp. 85-105, 2007.

[80] B. Raj, S. L. Mannan, P. R. V. RAP and M. D. Mathew, "Developement of fuels and structural materials for fast breeder ractors," *Sadhan a,* vol. 27, no. Part 5, pp. 527-558, 2002.

APPENDIX A

A.1. GODIVA MCNP6 Input

```
 Godiva  Solid Bare HEU sphere  HEU-MET-FAST-001
1          1        4.7984e-02     -1            imp:n=1
2          3       -1E-6            1 -2         imp:n=1
3          4       -1E-6            2 -3 #2      imp:n=1
4          5       -1E-6            3 -4 #2 #3   imp:n=1
5          0                        4            imp:n=0

1          so       8.7407
2          so       10
3          RPP      -20 20 -20 20 -20 20
4          so       60

kcode     10000     1.0  20   220
sdef   cel=1     erg=d1    rad=d2    pos=0.0 0.0 0.0
sp1    -3
si2    0.0    8.7407
sp2    -21    2
rand seed = 27
totnu
c ------------------------------------------------------ ENDF/B-VII -------
m1         92234.70c   4.9184e-04     92235.70c   4.4994e-02
           92238.70c   2.4984e-03
c ------------------------------------------------------------------------
m2         92234.70c   4.9184e-04     92235.70c   4.7244e-02
           92238.70c   2.4984e-03
m3    8016.70c    -1.0
m4    1001.70c    -1.0
m5    2004.70c    -.5
      8016.70c    -.5
c
print
```

A.2. GODIVA PHOENIX Input

```
GODIVA Burn
1                    !Number of MCNP materials to Burn
1  80c                  !MCNP material "m" Numbers
2.79722E+03          !Volume of Cells Containing the Materials
.5                  !Power in MWt
-200                 !Q-value for Fission
800                  !Total Number of Days Burned
8                    !Number of Outer Burn Steps
1                    !Number of Predictor Steps
0                    !Step to Restart After
/home/gspence/MCNP/MCNP_CODE/bin/mcnp6
/home/gspence/MCNP/MCNP_DATA/  ! Data path for MCNP
/home/gspence/scale/cmds/batch6.1          !Scale Executeable
/home/gspence/scale/  ! Data path for SCALE
1.0             !Fractional Importance Limit
```

```
1                !Flag for Intermediate keff Calculations
0                !# of isotopes to perturb (recommend < 3)
22                ! # of isotopes to print Activity (Ci)
441050
501250
511250
531350
541350
551330
551340
551370
601480
621490
631540
922340
922350
922380
942390
942400
942410
952410
952420
952421
962420
962440
22               !Number of Automatic Tally Isotopes
44105.80c
50125.80c
51125.80c
53135.80c
54135.80c
55133.80c
55134.80c
55137.80c
60148.80c
62149.80c
63154.80c
92234.80c
92235.80c
92238.80c
94239.80c
94240.80c
94241.80c
95241.80c
95242.80c
95642.80c
96242.80c
96244.80c
```

APPENDIX B

B.1. NRX MCNP6 Input

```
NRX Monteburns Benchmark Modeling
c Cell Cards
c
10 10  -18.7685   -20     13 -14                        imp:n=1  $ Fuel
2  2   -2.70      20 -2   13 -14                        imp:n=1  $ Clad
3  3   -.9827     2 -3    13 -14                        imp:n=1  $ Coolant
4  2   -2.70      3 -4    13 -14                        imp:n=1  $ Coolant Tube
5  4   -.00279    4 -5    13 -14                        imp:n=1  $ Air Gap
6  2   -2.70      5 -6    13 -14                        imp:n=1  $ Calandria Tube
7  5   -1.092     6 -8    11 -7   10 -12 9   13 -14     imp:n=1  $ Moderator
40 6   -2.10      -13   16 -8   11 -7   10 -12 9                          imp:n=1
$ Graphite Below
41 6   -2.10       14 -17 -8   11 -7   10 -12 9                          imp:n=1
$ Graphite Above
8  0              (7:-11:12:8:-9:-10:-13:14) #40 #41    imp:n=0

c Surface Cards
c
20    cz  1.73     $ Fuel Radius
21    cz  0.790151318 $ Fuel Radius
22    cz  1.343077479  $ Fuel Radius
2    cz  1.83     $ Clad Radius
3    cz  2.11     $ H20 Coolant
4    cz  2.21     $ Coolant tube (Al)
5    cz  2.86     $ Air gap
6    cz  3.02     $ Calandria tube (Al)
*7   p   1 1.73205 0  17.3    $ D20 Moderator
*8   px  8.65                 $ D20 Moderator
*9   p  -1 1.73205 0 -17.3    $ D20 Moderator
*10  p   1 1.73205 0 -17.3    $ D20 Moderator
*11  px -8.65                 $ D20 Moderator
*12   p  -1 1.73205 0  17.3    $ D20 Moderator
13  pz -153
14  pz  153
15  cz  20
16  pz -173
17  pz  173
18  pz -51
19  pz  51

c Data Cards
c
kcode 10000 1.0 25 225
sdef pos = 0 0 -153 axs = 0 0 1 rad = d1 ext = d2
si1 0 1.73
sp1 -21 2
si2 0 306
sp2 -21 0
rand seed = 9
c NatU
m10    92234.70c   -0.0054
```

```
       92235.70c   -0.7114
       92238.70c  -99.2832
c Al (2.7g/cc)
m2    13027.70c   1
c H20
m3    1001.70c    2
      8016.70c    1
mt3   lwtr.11t  $350k
c Air
m4    8016.66c    20
      7014.66c    80
c D20
m5    1002.70c    2
      8016.70c    1
mt5   hwtr.11t  $350k
c Graphite 2.10 g/cc
m6    6000.70c    1
mt6   grph.11t  $400k
```

B.2. NRX PHOENIX Input

```
Candu NRX @ 1300 MWd/t
1                 !Number of MCNP Materials to Burn
10 80c               !MCNP Material "m" Numbers
0                 !Volume of Cells Containing the Materials
0.20833           !Power in MWt
-200.0            !Q-value for Fission
0                 !Total Number of Days Burned
6                 !Number of Outer Burn Steps
0.395833  1.000
19.6042   1.000
79.00     1.000
79.00     1.000
79.00     1.000
80.00     1.000
1                 !Number of Predictor Steps
0                 !Step to Restart After
/home/gspence/MCNP/MCNP_CODE/bin/mcnp6
/home/gspence/MCNP/MCNP_DATA/  ! Data path for MCNP
/home/gspence/scale/cmds/batch6.1          !Scale Executeable
/home/gspence/scale/  ! Data path for SCALE
1.0             !Fractional Importance Limit
1                 !Flag for Intermediate keff Calculations
0
22                 ! # of isotopes to print Activity (Ci)
441050
501250
511250
531350
541350
551330
551340
551370
601480
621490
631540
922340
922350
922380
```

```
942390
942400
942410
952410
952420
952421
962420
962440
22                !Number of Automatic Tally Isotopes
44105.80c
50125.80c
51125.80c
53135.80c
54135.80c
55133.80c
55134.80c
55137.80c
60148.80c
62149.80c
63154.80c
92234.80c
92235.80c
92238.80c
94239.80c
94240.80c
94241.80c
95241.80c
95242.80c
95642.80c
96242.80c
96244.80c
```

APPENDIX C

C.1. Takahama-3 MCNP6 Input

```
Takahama-3 pin SF95 cell 4.11% enriched
c Density is 95% TD
1   1   -10.41   -9  3 -4         imp:n=1
3   2   -6.531    9 -2  3 -4      imp:n=1
4   3   -0.749  -5 6 -7 8 2 3 -4 imp:n=1
5   0   #1 #3 #4                 imp:n=0

1    cz    0.4025 $Fuel OD
2    cz    0.475 $Clad OD
9    cz    0.41  $Clad ID
*3   pz    0.0  $bottom
*4   pz    364.8 $top
c Increased boundary to maintain fuel/mod ratio
*5   px    .6624
*6   px   -.6624
*7   py    .6624
*8   py   -.6624

kcode 100 1.0 20 100
sdef pos = 0 0 0 axs = 0 0 1 rad = d1 ext = d2
si1 0 .41
sp1 -21 2
si2 0 364.8
sp2 -21 0
rand seed = 11
m1    92235.80c     -.036228911
      92238.80c     -.844900523
      92234.80c     -.000352593
      8016.80c      -.118517973
m2    40090.81c     96.0
      24052.81c      4.0
m3    1001.81c     0.66625
      8016.81c     0.33285
      5010.81c     0.00018
      5011.81c     0.00072
mt3   lwtr.62t
print
```

C.2. Takahama-3 PHOENIX Input

```
TK3
1                    !Number of MCNP Materials to Burn
1 80c                   !MCNP Material "m" Numbers
1.92652E+02                    !Volume of Cells Containing the Materials 126
rods@26.975cm^3 of fuel
0.0725               !Power in MWt
-200                 !Q-value for Fission
0.0                  !Total Number of Days Burned
32                   !Number of Outer Burn Steps
12  0.3069
```

```
8   1.2272
27  1.2276
35  1.2333
28  1.2211
21  1.2135
35  1.2091
35  1.1904
28  1.1908
27  1.1840
49  1.1674
15  1.1513
37  1.1357
19  1.1243
9   1.1175
88  0.0000
10  0.2633
11  1.0585
20  1.0687
23  1.0736
28  1.0719
28  1.0699
28  1.0677
35  1.0658
28  1.0636
34  1.0612
43  1.0570
28  1.0470
28  1.0370
35  1.0314
15  1.0268
8   1.0251
1                !Number of Predictor Steps
0                !Step to Restart After
/home/gspence/MCNP/MCNP_CODE/bin/mcnp6
/home/gspence/MCNP/MCNP_DATA/  ! Data path for MCNP
/home/gspence/scale/cmds/batch6.1          !Scale Executeable
/home/gspence/scale/  ! Data path for SCALE
1.0            !Fractional Importance Limit
1                !Flag for Intermediate keff Calculations
0
22                ! # of isotopes to print Activity (Ci)
441050
501250
511250
531350
541350
551330
551340
551370
601480
621490
631540
922340
922350
922380
942390
942400
942410
952410
```

```
952420
952421
962420
962440
22                !Number of Automatic Tally Isotopes
44105.80c
50125.80c
51125.80c
53135.80c
54135.80c
55133.80c
55134.80c
55137.80c
60148.80c
62149.80c
63154.80c
92234.80c
92235.80c
92238.80c
94239.80c
94240.80c
94241.80c
95241.80c
95242.80c
95642.80c
96242.80c
96244.80c
```

APPENDIX D

D.1. PFBR MCNP6 Input

This MCNP6 deck was created by Dr. Sunil Chirayath at Texas A&M University as part of the research into the PFBR. [79] It was modified slightly for validation purposes.

```
FBR Core FIRST CRITICAL With Depleted UO2 Axial and Radial Blanket
1    0     -1 17 -21 fill=1                        imp:n=1   $ Core inner
2    0     -101 102 -103 104 -105 106 lat=2 u=1   imp:n=1
      fill=-13:13 -13:13  0:0
      17 26R
      17 12R                17 17 6 6 6 6 6 6 6 6 6 17 17                17
      17 11R                17 6 6 6 6 6 6 6 6 6 6 6 6 6 17              17
      17 10R                6 6 6 6 9 9 9 9 9 9 9 6 6 6 6                17
      17 9R               6 6 6 9 9 9 9 9 9 9 9 9 9 6 6 6               17
      17 8R              6 6 9 9 9 9 8 8 8 8 8 9 9 9 9 6 6             17
      17 7R             6 6 9 9 9 8 8 8 8 8 8 8 8 9 9 9 6 6            17
      17 6R            6 6 9 9 8 8 8 8 7 23 7 8 8 8 8 9 9 6 6          17
      17 5R          6 6 9 9 8 8 8 19 7 7 7 7 19 8 8 8 9 9 6 6         17
      17 4R          6 6 9 9 8 8 7 7 7 7 7 7 7 7 7 8 8 9 9 6 6         17
      17 3R        6 6 9 9 8 8 23 7 7 27 7 7 23 7 7 23 8 8 9 9 6 6     17
      17 2R         6 6 9 9 8 8 7 7 7 7 7 7 7 7 7 7 7 8 8 9 9 6 6      17
      17 1R       17 6 6 9 9 8 8 7 7 7 7 7 7 7 7 7 7 8 8 9 9 6 6 17    17
      17     17 6 6 9 9 8 8 19 7 23 7 28 19 28 7 27 7 19 8 8 9 9 6 6 17  17
      17          17 6 6 9 9 8 8 7 7 7 7 7 7 7 7 7 7 8 8 9 9 6 6 17    17 1R
      17            6 6 9 9 8 8 7 7 7 7 7 7 7 7 7 7 7 8 8 9 9 6 6      17 2R
      17           6 6 9 9 8 8 23 7 7 27 7 7 23 7 7 23 8 8 9 9 6 6     17 3R
      17              6 6 9 9 8 8 7 7 7 7 7 7 7 7 7 8 8 9 9 6 6        17 4R
      17              6 6 9 9 8 8 8 19 7 7 7 7 19 8 8 8 9 9 6 6        17 5R
      17                6 6 9 9 8 8 8 8 7 23 7 8 8 8 8 9 9 6 6         17 6R
      17                 6 6 9 9 9 8 8 8 8 8 8 8 8 9 9 9 6 6           17 7R
      17                   6 6 9 9 9 9 8 8 8 8 8 9 9 9 9 6 6           17 8R
      17                    6 6 6 9 9 9 9 9 9 9 9 9 9 6 6 6            17 9R
      17                      6 6 6 6 9 9 9 9 9 9 9 6 6 6 6            17 10R
      17                      17 6 6 6 6 6 6 6 6 6 6 6 6 17            17 11R
      17                      17 17 6 6 6 6 6 6 6 6 6 17 17            17 12R
                                                                       17 26R
C   Universe 7 is FUEL SA CORE INNER
3  0 -401 402 -403 404 -405 406 15 -16 fill=2 u=7 imp:n=1   $ SA hex can inner
4  0      -201 202 -203 204 -205 206 lat=2  u=2   imp:n=1
      fill=-9:9 -9:9 0:0
      12 18R
      12 8R            11 11 11 11 11 11 11 11 11                       12
      12 7R           11 11 11 11 11 11 11 11 11 11 11                  12
      12 6R          11 11 11 11 11 11 11 11 11 11 11 11                12
      12 5R         11 11 11 11 11 11 11 11 11 11 11 11 11              12
      12 4R        11 11 11 11 11 11 11 11 11 11 11 11 11 11            12
      12 3R       11 11 11 11 11 11 11 11 11 11 11 11 11 11 11          12
      12 2R      11 11 11 11 11 11 11 11 11 11 11 11 11 11 11 11        12
      12 1R     11 11 11 11 11 11 11 11 11 11 11 11 11 11 11 11 11      12
      12         11 11 11 11 11 11 11 11 11 11 11 11 11 11 11 11 11     12
      12          11 11 11 11 11 11 11 11 11 11 11 11 11 11 11 11 11    12 1R
      12           11 11 11 11 11 11 11 11 11 11 11 11 11 11 11 11 11   12 2R
      12            11 11 11 11 11 11 11 11 11 11 11 11 11 11 11 11     12 3R
      12             11 11 11 11 11 11 11 11 11 11 11 11 11 11 11       12 4R
      12              11 11 11 11 11 11 11 11 11 11 11 11 11 11         12 5R
      12               11 11 11 11 11 11 11 11 11 11 11 11 11           12 6R
      12                11 11 11 11 11 11 11 11 11 11 11                12 7R
```

```
      12                11 11 11 11 11 11 11 11 11                        12 8R
                                                                          12 18R
5  2 -8.00 (-501 502 -503 504 -505 506)    &
(401:-402:403:-404:405:-406) 15 -16   u=7   imp:n=1   $ SA hex can
6  3 -0.90304 (501:-502:503:-504:505:-506) &
       15 -16                              u=7   imp:n=1   $ SA hex can outer
7  11 0.05969518 -10 -15                   u=7   imp:n=1   $ SA bottom
8  12 0.03004312 -10  16 -18               u=7   imp:n=1   $ SA top homo plenum
9  15 0.05386495 -10  18 -19               u=7   imp:n=1   $ Core top SS
10 16 0.05761362 -10  19                   u=7   imp:n=1   $ Core top B4C
11 0              -4    -2                 u=11  imp:n=1   $ plenum bot
13 5 -10.4259218   -4  2 -8              u=11  imp:n=1   $ ax blanket bot
14 24 -.0001785   -26 8 -9                 u=11  imp:n=1   $ fuel hole
15 1 -10.64258118  26 -4  8 -9            u=11  imp:n=1   $ fuel 10.7737803
17 5 -10.4259218   -4  9 -3              u=11  imp:n=1   $ ax blanket top
18 0              -4  3                    u=11  imp:n=1   $ plenum top
19 24 -.0001785  4 -5                       u=11  imp:n=1   $ fuel clad gap
20 2 -8.00      5 -6                       u=11  imp:n=1   $ fuel clad
21 3 -0.90304   6 -7                       u=11  imp:n=1   $ Na out pin
22 3 -0.90304     -7                       u=12  imp:n=1   $ Na filling tube
C Universe 8 is Fuel SA CORE OUTER
23 0 -401 402 -403 404 -405 406 15 -16 fill=3 u=8 imp:n=1   $ SA hex can inner
24 0      -201 202 -203 204 -205 206 lat=2  u=3   imp:n=1
      fill=-9:9 -9:9 0:0
      14 18R
      14 8R            13 13 13 13 13 13 13 13 13                      14
      14 7R           13 13 13 13 13 13 13 13 13 13                    14
      14 6R          13 13 13 13 13 13 13 13 13 13 13                  14
      14 5R         13 13 13 13 13 13 13 13 13 13 13 13                14
      14 4R        13 13 13 13 13 13 13 13 13 13 13 13 13              14
      14 3R       13 13 13 13 13 13 13 13 13 13 13 13 13 13            14
      14 2R      13 13 13 13 13 13 13 13 13 13 13 13 13 13 13          14
      14 1R     13 13 13 13 13 13 13 13 13 13 13 13 13 13 13 13        14
      14       13 13 13 13 13 13 13 13 13 13 13 13 13 13 13 13 13      14
      14        13 13 13 13 13 13 13 13 13 13 13 13 13 13 13 13        14 1R
      14         13 13 13 13 13 13 13 13 13 13 13 13 13 13 13          14 2R
      14          13 13 13 13 13 13 13 13 13 13 13 13 13 13            14 3R
      14           13 13 13 13 13 13 13 13 13 13 13 13 13              14 4R
      14            13 13 13 13 13 13 13 13 13 13 13 13                14 5R
      14             13 13 13 13 13 13 13 13 13 13 13                  14 6R
      14              13 13 13 13 13 13 13 13 13 13                    14 7R
      14               13 13 13 13 13 13 13 13 13                      14 8R
      14 18R
25 2 -8.00 (-501 502 -503 504 -505 506)    &
      (401:-402:403:-404:405:-406) 15 -16   u=8   imp:n=1   $ SA hex can
26 3 -0.90304 (501:-502:503:-504:505:-506) &
       15 -16                              u=8   imp:n=1   $ SA hex can outer
27 11 0.05969518 -10 -15                   u=8   imp:n=1   $ SA bottom
28 12 0.03004312 -10  16 -18               u=8   imp:n=1   $ SA top homo plenum
29 15 0.05386495 -10  18 -19               u=8   imp:n=1   $ Core top SS
30 16 0.05761362 -10  19                   u=8   imp:n=1   $ Core top B4C
31 0              -4    -2                 u=13  imp:n=1   $ plenum bot
33 5 -10.4259218   -4  2 -8              u=13  imp:n=1   $ ax blanket bot
34 24 -.0001785   -26 8 -9                 u=13  imp:n=1   $ fuel hole
35 4 -10.67464722  26 -4  8 -9            u=13  imp:n=1   $ fuel 10.80996965
37 5 -10.4259218   -4  9 -3              u=13  imp:n=1   $ ax blanket top
38 0              -4  3                    u=13  imp:n=1   $ plenum top
39 24 -.0001785  4 -5                       u=13  imp:n=1   $ fuel clad gap
40 2 -8.00      5 -6                       u=13  imp:n=1   $ fuel clad
41 3 -0.90304   6 -7                       u=13  imp:n=1   $ Na out pin
42 3 -0.90304     -7                       u=14  imp:n=1   $ Na filling tube
C Universe 4 is Na tube of FA size
43  3 -0.90304     -10                     u=4   imp:n=1   $ NA filling
C Universe 9 is Radial Blanket SA
44 0 -401 402 -403 404 -405 406 22 -20 fill=5 u=9 imp:n=1   $ SA hex can inner
45 0 -301 302 -303 304 -305 306 lat=2       u=5   imp:n=1
      fill=-5:5 -5:5 0:0
```

```
      16 10R
      16 4R                 15 15 15 15 15                16
      16 3R                15 15 15 15 15 15              16
      16 2R               15 15 15 15 15 15 15            16
      16 1R              15 15 15 15 15 15 15 15          16
      16                15 15 15 15 15 15 15 15 15        16
      16                 15 15 15 15 15 15 15 15          16 1R
      16                  15 15 15 15 15 15 15            16 2R
      16                   15 15 15 15 15 15              16 3R
      16                    15 15 15 15 15                16 4R
      16 10R
46 2 -8.00 (-501 502 -503 504 -505 506)    &
     (401:-402:403:-404:405:-406) 22 -20    u=9   imp:n=1   $ SA hex can
47 3 -0.90304 (501:-502:503:-504:505:-506) &
      22 -20                                u=9   imp:n=1 $ SA hex can out
48 11 0.05969518 -10 -15                    u=9   imp:n=1   $ SA bottom
49 13 0.06846700 -10  15 -22                u=9   imp:n=1   $ RBPSS
50 14 0.02912191 -10  20 -18                u=9   imp:n=1   $ RBPT
51 15 0.05386495 -10  18 -19                u=9   imp:n=1   $ RBSS top
52 16 0.05761362 -10  19                    u=9   imp:n=1   $ RBB4C top
53 0               -11 -2                   u=15  imp:n=1   $ rad blank ple bot
54 6 -10.59230329 -11  2 -3                 u=15  imp:n=1   $ rad blanket
55 0              -11  3                    u=15  imp:n=1   $ rad blank ple top
56 24 -.0001785    11 -12                   u=15  imp:n=1   $ blank clad gap
57 2 -8.00         12 -13                   u=15  imp:n=1   $ blanket clad
58 3 -0.90304      13 -10                   u=15  imp:n=1   $ NA out blanket
59 3 -0.90304     -10                       u=16  imp:n=1   $ NA filling tube
C Universe 6 is SS reflector SA
60 11 0.05969518  -10 -15                   u=6   imp:n=1   $ SS Refl Ass bot
61 7  0.09365394  -10  15 -8                u=6   imp:n=1   $ SS Reflector B4C
62 8  0.06154800  -10  8  -20               u=6   imp:n=1   $ SS Reflector
63 14 0.02912191  -10  20 -18               u=6   imp:n=1   $ SS reflector top
64 7  0.09365394  -10  18                   u=6   imp:n=1   $ SS refle B4C top
C Universe 17 is B4C Shield SA
65 11 0.05969518  -10  -15                  u=17  imp:n=1   $ B4C SHLD bottom
66 17 0.01835245  -10  15 -23               u=17  imp:n=1   $ SHLD Plenum bot
67 7  0.09365394   -10 23 -24               u=17  imp:n=1   $ B4C Shld I layer
68 17 0.01835245  -10  24 -25               u=17  imp:n=1   $ SHLD Plenum top
69 18 0.06221962  -10  25                   u=17  imp:n=1   $ SHLD SS top
C Universe 18 is CSR/DSR
70 9  0.03393119   -10 -8                   u=18  imp:n=1   $ CSR/DSR bottom
71 10 0.06340921   -10  8 -14               u=18  imp:n=1   $ CSR/DSR
72 9  0.03393119   -10  14                  u=18  imp:n=1   $ CSR/DSR top
C Universe 19 is Diluent SA
73 11 0.05969518 -10 -15                    u=19  imp:n=1   $ SA bottom
74 13 0.06846700 -10  15 -22                u=19  imp:n=1   $ RBPSS
75 20 0.02324489 -10  22 -2                 u=19  imp:n=1   $ RB Plenum bot
76 19 0.05133189 -10  2  -3                 u=19  imp:n=1   $ Diluent with RBP
77 20 0.02324489 -10  3  -20                u=19  imp:n=1   $ RB Plenum top
78 14 0.02912191 -10  20 -18                u=19  imp:n=1   $ RBPT
79 15 0.05386495 -10  18 -19                u=19  imp:n=1   $ RBSS top
80 16 0.05761362 -10  19                    u=19  imp:n=1   $ RBB4C top
C Universe 23 is pinwise CSR
81 0 -401 402 -403 404 -405 406 36 -37 fill=22 u=23 imp:n=1 $ SA hex can inner
82 0 -601 602 -603 604 -605 606 lat=2       u=22  imp:n=1
      fill=-3:3 -3:3 0:0
      21 6R
      21 2R                   20 20 20                  21
      21 1R                 20 20 20 20                 21
      21                   20 20 20 20 20               21
      21                    20 20 20 20                 21 1R
      21                      20 20 20                  21 2R
      21 6R
83 2 -8.00 (-501 502 -503 504 -505 506)    &
     (401:-402:403:-404:405:-406) 36 -37    u=23  imp:n=1   $ SA hex can
84 3 -0.90304 (501:-502:503:-504:505:-506) &
      36 -37                                u=23  imp:n=1   $ SA hex can out
```

```
85 9 0.03393119 -10 -36                    u=23  imp:n=1   $ CSR Follower bot
86 9 0.03393119 -10  37                    u=23  imp:n=1   $ CSR Follower top
87 22 -2.4        -27 -40                  u=20  imp:n=1   $ CSR pin bot
88 21 -2.4        -27  40 -41              u=20  imp:n=1   $ CSR pin mid
89 22 -2.4        -27  41                  u=20  imp:n=1   $ CSR pin top
90 24 -.0001785    27 -28                  u=20  imp:n=1   $ CSR clad gap
91 2 -8.00         28 -29                  u=20  imp:n=1   $ CSR clad
92 3 -0.90304      29 -10                  u=20  imp:n=1   $ NA out CSR
93 3 -0.90304     -10                      u=21  imp:n=1   $ NA filling tube
C Universe 27 is pinwise DSR
94 0 -401 402 -403 404 -405 406 38 -39 fill=26 u=27 imp:n=1 $ SA hex can inner
95 0 -601 602 -603 604 -605 606 lat=2      u=26  imp:n=1
      fill=-3:3 -3:3 0:0
      25 6R
      25 2R                    24 24 24                  25
      25 1R                  24 24 24 24                 25
      25                    24 24 24 24 24               25
      25                     24 24 24 24                 25 1R
      25                       24 24 24                  25 2R
      25 6R
96 2 -8.00 (-501 502 -503 504 -505 506)    &
     (401:-402:403:-404:405:-406) 38 -39    u=27  imp:n=1   $ SA hex can
97 3 -0.90304 (501:-502:503:-504:505:-506) &
      38 -39                               u=27  imp:n=1   $ SA hex can out
98 9 0.03393119 -10 -38                    u=27  imp:n=1   $ DSR Follower bot
99 9 0.03393119 -10  39                    u=27  imp:n=1   $ DSR Follower top
100  21 -2.4        -33                    u=24  imp:n=1   $ DSR pin mid
101  24 -.0001785    33 -34                u=24  imp:n=1   $ DSR clad gap
102  2 -8.00         34 -35                u=24  imp:n=1   $ DSR clad
103  3 -0.90304      35 -10                u=24  imp:n=1   $ NA out DSR
104  3 -0.90304     -10                    u=25  imp:n=1   $ NA filling tube
C Universe 28 is ALSO Diluent SA (for Monteburns purpose modified)
105 11 0.05969518 -10 -15                  u=28  imp:n=1   $ SA bottom
106 13 0.06846700 -10  15 -22              u=28  imp:n=1   $ RBPSS
107 20 0.02324489 -10  22 -2               u=28  imp:n=1   $ RB Plenum bot
108 23 0.05133189 -10  2  -3               u=28  imp:n=1   $ Diluent with RBP
109 20 0.02324489 -10  3  -20              u=28  imp:n=1   $ RB Plenum top
110 14 0.02912191 -10  20 -18              u=28  imp:n=1   $ RBPT
111 15 0.05386495 -10  18 -19              u=28  imp:n=1   $ RBSS top
112 16 0.05761362 -10  19                  u=28  imp:n=1   $ RBB4C top
113 0 1:-17:21 imp:n=0

1    cz  155                                               $ core vessel rad
2    pz  0                                                 $ blanket bottom
3    pz  160                                               $ blanket top
4    cz  0.2775                                            $ fuel pellet rad
5    cz  0.285                                             $ fuel clad ID
6    cz  0.33                                              $ fuel clad OD
7    cz  5.0                                               $ outer pin Na
8    pz  30                                                $ bot blank end
9    pz  130                                               $ top blank start
10   cz  20                                                $ dummy NA
11   cz  0.638                                             $ radi blank rad
12   cz  0.6565                                            $ blank clad ID
13   cz  0.7165                                            $ blank clad OD
14   pz  141                                               $ CRF top Start
15   pz  -75                                               $ plenum bottom
16   pz  183                                               $ plenum top
17   pz  -101                                              $ SA bottom
18   pz  191.5                                             $ remaining plenum
19   pz  257.0                                             $ SA SS top
20   pz  170                                               $ Rad blnk ple top
21   pz  267                                               $ Core B4C top
22   pz  -60                                               $ RB ple bot SS
23   pz  3.9                                               $ SHLD plenum bot
24   pz  238.2                                             $ B4C shld top
25   pz  248.4                                             $ SHPL top
```

```
26   cz  0.09                                                    $ fuel annular rad
27   cz  0.87                                                    $ CSRB4C pellet OR
28   cz  1.02                                                    $ CSRB4C clad IR
29   cz  1.12                                                    $ CSRB4C clad OR
C The following three cards are not required any more
C 30   pz  50                                                    $ CSRnatB4C bot
C 31   pz  121                                                   $ CSRnatB4C top
C 32   pz  131                                                   $ DSRB4C top
33   cz  0.89                                                    $ DSRB4C pellet OR
34   cz  1.00                                                    $ DSRB4C clad IR
35   cz  1.07                                                    $ DSRB4C clad OR
C ************************************************************************
C The following PZ's are for pin wise CSR and DSR inserion and withdrawal
C Change the comment card accordingly
C ************************************************************************
C 36   pz  29.0      $ CSR DOWN (bottom edge)
C 37   pz 140.0      $ CSR DOWN (top edge)
36   pz 137.5      $ CSR UP   (bottom edge)
37   pz 248.5      $ CSR UP   (top edge)
C 38   pz  29.5      $ DSR DOWN (bottom edge)
C 39   pz 130.5      $ DSR DOWN (top edge)
38   pz 131.5      $ DSR UP (bottom edge)
39   pz 232.5      $ DSR UP (top edge)
C ********************************************************************************
C following pairs are CSR down &  up >>>  how the pin axial profile change
C ********************************************************************************
C 40   pz  49.0      $ CSR DOWN (bottom nat B4C pin top)
C 41   pz 120.0      $ CSR DOWN (mid enrich B4C pin top)
40   pz 157.5      $ CSR UP   (bottom nat B4C pin top)
41   pz 228.5      $ CSR UP   (mid enrich B4C pin top)
C ********************************************************************************
101  px  6.75                                                    $ hexside FA
102  px -6.75                                                    $ hexside FA
103  p   1  1.7320508076 0  13.5                                 $ hexside FA
104  p   1  1.7320508076 0 -13.5                                 $ hexside FA
105  p  -1  1.7320508076 0  13.5                                 $ hexside FA
106  p  -1  1.7320508076 0 -13.5                                 $ hexside FA
201  py  0.4125                                                  $ hexside pin
202  py -0.4125                                                  $ hexside pin
203  p   1.7320508076  1 0  0.825                                $ hexside pin
204  p   1.7320508076  1 0 -0.825                               $ hexside pin
205  p   1.7320508076 -1 0  0.825                                $ hexside pin
206  p   1.7320508076 -1 0 -0.825                               $ hexside pin
301  py  0.8                                                     $ hexside pin
302  py -0.8                                                     $ hexside pin
303  p   1.7320508076  1 0  1.6                                 $ hexside pin
304  p   1.7320508076  1 0 -1.6                                 $ hexside pin
305  p   1.7320508076 -1 0  1.6                                 $ hexside pin
306  p   1.7320508076 -1 0 -1.6                                 $ hexside pin
401  px  6.26                                                    $ hexside FA
402  px -6.26                                                    $ hexside FA
403  p   1  1.7320508076 0  12.52                                $ hexside FA
404  p   1  1.7320508076 0 -12.52                                $ hexside FA
405  p  -1  1.7320508076 0  12.52                                $ hexside FA
406  p  -1  1.7320508076 0 -12.52                                $ hexside FA
501  px  6.58                                                    $ hexside FA
502  px -6.58                                                    $ hexside FA
503  p   1  1.7320508076 0  13.16                                $ hexside FA
504  p   1  1.7320508076 0 -13.16                                $ hexside FA
505  p  -1  1.7320508076 0  13.16                                $ hexside FA
506  p  -1  1.7320508076 0 -13.16                                $ hexside FA
601  py  1.2                                                     $ hexside pin
602  py -1.2                                                     $ hexside pin
603  p   1.7320508076  1 0  2.4                                 $ hexside pin
604  p   1.7320508076  1 0 -2.4                                 $ hexside pin
605  p   1.7320508076 -1 0  2.4                                 $ hexside pin
606  p   1.7320508076 -1 0 -2.4
```

```
kcode 5000 1 25 150 15000
sdef pos = 0 0 0 axs = 0 0 1 rad = d1 ext = d2
si1 0 155
sp1 0 1
si2 s d3 d4 d5
sp2 0.375 0.25 0.375
si3 0 30
sp3 0 1
si4 30 130
sp4 0 1
si5 130 160
sp5 0 1
m1     92235.80c -0.0017256
       92238.80c -0.6973080
       94239.80c -0.1254001
       94240.80c -0.0450321  $ -0.04496
       94241.80c -0.0096691  $ -0.00965
       94242.80c -0.0024919  $ -0.00249
        8016.80c -0.1183732  $ -0.11837  changed wt as per Pu buildup table core I
m2     26000.55c -0.66598
        6000.66c -0.00052
       24000.50c -0.13800
       28000.50c -0.15200
       42000.66c -0.01460
       14000.60c -0.00920
       25055.60c -0.01740
       22000.62c -0.00230                                    $ SS
m3     11023.62c 1.0                                         $ Na
m4     92235.80c -0.0015732  $ -0.00157
       92238.80c -0.6357256  $ -0.63568
       94239.80c -0.1678273  $ -0.16786
       94240.80c -0.0602681  $ -0.06028
       94241.80c -0.0129404  $ -0.01294
       94242.80c -0.0033350  $ -0.00334
        8016.80c -0.1183303  $ -0.11833  changed wt as per Pu buildup table  core II
m5     92235.80c -0.00218
       92238.80c -0.87932
        8016.80c -0.11850                                    $ axial blanket
m6     92235.80c -0.00218
       92238.80c -0.87932
        8016.80c -0.11850                                    $ radial blanket
m7     26054.62c 0.49285e-03
       26056.62c 0.77367e-02
       26057.62c 0.17867e-03
       26058.62c 0.23778e-04
       24050.62c 0.83368e-04
       24052.62c 0.16077e-02
       24053.62c 0.18230e-03
       24054.62c 0.45377e-04
       28058.62c 0.12397e-02
       28060.62c 0.47752e-03
       28061.62c 0.20759e-04
       28062.62c 0.66175e-04
       28064.62c 0.16862e-04
       42000.66c 0.16722e-03
        6012.50c 0.15150e-01
       11023.62c 0.55700e-02
        1001.62c 0.95384e-20
       14000.60c 0.15859e-03
       25055.62c 0.25943e-03
        5010.66c 0.11915e-01
        5011.66c 0.48262e-01                                 $ B4C Shld & SS bot
m8     26054.62c 0.25312e-02
       26056.62c 0.39734e-01
       26057.62c 0.91763e-03
       26058.62c 0.12212e-03
```

```
        24050.62c 0.54017e-04
        24052.62c 0.10417e-02
        24053.62c 0.11812e-03
        24054.62c 0.29402e-04
        28058.62c 0.52485e-02
        28060.62c 0.20217e-02
        28061.62c 0.87891e-04
        28062.62c 0.28017e-03
        28064.62c 0.71392e-04
        42000.66c 0.96251e-03
         6012.50c 0.83109e-04
        11023.62c 0.64104e-02
         1001.62c 0.95384e-20
        14000.60c 0.65748e-03
        25055.62c 0.11766e-02                          $ SS Reflector
m9      26054.62c 0.54798e-03
        26056.62c 0.86021e-02
        26057.62c 0.19866e-03
        26058.62c 0.26438e-04
        24050.62c 0.92692e-04
        24052.62c 0.17875e-02
        24053.62c 0.20268e-03
        24054.62c 0.50453e-04
        28058.62c 0.13783e-02
        28060.62c 0.53091e-03
        28061.62c 0.23080e-04
        28062.62c 0.73574e-04
        28064.62c 0.18748e-04
        42000.66c 0.18592e-03
         6012.50c 0.28365e-04
        11023.62c 0.19719e-01
         1001.62c 0.95384e-20
        14000.60c 0.17636e-03
        25055.62c 0.28844e-03                          $ CSR/DSR follower
m10     26054.62c 0.62343e-03
        26056.62c 0.97865e-02
        26057.62c 0.22601e-03
        26058.62c 0.30078e-04
        24050.62c 0.10546e-03
        24052.62c 0.20336e-02
        24053.62c 0.23060e-03
        24054.62c 0.57401e-04
        28058.62c 0.15682e-02
        28060.62c 0.60405e-03
        28061.62c 0.26260e-04
        28062.62c 0.83709e-04
        28064.62c 0.21330e-04
        42000.66c 0.21153e-03
         5010.66c 0.15779e-01
         5011.66c 0.12131e-01
         6012.50c 0.69823e-02
        11023.62c 0.12380e-01
         1001.62c 0.95384e-20
        14000.60c 0.20061e-03
        25055.62c 0.32817e-03                          $ CSR/DSR homo
m11     26054.62c 0.19242e-02
        26056.62c 0.30205e-01
        26057.62c 0.69757e-03
        26058.62c 0.92834e-04
        24050.62c 0.32548e-03
        24052.62c 0.62765e-02
        24053.62c 0.71170e-03
        24054.62c 0.17716e-03
        28058.62c 0.48398e-02
        28060.62c 0.18643e-02
        28061.62c 0.81046e-04
        28062.62c 0.25835e-03
```

```
        28064.62c 0.65832e-04
        42000.66c 0.65284e-03
         6012.50c 0.99601e-04
        11023.62c 0.97907e-02
         1001.62c 0.95384e-20
        14000.60c 0.61914e-03
        25055.62c 0.10128e-02                    $ SA bottom
m12     26054.62c 0.78387e-03
        26056.62c 0.12305e-01
        26057.62c 0.28418e-03
        26058.62c 0.37819e-04
        24050.62c 0.13260e-03
        24052.62c 0.25571e-02
        24053.62c 0.28995e-03
        24054.62c 0.72175e-04
        28058.62c 0.19717e-02
        28060.62c 0.75950e-03
        28061.62c 0.33018e-04
        28062.62c 0.10525e-03
        28064.62c 0.26820e-04
        42000.66c 0.26597e-03
         6012.50c 0.40578e-04
        11023.62c 0.97126e-02
         1001.62c 0.99184e-20
        14000.60c 0.25224e-03
        25055.62c 0.41263e-03                    $ Core Plenum homog
m13     26054.62c 0.23927e-02
        26056.62c 0.37560e-01
        26057.62c 0.86743e-03
        26058.62c 0.11544e-03
        24050.62c 0.40474e-03
        24052.62c 0.78049e-02
        24053.62c 0.88502e-03
        24054.62c 0.22030e-03
        28058.62c 0.60183e-02
        28060.62c 0.23182e-02
        28061.62c 0.10078e-03
        28062.62c 0.32126e-03
        28064.62c 0.81863e-04
        42000.66c 0.81182e-03
         6012.50c 0.12386e-03
        11023.62c 0.64104e-02
         1001.62c 0.95384e-20
        14000.60c 0.76992e-03
        25055.62c 0.12595e-02                    $ RBPBSS
m14     26054.62c 0.29254e-03
        26056.62c 0.45923e-02
        26057.62c 0.10606e-03
        26058.62c 0.14114e-04
        24050.62c 0.49438e-04
        24052.62c 0.95424e-03
        24053.62c 0.10820e-03
        24054.62c 0.26934e-04
        28058.62c 0.73597e-03
        28060.62c 0.28349e-03
        28061.62c 0.12324e-04
        28062.62c 0.39286e-04
        28064.62c 0.10011e-04
        42000.66c 0.91980e-04
         6012.50c 0.10890e-04
        11023.62c 0.21539e-01
        14000.60c 0.94113e-04
        25055.62c 0.15398e-03                    $ RBPT/RFTSS1
m15      6012.50c 0.83867e-04
        14000.60c 0.52075e-03
        25055.62c 0.85201e-03
        26054.62c 0.16187e-02
```

```
        26056.62c 0.25410e-01
        26057.62c 0.58684e-03
        26058.62c 0.78097e-04
        24050.62c 0.27381e-03
        24052.62c 0.52802e-02
        24053.62c 0.59873e-03
        24054.62c 0.14904e-03
        28058.62c 0.40722e-02
        28060.62c 0.15686e-02
        28061.62c 0.68192e-04
        28062.62c 0.21738e-03
        28064.62c 0.55391e-04
        42000.66c 0.54889e-03
        11023.62c 0.11882e-01                          $ Core-SS
m16      5010.66c 0.47121e-02
         5011.66c 0.19329e-01
         6012.50c 0.60415e-02
        14000.60c 0.19450e-03
        25055.62c 0.31822e-03
        42000.66c 0.20501e-03
        11023.62c 0.11882e-01
        26054.62c 0.60458e-03
        26056.62c 0.94907e-02
        26057.62c 0.21918e-03
        26058.62c 0.29169e-04
        24050.62c 0.10227e-03
        24052.62c 0.19721e-02
        24053.62c 0.22362e-03
        24054.62c 0.55664e-04
        28058.62c 0.15209e-02
        28060.62c 0.58586e-03
        28061.62c 0.25469e-04
        28062.62c 0.81189e-04
        28064.62c 0.20688e-04                          $ Core B4C
m17     26054.62c 0.49285e-03
        26056.62c 0.77367e-02
        26057.62c 0.17867e-03
        26058.62c 0.23778e-04
        24050.62c 0.83368e-04
        24052.62c 0.16077e-02
        24053.62c 0.18230e-03
        24054.62c 0.45377e-04
        28058.62c 0.12397e-02
        28060.62c 0.47752e-03
        28061.62c 0.20759e-04
        28062.62c 0.66175e-04
        28064.62c 0.16862e-04
        42000.66c 0.16722e-03
         6012.50c 0.25512e-04
        11023.62c 0.55700e-02
         1001.62c 0.95384e-20
        14000.60c 0.15859e-03
        25055.62c 0.25943e-03                          $ SHPLenum
m18     26054.62c 0.20590e-02
        26056.62c 0.32322e-01
        26057.62c 0.74646e-03
        26058.62c 0.99340e-04
        24050.62c 0.34829e-03
        24052.62c 0.67164e-02
        24053.62c 0.76158e-03
        24054.62c 0.18957e-03
        28058.62c 0.51790e-02
        28060.62c 0.19949e-02
        28061.62c 0.86726e-04
        28062.62c 0.27646e-03
        28064.62c 0.70445e-04
        42000.66c 0.69860e-03
```

```
         6012.50c 0.10658e-03
        11023.62c 0.88178e-02
         1001.62c 0.95384e-20
        14000.60c 0.66254e-03
        25055.62c 0.10838e-02                                   $ SHLD SS top
m19     92235.80c 0.187309e-04
        92238.80c 0.747364e-02
        26000.55c 0.132470e-01
        24000.50c 0.301425e-02
        28000.50c 0.286071e-02
         8016.80c 0.149847e-01
         6012.50c 0.400788e-04
        11023.62c 0.903609e-02
        14000.60c 0.249138e-03
        25055.62c 0.407556e-03                                  $ diluent homog
m20     26054.62c 0.63886e-03
        26056.62c 0.10029e-01
        26057.62c 0.23161e-03
        26058.62c 0.30823e-04
        24050.62c 0.10807e-03
        24052.62c 0.20840e-02
        24053.62c 0.23631e-03
        24054.62c 0.58822e-04
        28058.62c 0.16070e-02
        28060.62c 0.61899e-03
        28061.62c 0.26910e-04
        28062.62c 0.85781e-04
        28064.62c 0.21858e-04
        42000.66c 0.21676e-03
         6012.50c 0.33070e-04
        11023.62c 0.66755e-02
         1001.62c 0.95384e-20
        14000.60c 0.20557e-03
        25055.62c 0.33629e-03                                   $ Blanket plenum
m21      5010.66c 0.52
         5011.66c 0.28
         6012.50c 0.20                                          $ pinwise CSRmid/DSR
m22      5010.66c 0.1592
         5011.66c 0.6408
         6012.50c 0.2000                                        $ pinwise CSRtop/bot
m23     92235.80c 0.187309e-04
        92238.80c 0.747364e-02
        26000.55c 0.132470e-01
        24000.50c 0.301425e-02
        28000.50c 0.286071e-02
         8016.60c 0.149847e-01
         6012.50c 0.400788e-04
        11023.62c 0.903609e-02
        14000.60c 0.249138e-03
        25055.62c 0.407556e-03                                  $ diluent homog  for
monteburns purpose
m24     002004.73c 1.0
c tmp 6.42e-8 12r 1.011e-7 6.42e-8 15r 1.011e-7 6.42e-8 77r
```

D.2. PFBR PHOENIX Input

```
FBR Core Irradiation
6                       !Number of MCNP materials to Burn
1  80c                     !MCNP material "m" Numbers
4  80c                     !MCNP material "m" Numbers
5  80c                     !MCNP material "m" Numbers
6  80c                     !MCNP material "m" Numbers
19 80c                     !MCNP material "m" Numbers
23 80c                     !MCNP material "m" Numbers
```

```
413381.36             !Volume of Cells Containing the Materials
422776.40             !Volume of Cells Containing the Materials
501694.66             !Volume of Cells Containing the Materials
1422806.69            !Volume of Cells Containing the Materials
176773.11             !Volume of Cells Containing the Materials
50506.6               !Volume of Cells Containing the Materials
1250                  !Power in MWt
-196.0                !Q-value for Fission
0                  !Total Number of Days Burned
8                  !Number of Outer Burn Steps
0.395833 1.0           !If Days = 0, read in days burned & power fraction for
each
29.6042 1.0           ! of the Outer Burn Steps specified above
30 1.0             ! if days burned > 0, this section is ignored
30 1.0             !If Days = 0, read in days burned & power fraction for each
30 1.0             ! of the Outer Burn Steps specified above
30 1.0             ! if days burned > 0, this section is ignored
30 1.0             ! of the Outer Burn Steps specified above
45 0.0             ! if days burned > 0, this section is ignored
1                  !Number of Predictor Steps
0                  !Step to Restart After
mcnp6.mpi 10
/usr/local/mcnp6-data/  ! Data path for MCNP
/usr/local/scale-6.1/cmds/batch6.1       !Scale Executeable
/usr/local/scale-6.1/  ! Data path for SCALE
1.0             !Fractional Importance Limit
1                  !Flag for Intermediate keff Calculations
2                  !# of isotopes to perturb (recommend < 3)
94239 5            !Isotope, % perturbation
94239 10            !Isotope, % perturbation
22                  ! # of isotopes to print Activity (Ci)
441050
501250
511250
531350
541350
551330
551340
551370
601480
621490
631540
922340
922350
922380
942390
942400
942410
952410
952420
952421
962420
962440
22                 !Number of Automatic Tally Isotopes
44105.80c
50125.80c
51125.80c
53135.80c
54135.80c
```

```
55133.80c
55134.80c
55137.80c
60148.80c
62149.80c
63154.80c
92234.80c
92235.80c
92238.80c
94239.80c
94240.80c
94241.80c
95241.80c
95242.80c
95642.80c
96242.80c
96244.80c
22                !Number of Automatic Tally Isotopes
44105.80c
50125.80c
51125.80c
53135.80c
54135.80c
55133.80c
55134.80c
55137.80c
60148.80c
62149.80c
63154.80c
92234.80c
92235.80c
92238.80c
94239.80c
94240.80c
94241.80c
95241.80c
95242.80c
95642.80c
96242.80c
96244.80c
22                !Number of Automatic Tally Isotopes
44105.80c
50125.80c
51125.80c
53135.80c
54135.80c
55133.80c
55134.80c
55137.80c
60148.80c
62149.80c
63154.80c
92234.80c
92235.80c
92238.80c
94239.80c
94240.80c
94241.80c
95241.80c
```

```
95242.80c
95642.80c
96242.80c
96244.80c
22                !Number of Automatic Tally Isotopes
44105.80c
50125.80c
51125.80c
53135.80c
54135.80c
55133.80c
55134.80c
55137.80c
60148.80c
62149.80c
63154.80c
92234.80c
92235.80c
92238.80c
94239.80c
94240.80c
94241.80c
95241.80c
95242.80c
95642.80c
96242.80c
96244.80c
22                !Number of Automatic Tally Isotopes
44105.80c
50125.80c
51125.80c
53135.80c
54135.80c
55133.80c
55134.80c
55137.80c
60148.80c
62149.80c
63154.80c
92234.80c
92235.80c
92238.80c
94239.80c
94240.80c
94241.80c
95241.80c
95242.80c
95642.80c
96242.80c
96244.80c
22                !Number of Automatic Tally Isotopes
44105.80c
50125.80c
51125.80c
53135.80c
54135.80c
55133.80c
55134.80c
55137.80c
```

60148.80c
62149.80c
63154.80c
92234.80c
92235.80c
92238.80c
94239.80c
94240.80c
94241.80c
95241.80c
95242.80c
95642.80c
96242.80c
96244.80c
95642.80c
96242.80c
96244.80c